

# RESEARCH REPORT



## Fire Performance of Houses. Phase I. Study of Unprotected Floor Assemblies in Basement Fire Scenarios Part I



## CMHC—HOME TO CANADIANS

Canada Mortgage and Housing Corporation (CMHC) has been Canada's national housing agency for more than 60 years.

Together with other housing stakeholders, we help ensure that Canada maintains one of the best housing systems in the world. We are committed to helping Canadians access a wide choice of quality, affordable homes, while making vibrant, healthy communities and cities a reality across the country.

For more information, visit our website at **[www.cmhc.ca](http://www.cmhc.ca)**

You can also reach us by phone at 1-800-668-2642  
or by fax at 1-800-245-9274.



National Research  
Council Canada

Conseil national  
de recherches Canada



## **Fire Performance of Houses**

### **Phase I**

### **Study of Unprotected Floor Assemblies in Basement Fire Scenarios**

### **Part 1 – Results of Tests UF-01 and UF-02 (Solid Wood Joists)**

Research Report: IRC-RR-246

Date: March 31, 2009

Authors: N. Bénichou, J.Z. Su, A.C.  
Bwalya, G.D. Loughheed, B.C.  
Taber, P. Leroux, A.H. Kashef, C.  
McCartney, J.R. Thomas

INSTITUTE FOR RESEARCH IN CONSTRUCTION  
Fire Research Program

## TABLE OF CONTENTS

TABLE OF CONTENTS .....	i
LIST OF FIGURES .....	iii
LIST OF TABLES .....	v
ABSTRACT .....	vi
<b>1 INTRODUCTION .....</b>	<b>1</b>
<b>1.1 Background .....</b>	<b>1</b>
<b>1.2 Goals of the Research .....</b>	<b>2</b>
<b>1.3 General Research Approach .....</b>	<b>2</b>
<b>1.4 Scope of the Research Project .....</b>	<b>3</b>
<b>1.5 Content of this Document .....</b>	<b>3</b>
<b>2 EXPERIMENTAL STUDY .....</b>	<b>4</b>
<b>2.1 Geometry - Compartments in the Facility .....</b>	<b>4</b>
2.1.1 Fire Compartment - Basement .....	4
2.1.2 First Storey .....	5
2.1.3 Second Storey .....	5
<b>2.2 Lining Materials in Compartments .....</b>	<b>7</b>
<b>2.3 Openings and their States .....</b>	<b>7</b>
<b>2.4 Fuel Load in the Fire Compartment .....</b>	<b>8</b>
<b>2.5 Instrumentation in the Different Compartments and Exterior .....</b>	<b>9</b>
2.5.1 Fire Compartment in Basement .....	9
2.5.2 First Storey .....	10
2.5.3 Second Storey .....	11
2.5.4 Exterior .....	12
<b>2.6 Testing Procedure .....</b>	<b>12</b>
<b>2.7 Construction Details of the Floor Assemblies .....</b>	<b>13</b>
2.7.1 Floor Assemblies with Solid Wood Joists .....	13
<b>2.8 Instrumentation of the Floor Assemblies .....</b>	<b>18</b>
2.8.1 Temperatures in the Floor Assemblies .....	18
2.8.2 Flame Penetration through the Floor Assemblies .....	20
2.8.3 Deflection of the Floor Assemblies .....	22
<b>2.9 Loading of the Floor Assemblies .....</b>	<b>22</b>
<b>3 RESULTS OF THE TESTS .....</b>	<b>24</b>
<b>3.1 Recording of Results .....</b>	<b>24</b>
<b>3.2 Observations and Recordings .....</b>	<b>24</b>
<b>3.3 Time-temperature Curves at Different Locations .....</b>	<b>24</b>
3.3.1 Temperatures in the Compartments .....	24
3.3.2 Temperatures at the Window in the Basement .....	39
3.3.3 Temperatures at the Doorway to the Basement .....	40
3.3.4 Temperatures on the First Storey at the Top of the Stairs from the Basement .....	41
3.3.5 Temperatures on the Second Storey at the Top of the Stairs .....	43
3.3.6 Temperatures at the Outside Doorway on the First Storey .....	44
3.3.7 Temperatures on the First Storey on the Unexposed Side of the Floor Assemblies .....	46
3.3.8 Temperatures on the Exposed Side of the Floor Assemblies .....	50
<b>3.4 Deflection Measurements Results and Structural Performance .....</b>	<b>66</b>
3.4.1 For Test UF-01 .....	66

3.4.2	For Test UF-02.....	69
<b>3.5</b>	<b>Flame Penetration Results .....</b>	<b>72</b>
3.5.1	For Test UF-01.....	73
3.5.2	For Test UF-02.....	73
<b>3.6</b>	<b>Detection Times.....</b>	<b>74</b>
<b>3.7</b>	<b>Results of Smoke and Gas Measurements and Tenability Analysis .....</b>	<b>75</b>
3.7.1	Exposure to Toxic Gases.....	77
3.7.2	Exposure to Heat.....	84
3.7.3	Visual Obscuration by Smoke .....	85
3.7.4	Summary of Estimation of Time to Incapacitation.....	87
<b>3.8</b>	<b>The Sequence of Events.....</b>	<b>97</b>
4	SUMMARY.....	99
5	ACKNOWLEDGMENTS.....	99
6	REFERENCES .....	100

## LIST OF FIGURES

Figure 1. Possible chronological sequence of events affecting the life safety of occupants in a fire situation.....	2
Figure 2. Three-storey facility.....	4
Figure 3. Basement level layout.....	5
Figure 4. First storey layout.....	6
Figure 5. Second storey layout .....	6
Figure 6. Fuel package .....	8
Figure 7. Arrangement of the fuel package in the fire compartment .....	9
Figure 8. Fire Compartment instrumentation .....	10
Figure 9. First storey instrumentation.....	11
Figure 10. Second storey instrumentation .....	12
Figure 11. Solid wood joist layout details.....	14
Figure 12. Solid wood joist overlap details.....	15
Figure 13. End connection details and supports.....	15
Figure 14. Cross bracing details.....	16
Figure 15. Subfloor layout.....	17
Figure 16. Subfloor nail pattern and nail description.....	18
Figure 17. Thermocouples locations.....	19
Figure 18. Thermocouples locations reflecting the different sections shown in Figure 17 .....	20
Figure 19. Wire mesh device to detect flame penetration.....	21
Figure 20. Loading blocks and locations of the deflection measurement points on the unexposed side of the floor .....	22
Figure 21. Loading blocks restraining system.....	23
Figure 22. TC Trees in the basement for UF-01 .....	26
Figure 23. TC Trees in the basement for UF-02 .....	29
Figure 24. TC trees in the first storey for UF-01.....	32
Figure 25. TC trees in the first storey for UF-02.....	34
Figure 26. TC trees in the second storey bedrooms for UF-01 .....	37
Figure 27. TC trees in the second storey bedrooms for UF-02.....	38
Figure 28. Temperatures at the window in the basement for UF-01 .....	39
Figure 29. Temperatures at the window in the basement for UF-02.....	40
Figure 30. Temperatures at the exposed side [basement side] of the basement door for Test UF-02 .....	41
Figure 31. Temperatures on the first storey at the top of the stairs from the basement for Test UF-01 .....	42
Figure 32. Temperatures on the first storey at the top of the stairs from the basement [unexposed side of basement door] for Test UF-02 .....	42
Figure 33. Temperatures on the second storey at the stairs for UF-01 .....	43
Figure 34. Temperatures on the second storey at the stairs for UF-02 .....	44
Figure 35. Temperatures at the outside doorway on the first storey for UF-01.....	45
Figure 36. Temperatures at the outside doorway on the first storey for UF-02.....	45
Figure 37. Temperatures at the unexposed side of subfloor for UF-01 .....	47
Figure 38. Temperatures at the unexposed side of subfloor for UF-02 .....	49
Figure 39. Temperatures at the exposed side for UF-01 .....	52
Figure 40. Temperatures at the exposed side for UF-02 .....	60
Figure 41. Deflection points measured .....	67
Figure 42. Deflection measurements for rows 1, 2 and 3 for UF-01 .....	68

Figure 43. Deflection measurements for rows 1, 2 and 3 for UF-02 .....	70
Figure 44. Picture showing the north side holding the concrete blocks for UF-02 .....	72
Figure 45. Results of flame sensors at different joints .....	74
Figure 46. CO measurements for Test UF-01 .....	89
Figure 47. O <sub>2</sub> measurements for Test UF-01 .....	89
Figure 48. CO <sub>2</sub> measurements for Test UF-01 .....	90
Figure 49. Optical density measurements for Test UF-01 .....	91
Figure 50. CO measurements for Test UF-02 .....	92
Figure 51. O <sub>2</sub> measurements for Test UF-02 .....	92
Figure 52. CO <sub>2</sub> measurements for Test UF-02 .....	93
Figure 53. Optical density measurements for Test UF-02 .....	94
Figure 54. Time remaining to incapacitation versus onset of exposure for Test UF-01 .....	95
Figure 55. Time remaining to incapacitation versus onset of exposure for Test UF-02 .....	96
Figure 56. Sequence of fire events in Test UF-01 .....	98
Figure 57. Sequence of fire events in Test UF-02 .....	98

## LIST OF TABLES

Table 1. Reserve Live Load Capacity .....	23
Table 2. Smoke Alarm Activation Times after Ignition .....	75
Table 3. Maximum CO and CO <sub>2</sub> Concentrations and Minimum O <sub>2</sub> Concentration .....	78
Table 4. Tenability Limits for Incapacitation or Death after 5-min Exposure .....	78
Table 5. Time to the Specified Fractional Effective Dose for Exposure to O <sub>2</sub> Vitiating, CO <sub>2</sub> and CO .....	82
Table 6. FED due to CO, CO <sub>2</sub> , O <sub>2</sub> Vitiating at Specified Time .....	83
Table 7. Time to the Specified FED for Exposure to Convected Heat .....	85
Table 8. Time to the Specified Smoke Optical Density .....	87
Table 9. Summary of Estimation of Time to Specified FED and OD .....	87
Table A 1. Test Summary for Test UF-01 .....	103
Table A 2. Test Summary for Test UF-02 .....	104

## **ABSTRACT**

This report documents part of the research project involving a series of full-scale fire experiments in a test facility that simulated a two-storey single-family house with a severe, fast growing fire originating in an unfinished basement to study the fire performance of the floor/ceiling assembly constructed over the basement. The report presents the results and analysis of Test UF-01 and Test UF-02 carried out in the test house with an unprotected solid wood floor/ceiling assembly above the basement. The two tests were identical except for the state of the door in the doorway leading from the first storey to the basement, which was absent in Test UF-01 (i.e. completely open basement doorway) and completely closed in Test UF-02 (i.e. closed basement doorway). A number of measurements were taken at various locations during the tests such as temperatures, smoke alarm activation times, smoke optical density, floor deflection and concentrations of CO, CO<sub>2</sub> and O<sub>2</sub>. For these two tests, untenable conditions on the upper storeys were reached before failure of the test floor assembly. The results showed that closing the door to the basement delayed the failure of the unprotected floor assembly over the basement as well as the onset of untenable conditions on the upper storeys.

# **FIRE PERFORMANCE OF HOUSES**

## **PHASE I**

### **STUDY OF UNPROTECTED FLOOR ASSEMBLIES IN BASEMENT FIRE SCENARIOS**

#### **Part 1 – Results of Tests UF-01 and UF-02 (Solid Wood Joists)**

N. Bénichou, J.Z. Su, A.C. Bwalya, G.D. Loughheed, B.C. Taber, P. Leroux, A.H. Kashef, C. McCartney and J.R. Thomas

## **1 INTRODUCTION**

### **1.1 Background**

Risk of fires in buildings and concerns about their potential consequences are always present. Canada's fire death rate has continuously declined for the last three decades; much of this decline is attributed to the introduction of residential smoke alarms (this is also the case in the United States). With the advent of new materials and innovative products for use in construction of single-family houses, there is a need to understand what impacts these materials and products will have on occupant life safety under fire conditions and a need to develop a technical basis for the evaluation of their fire performance.

The National Building Code of Canada (NBCC) [1] generally intends that major structural load-bearing elements (floors, walls and roofs) have sufficient fire resistance to limit the probability of premature failure or collapse during the time required for occupants to evacuate safely [2]. Historically, the NBCC has not specified a minimum level of fire performance (fire resistance) of these structural elements in single-family houses.

In Canada, the Canadian Construction Materials Centre (CCMC) is called upon to evaluate the use of new materials and innovative construction products for compliance with the NBCC. Some of the more recent innovative structural products, seeking recognition for use in housing, are made of new composite and non-traditional materials that may have unknown fire behaviour. When evaluating new structural products, part of the CCMC challenge is related to the fact that no guidance or criteria are provided in the NBCC regarding the fire performance of structural systems used in single-family houses.

The Canadian Commission on Construction Materials Evaluation (CCCME) guides the operation of CCMC. Through the CCCME, CCMC sought the views of the Canadian Commission on Building and Fire Codes (CCBFC), which guides the development of the NBCC. After review and discussion, both the CCBFC and CCCME agreed that a study on the factors that affect the life safety of occupants of single-family houses should be conducted.

## 1.2 Goals of the Research

The National Research Council of Canada Institute for Research in Construction (NRC-IRC) undertook research into fires in single-family houses to understand the impact of residential construction products and systems on occupant life safety.

This research project sought to achieve the following goals:

1. To determine the significance of the fire performance of structural materials used in houses to the life safety of occupants.
2. To identify methods of measuring the fire performance of unprotected structural elements used in houses.
3. To measure and establish the fire performance of traditional house construction to facilitate the evaluation of the fire performance of innovative construction products and systems.

## 1.3 General Research Approach

Figure 1 shows a possible chronological sequence of relevant critical events that might occur in a fire scenario. It is acknowledged that the chronology of the occurrence of events may differ, and in some cases can shift in ordering.

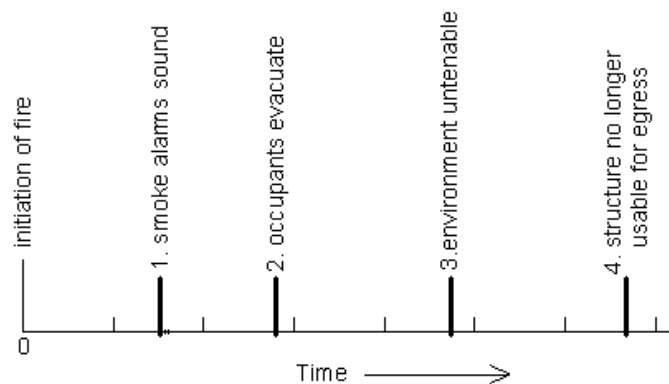


**Figure 1. Possible chronological sequence of events affecting the life safety of occupants in a fire situation**

The research sought to establish, through experimental studies and using specific fire test scenarios, the typical sequence of the following events (measured from initiation of a fire), using a test facility intended to represent a typical code-compliant single-family house:

1. Sounding of smoke alarms (Event 1 as shown in Figure 1).
2. Loss of tenability within the environment of the first, second or subsequent storey(s) (Event 3).
3. Loss of integrity of the floor assembly and/or loss of its function as a viable egress route on the first or second storey(s)<sup>1</sup> (Event 4).

---

<sup>1</sup> The state of the egress route(s) on the first storey is relevant to the evaluation of the performance of the basement foundation walls and floor structure constructed over the basement;

The research also sought to establish a basis for prediction or estimation of the required safe egress times expected for ambulatory occupants assuming a tenable indoor environment and a structurally sound evacuation route. A review of the literature on the waking effectiveness of occupants to smoke alarms, the delay time to start evacuation and the timing of escape in single-family houses was conducted. The objective of the review was to identify a range of estimated times families would take to awake, prepare and move out of their home after perceiving the sound of a smoke alarm during the night in winter conditions (Event 2 shown in Figure 1). This literature review was a separate but parallel study to the experimental studies. The results of the literature review are provided in Reference [3].

#### **1.4 Scope of the Research Project**

The overall research consisted of a number of phases of experimental studies with each phase investigating a specified structural element based on specified fire scenarios.

Phase 1 (2004 to 2007) of the experimental study focused on basement fires and their impacts on the structural integrity of unprotected floor assemblies above a basement and the tenability conditions in a full-scale test facility. It is acknowledged that, a basement is not the most frequent site of household fires but it is the fire location that is most likely to create the greatest challenge to the structural integrity of the 1<sup>st</sup> storey structure, which typically provides the main egress routes. The study of fires originating in basements also provides a good model for the migration of combustion products throughout the house and its egress paths. The data collected during this phase of the project provided important indicators for identifying and evaluating the sequence for the occurrence of critical events shown in Figure 1.

This research focused on the life safety of occupants in single-family houses. The safety of emergency responders in a fire originating in single-family houses was not within the scope of this research project. Technical data collected during this research could aid in clarifying the potential risks associated with firefighting activities.

#### **1.5 Content of this Document**

This report documents the results of the first phase of the work involving an experimental study of the structural fire performance of the floor/ceiling assembly (1<sup>st</sup> storey) constructed over the basement level of a test house. Specifically, this report contains the data and analysis of the first two tests (UF-01 and UF-02) of the Phase I study carried out in a test house with an unprotected solid wood joist floor/ceiling assembly. This includes results on the fire scenarios, tenability, structural integrity, and the sequence of Events 1, 3 and 4, as illustrated in Figure 1.

---

the state of the egress route on the second storey is relevant to the evaluation of the performance of the above-grade wall structures and floor structure over the first storey.

## 2 EXPERIMENTAL STUDY

To undertake this research, NRC-IRC constructed a three-level experimental facility, representing a typical two-storey detached single-family house with a basement. The facility allows the study of structural fire performance, as well as smoke movement and tenability under fire conditions for single-family houses. The facility has a total floor area of approximately 95 m<sup>2</sup> per storey and is shown in Figure 2.



**Figure 2. Three-storey facility**

### 2.1 Geometry - Compartments in the Facility

#### 2.1.1 Fire Compartment - Basement

The layout of the basement is shown in Figure 3. The basement was partitioned to create a fire room representing a 27.6 m<sup>2</sup> basement living area, or about 1/4 of the total basement area. This compartment size was chosen based on a survey carried out by NRC [4]. The area of the basement that was not used for the fire compartment was blocked off during the fire tests. The height of the basement was 2.44 m. The ceiling clear height depended on the depth of the floor assembly being tested. A rectangular exterior opening measuring 2.0 m wide by 0.5 m high and located 1.8 m above the floor was provided in the south wall of the fire room. The size of the opening was chosen based on the results of the survey carried out by NRC [4]. A 0.91 m wide by 2.05 m high doorway opening located on the north wall of the fire room led into an empty stairwell enclosure (without a staircase). At the top of this stairwell, a 0.81 m wide by 2.05 m high doorway led into the first storey, as shown in Figure 4. This doorway either had no door (open basement doorway) or had a door in the closed position (closed basement doorway), depending on the scenario being studied. There is no requirement for a basement door in the NBCC. Section on “Openings and their States” provides more details.

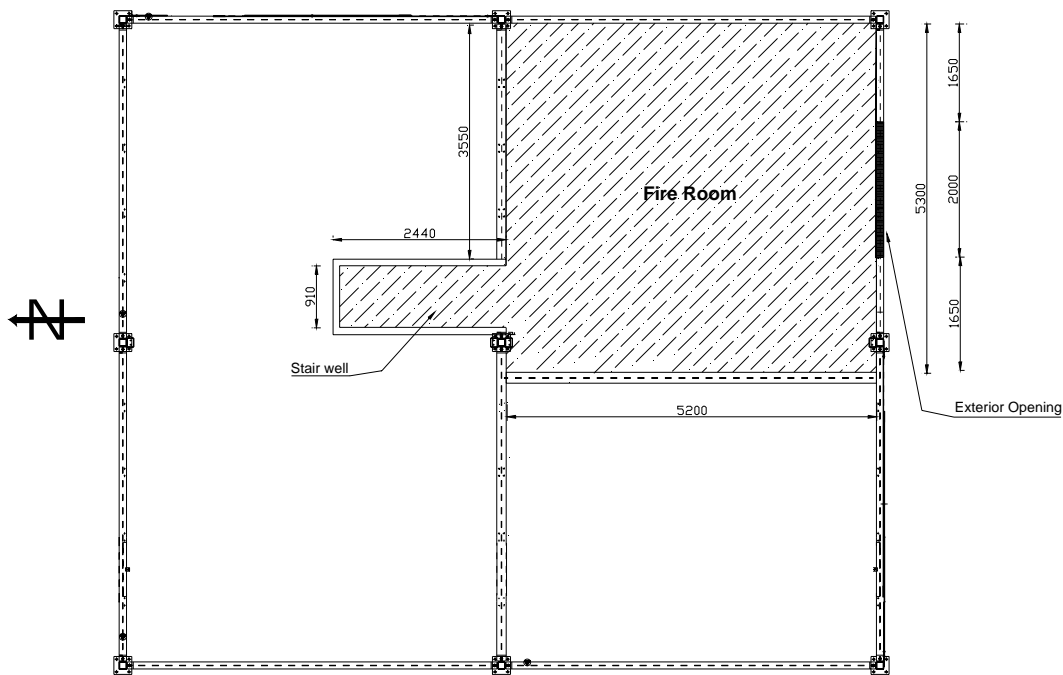


**Figure 3. Basement level layout (dimensions in mm)**

### 2.1.2 First Storey

The first storey had an open-plan layout with no partitions, as shown in Figure 4. A test floor assembly was constructed on the first storey directly above the fire room for each experiment. The remainder of the floor on the first storey was constructed out of non-combustible materials. The height of the storey was about 2.44 m. As shown in Figure 4, this storey had 2 door openings: a door opening to the outside (dimensions of 0.89 m by 2.07 m) and a door opening that connected the basement to the first storey (dimensions of 0.81 m by 2.05 m). This storey also connected to the 2<sup>nd</sup> storey by a staircase in the middle of the storey area. This staircase to the second storey was not enclosed. The floor being tested was positioned in the southeast quarter of the first storey, on top of the fire compartment.

### 2.1.3 Second Storey

The layout of the second storey is shown in Figure 5. This storey was partitioned to contain two identical bedrooms with dimensions of 3.75 m by 4.47 m connected by a corridor with dimensions of 1.1 m x 4.45 m. The height of the storey was 2.44 m. In all tests, the door of the southeast bedroom remained closed whereas the door on the southwest bedroom was kept open. The size of the door openings was 0.81 m by 2.05 m. The remaining area of the second storey that was not used was blocked off during the fire tests.

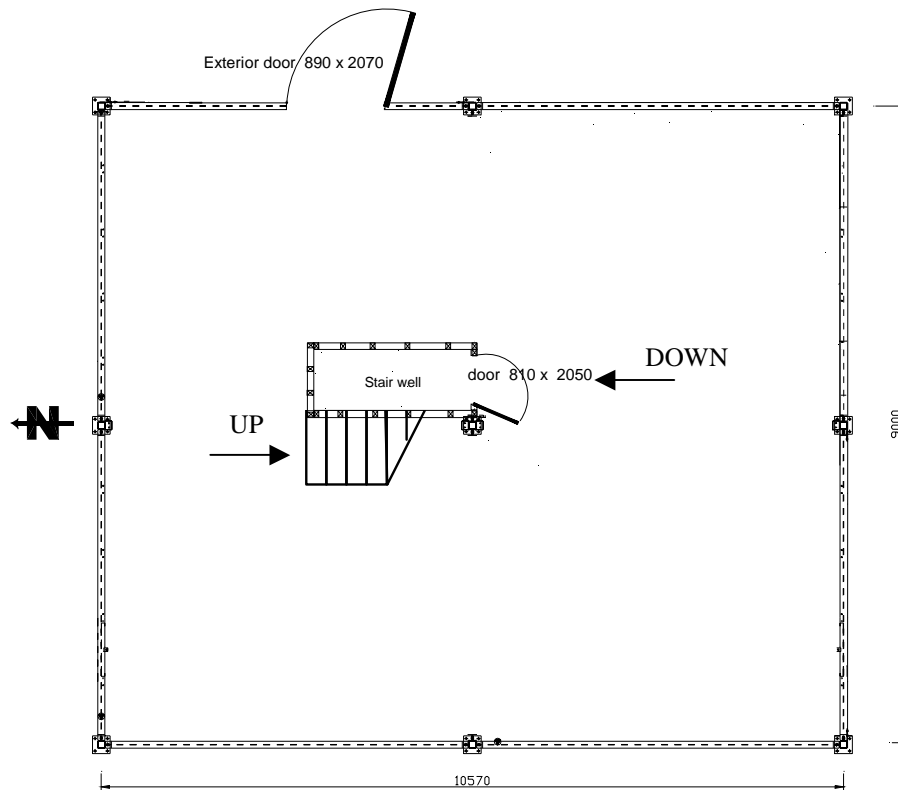


**Figure 4. First storey layout (dimensions in mm)**

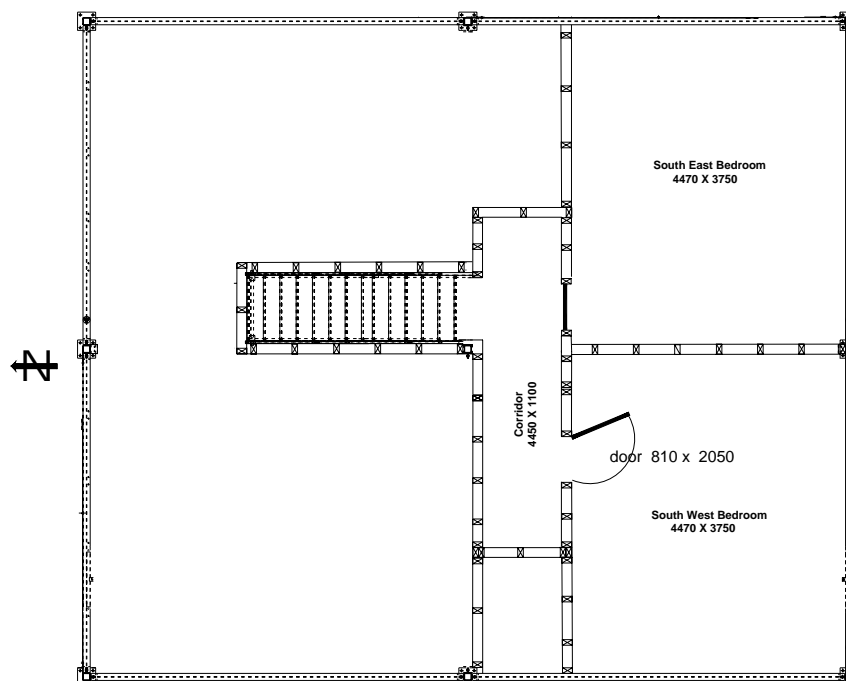


**Figure 5. Second storey layout (dimensions in mm)**

## **2.2 Lining Materials in Compartments**

The compartments were lined with different materials. For the basement level, the walls of the fire compartment were lined with 12.7 mm thick regular gypsum board. There was no ceiling finish in the fire compartment, so the floor assembly, including both the framing supports (joists) and the underside of the subfloor (oriented strand board, OSB), was unprotected and exposed. For the first and second storeys, cement board covered the walls, and the ceilings were covered with 12.7-mm thick regular gypsum board. There was no finished floor in the 1<sup>st</sup> storey, so the upper surface of the OSB subfloor used on the floor assembly being tested was exposed. In the remainder of the compartment on the first storey, the floor was noncombustible. The OSB that was used for the subfloor was chosen on the basis of a study on the performance of different OSBs when exposed to fire [5].

## **2.3 Openings and their States**

The openings included: on the basement level, a rough window opening; on the first storey, a door opening to the outside and a door opening at the top of the empty stairwell enclosure (contained no stairs) leading from the basement level; on the second storey, a door opening in the corridor at the top of the stairs leading from the first storey and door openings from the corridor leading to each of the two bedrooms. The size of all the doorways were typical of those used in housing. The single window opening in the basement (2.0 m x 0.5 m) represents an area equal to the size of two typical basement windows.

The doors on the door openings were inexpensive moulded-fibreboard hollow-core interior doors with minimum size styles and rails or solid-core exterior wood doors. The rough window opening in the basement level was covered with a noncombustible panel that could open at the appropriate time in each fire test.

At the start of a test, the rough window opening in the basement and the exterior door on the first storey leading to the outside were closed. Both were opened at critical times during a test (see Section 2.6 Testing Procedure). The doorway on the first storey leading to the basement either had a door in the opening in the closed position (closed basement doorway) or had no door (open basement doorway) depending on the scenario being studied. In Test UF-01, the open basement doorway was used; in Test UF-02, the closed basement doorway was used. On the second storey, during the test, the door to the southwest bedroom was open, and the door to the southeast bedroom was closed.

There was no heating, ventilating and air-conditioning or plumbing system installed in the test house, i.e., no associated mechanical openings in the floor.

## 2.4 Fuel Load in the Fire Compartment

The selection of the fuel load and its arrangement in the fire compartment was a critical element in this experimental work. A study was conducted to select the fire scenario and fuel package, which was used in this phase of the project [6]. This fuel package consisted of a mock-up sofa constructed with 9 kg of exposed polyurethane foam (PUF), the dominant combustible constituent of upholstered furniture, and 190 kg of wood cribs beside and underneath the mock-up sofa. A photograph of the fuel package is shown in Figure 6. The mock-up sofa was constructed with 6 blocks of flexible polyurethane foam (with a density of  $32.8 \text{ kg/m}^3$ ) placed on a metal frame. Each block was 610 mm long by 610 mm wide and 100 mm or 150 mm thick. The 150-mm thick foam blocks were used for the backrest and the 100 mm thick foam blocks for the seat cushion. The PUF foam was used without any upholstery fabric that is used in typical upholstered furniture. The wood cribs were made with spruce lumber pieces, each piece measuring 38 mm x 89 mm x 800 mm. For the small cribs located under the mock-up sofa, four layers with six pieces per layer were used. The other two cribs used eight layers.

The placement of the fuel package in the basement fire compartment is illustrated in Figure 7. The mock-up sofa was located at the center of the floor area. The mock-up sofa was ignited in accordance with the ASTM 1537 test protocol [7] and the wood cribs provided the remaining fire load to sustain the fire for the desired period of time.



**Figure 6.** Fuel package

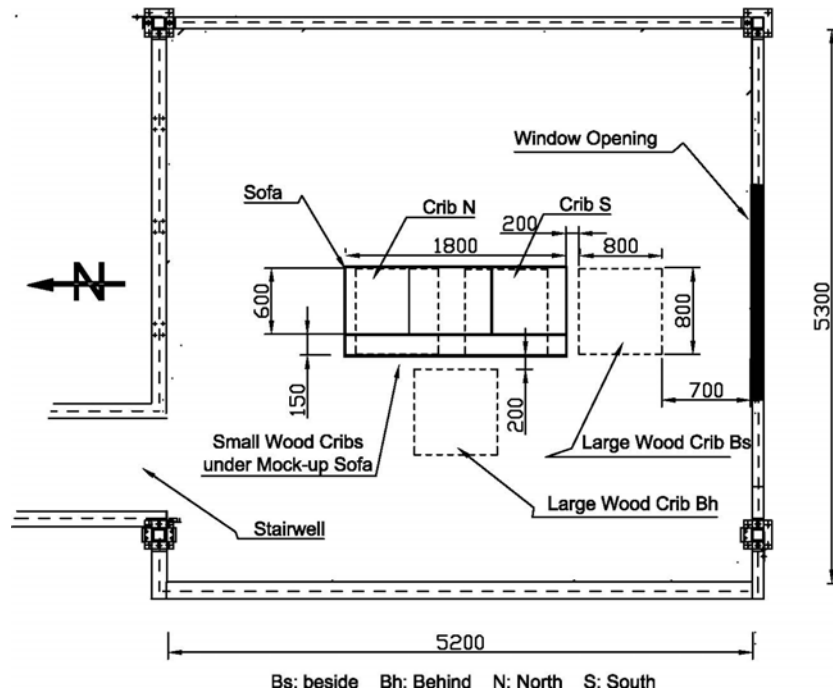


**Figure 7. Arrangement of the fuel package in the fire compartment**  
(dimensions in mm)

## 2.5 Instrumentation in the Different Compartments and Exterior

The following is a summary of the instrumentation installed inside and around the exterior of the test facility.

### 2.5.1 Fire Compartment in Basement

The instrumentation in the basement fire room included the following:

- Four vertical arrays of thermocouples located at the quarter points of the fire room to measure temperatures at heights of 0.4, 0.9, 1.4, 1.9 and 2.4 m above the floor level.
- Thermocouples located at the basement exterior opening (window) to measure the temperature at the simulated window and the temperature of the gas plume after the mock-window was opened.
- Thermocouples located on the exposed side of the door to the basement at the centre and at three heights: 0.9, 1.4 and 1.9 m (for UF-02 only).
- Residential photoelectric smoke alarms located near the stairwell.
- Air velocity measurements at the basement exterior opening (window).
- Differential pressure measurement between the fire compartment and the exterior of the test facility, located 2.0 m above the floor.
- Video recording of the burning fuel package.
- Thermocouples measuring temperatures in the wood cribs.

The positioning of the instrumentation in the fire compartment on the basement level is shown in Figure 8.

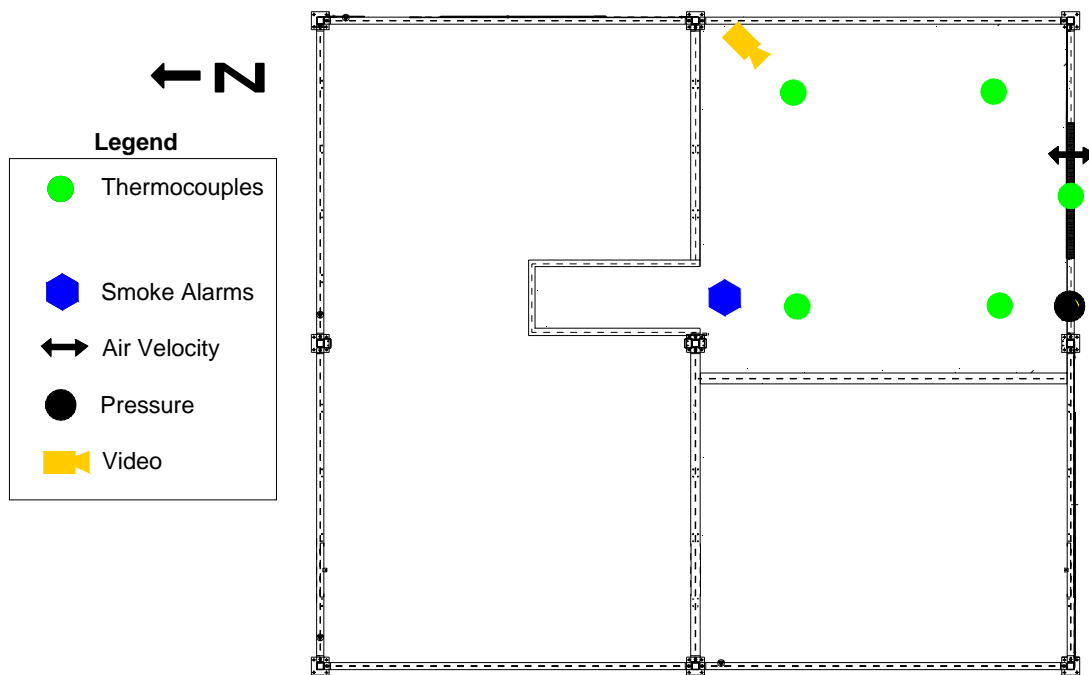


**Figure 8. Fire Compartment instrumentation**

### 2.5.2 First Storey

The instrumentation on the first storey included the following:

- Four vertical thermocouple arrays at the quarter points of the whole floor area.
- One vertical thermocouple array located at the door opening of the stairwell from the basement level.
- Gas sampling ports at the southwest quarter point, including:
  - CO/CO<sub>2</sub>/O<sub>2</sub> at 0.9 m and 1.5 m above the floor.
  - Fourier Transform Infrared Spectroscopy (FTIR) at 1.5 m above the floor.
- Smoke density measurements at the southwest quarter point at 0.9 m and 1.5 m above the floor.
- Residential ionization and photoelectric smoke alarms located on the ceiling near the doorway to the basement.
- Air velocity measurements located at top of the basement stairwell at ceiling height and at 1.5 m above the floor.
- Differential pressure measurement between the fire compartment in the basement level and the first storey.
- Video recording from two locations.

The positioning of the instrumentation on the first storey is shown in Figure 9.

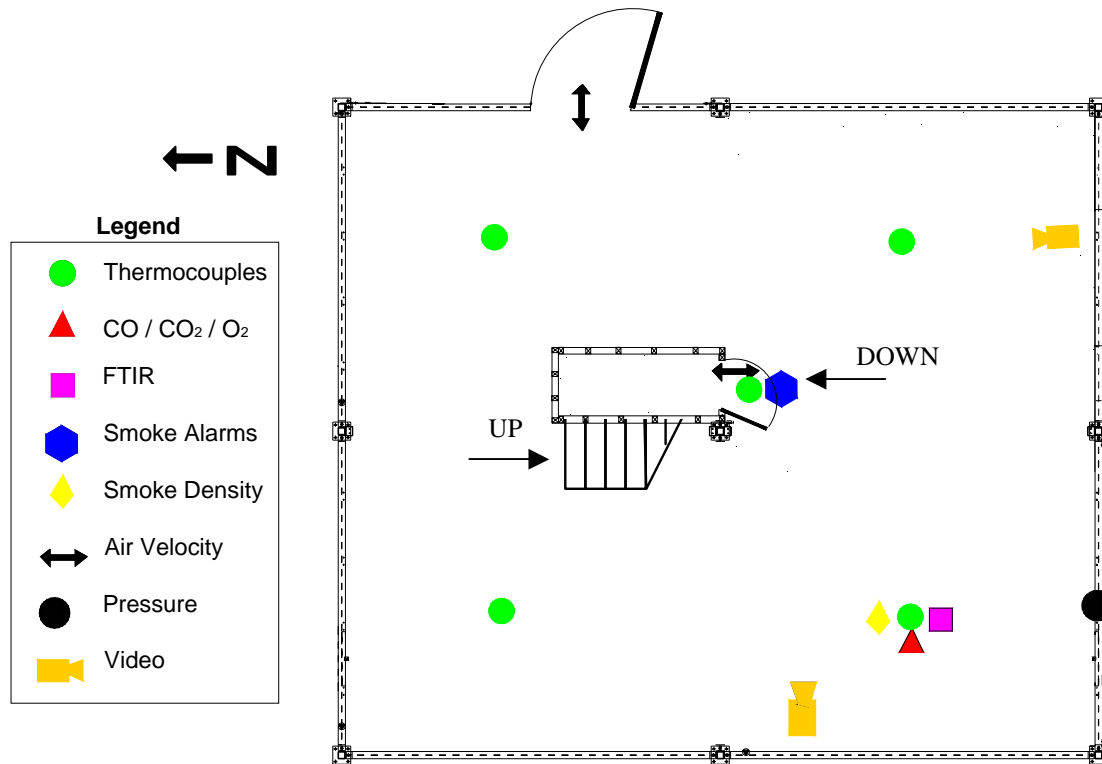


**Figure 9. First storey instrumentation**

### 2.5.3 Second Storey

The instrumentation on the second storey included the following:

- One vertical thermocouple array in the corridor at the top of the stairs.
- One vertical thermocouple array in the center of each bedroom.
- Residential ionization and photoelectric smoke alarms located on the ceiling in the corridor at the top of the stairs.
- Residential ionization and photoelectric smoke alarms located on the ceiling at the centre of each bedroom.
- Gas analysis (CO/CO<sub>2</sub>/O<sub>2</sub>) in the corridor at the top of the stairs at 0.9 m and 1.5 m above the floor.
- Smoke density measurements in the corridor at the top of the stairs at 0.9 m and 1.5 m above the floor.
- Air velocity measurements located at the top of the stairs at ceiling height and at 1.5 m above the floor.
- Video recording in the corridor.

The positioning of the instrumentation on the second storey is shown in Figure 10.

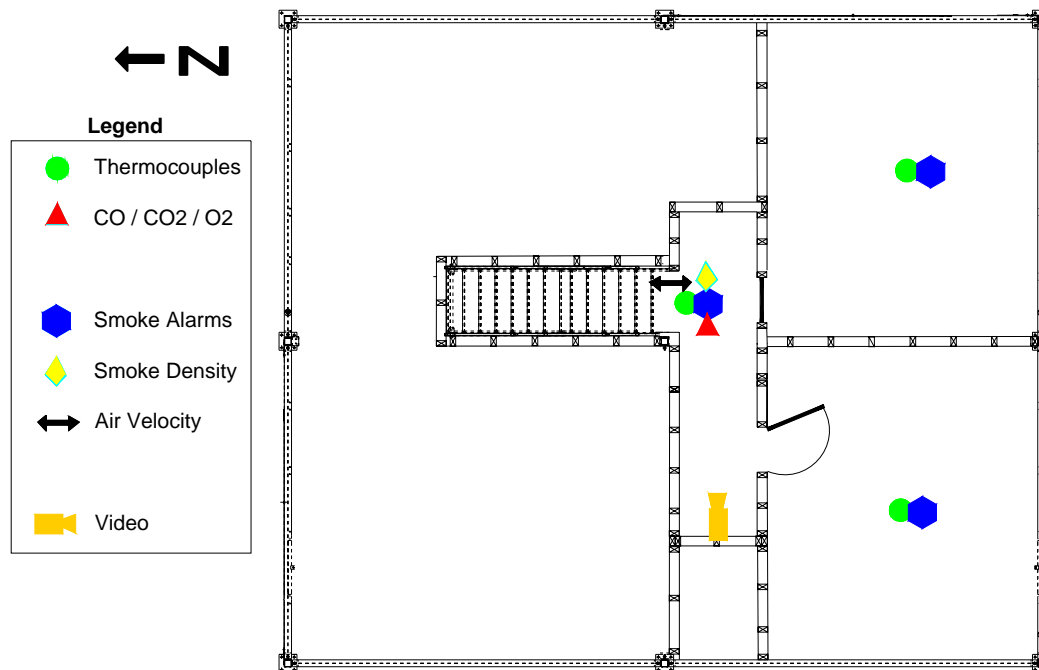


**Figure 10. Second storey instrumentation**

#### 2.5.4 Exterior

Instrumentation of the facility exterior included the following:

- Air velocity measurements located at the basement window opening.
- Air velocity measurements located at the exterior door opening on the first storey.
- Video recording of the exterior window opening in the fire compartment on the basement level and the exterior door opening on the first storey.

## 2.6 Testing Procedure

The mock-up sofa was ignited in accordance with the ASTM 1537 test protocol [7] and data was collected at 5 s intervals throughout each test.

The non-combustible panel that covered the fire room's exterior rough window opening during the initial stage of each test was manually removed when the temperature measured at the top-center of the opening reached 300°C. The removal of the panel was to provide ventilation air necessary for combustion.

The exterior door on the first storey was opened at 180 s after ignition and left open, simulating a situation where some occupants, who would have been in the test house, escaped leaving the exterior door open while other occupants may still have been inside the house.

The tests were terminated by extinguishing the fires using a manually operated sprinkler system when one of the following occurred (singly or in combination):

- Excessive flame penetration through the floor assembly;
- Structure failure of any part of the floor assembly;
- Compromise of safety of the test facility.

## **2.7 Construction Details of the Floor Assemblies**

Eleven full-scale floor assemblies were tested in this first phase of the project. In each test, the floor assembly was installed in the three-storey test facility to create the ceiling portion over the fire compartment in the basement level. The floor assemblies had no ceiling sheathing attached on the underside, leaving the framing members and the subfloor exposed and unprotected from exposure to the fire from the burning fuel package.

For each type of floor assembly tested, the floor joist/truss spans were either chosen from the appendices of the NBCC or calculated based on the ultimate and serviceability limit states. Therefore, the floor joists/trusses could either span the entire length of the fire compartment space or require an intermediate beam support for shorter spans. When designing the assemblies, various aspects were considered including what is typically used for framing and subfloor materials in housing today, consideration of serviceability limit states, typical spacing, typical spans, typical depths, etc. As well, the assemblies were loaded at 50% of the specified load in the NBCC (see Section 2.9).

Details of the first two floor assemblies tested (solid wood joists) are provided below.

### **2.7.1 Floor Assemblies with Solid Wood Joists**

The first two tests, documented in this report, were conducted using wood frame floor assemblies constructed using solid wood joists and an OSB subfloor. The overall dimensions of the wood joist assemblies were 5054 mm by 5175 mm. Specific dimensions of the various components of the assemblies are provided in Figure 11 to Figure 16.

The solid wood joists were manufactured using spruce-pine-fir (SPF) lumber bearing a grade-stamp 'No.2 and better'. The structural members were 235 mm deep by 38 mm wide (nominal 2x10), and were spaced at 400 mm on centre (Figure 11). The joist span length chosen was 4.17 m (Figure 11) taken from the span tables of the NBCC [1]. This corresponds to the maximum span allowed for wood floor joists of SPF lumber graded as 'No.2 and better', and constructed with cross-bridging mid-span and the joists spaced at 400 mm o.c. Since the maximum span allowed for the wood joists was shorter than the length of the fire compartment, a beam was used as an intermediate support at the end of the 4.17-m span and a set of shorter joists were used to increase the span of the floor to extend to the end of the fire compartment. Figure 12 and Figure 13 show the details of the joint overlap and the supporting beams.

The wood joist floor assembly was supported by three horizontal beams, each of which was supported by three columns (a total of nine columns for each floor assembly). The beams were bolted to the columns, which were stiffened by bars and rested stably on the floor under the weight of the assembly and beams.

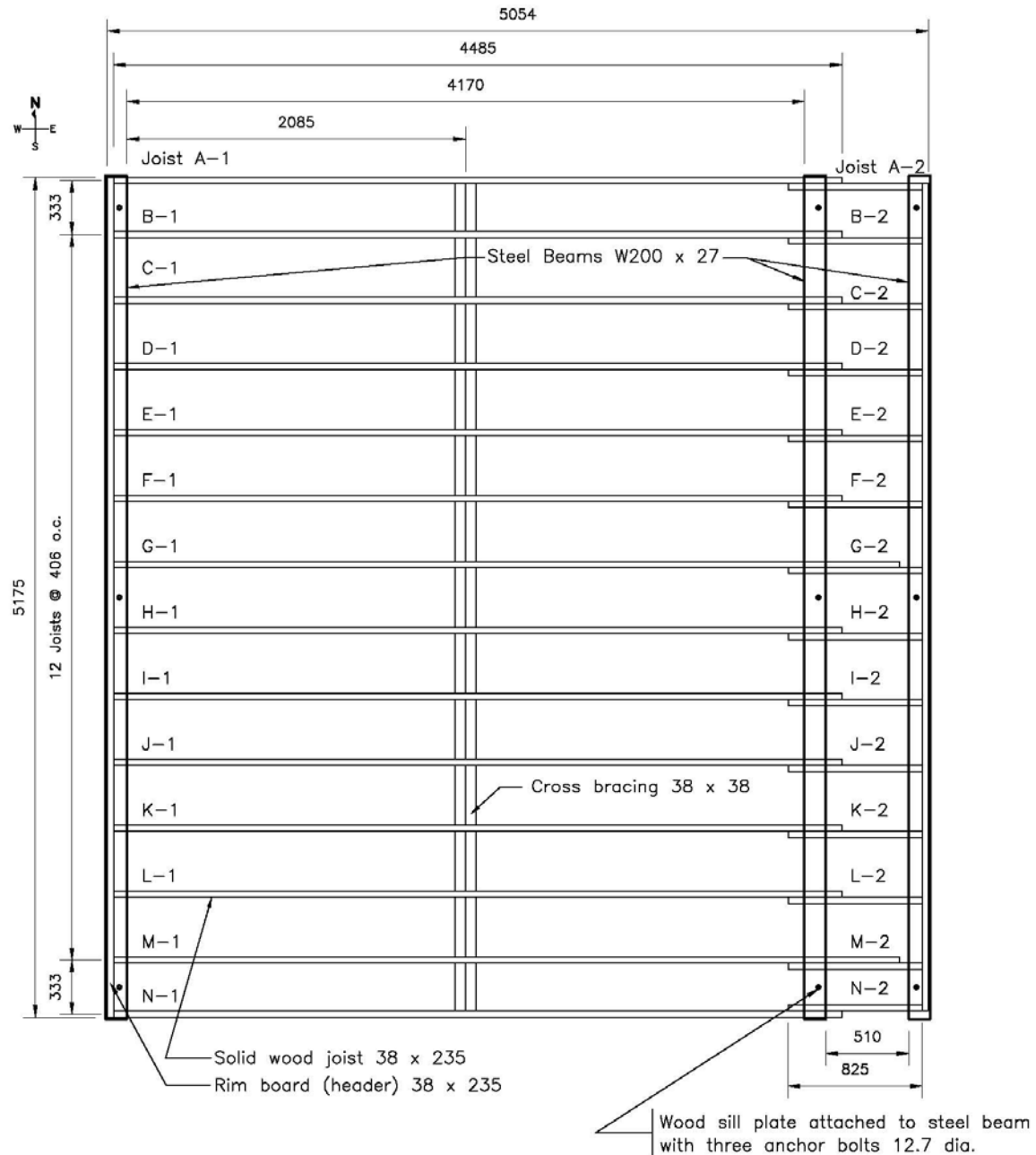


**Figure 11. Solid wood joist layout details** (all dimensions in mm).

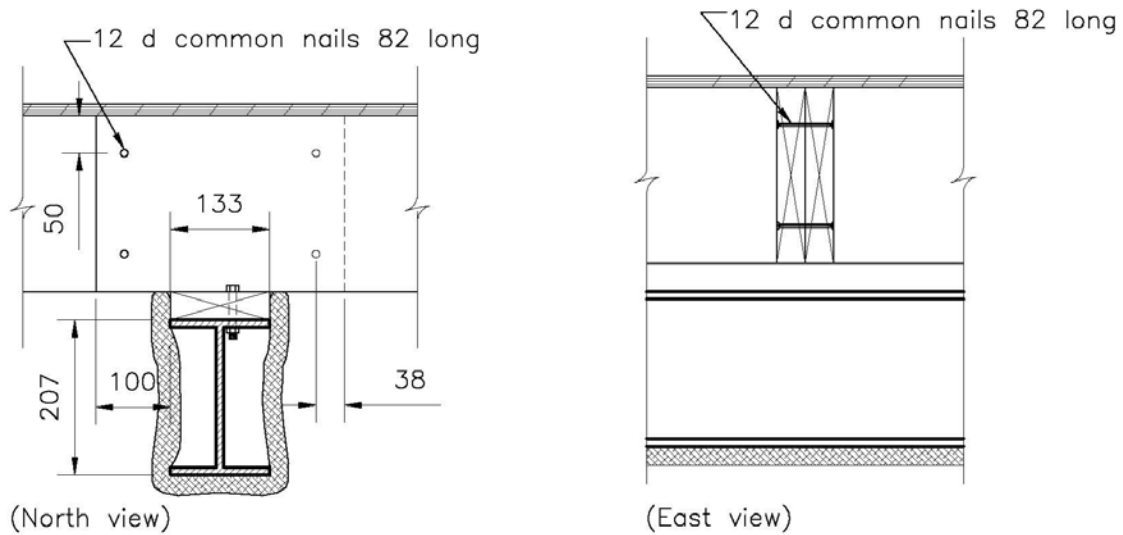


**Figure 12. Solid wood joist overlap details** (all dimensions in mm).

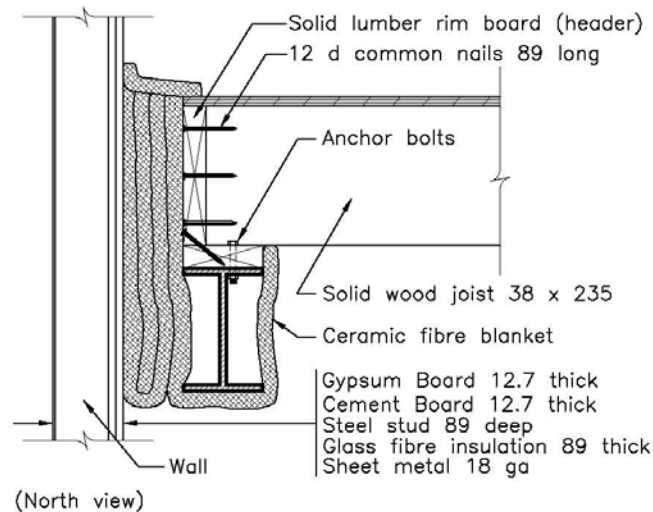
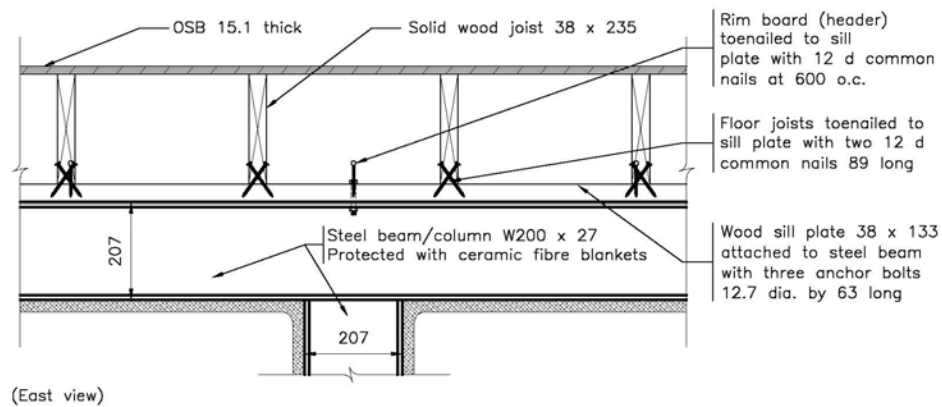


**Figure 13. End connection details and supports** (all dimensions in mm).

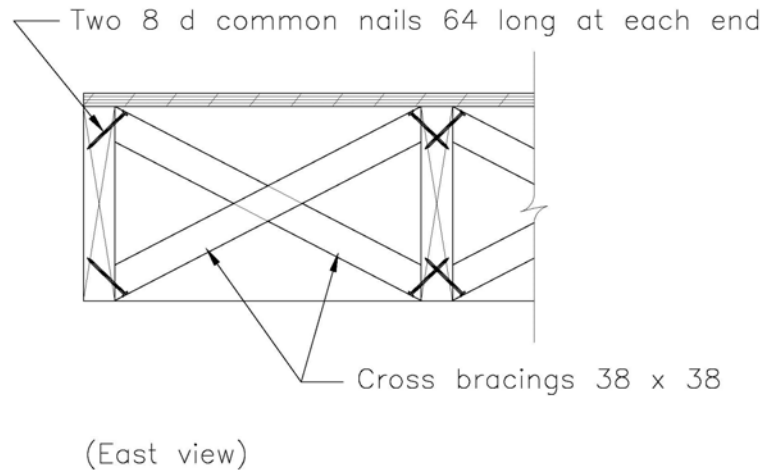


**Figure 14. Cross bracing details** (all dimensions in mm).

Figure 13 also shows the details of the end connection. Ceramic fibre blankets were used to fill any gaps between the assembly and the end walls. Ceramic fibre blankets were also used to protect the steel beams and columns so that they were not subjected to fire and would not fail during the tests.

In the solid wood joist test assemblies (UF-01 and UF-02), rim boards (headers) made of solid lumber 38 mm by 235 mm, were placed at the east and west sides of the floors as shown in Figure 11. In both of these assemblies, one row of diagonal wood cross-bracing, 38 mm thick by 38 mm wide was placed at the centre of the longer span of the assembly between the joists. Details of the cross-bracing and its location within the joist layout for the above-mentioned assemblies are shown in Figure 11 and Figure 14.

OSB was used as the subfloor material in the floor assemblies. The specific OSB material used was selected based on a separate study documented in reference [5]. The subfloor panels were 15.1 mm thick in both assemblies, with a full panel size being 1.2 x 2.4 m. The longer panel edges had a tongue and groove profile while the short panel edges were square-butt ends. Figure 15 shows the layout of the subfloor. The nailing pattern and description of nails used to attach the OSB panels to the wood joists and rim board (header) are shown in Figure 16.

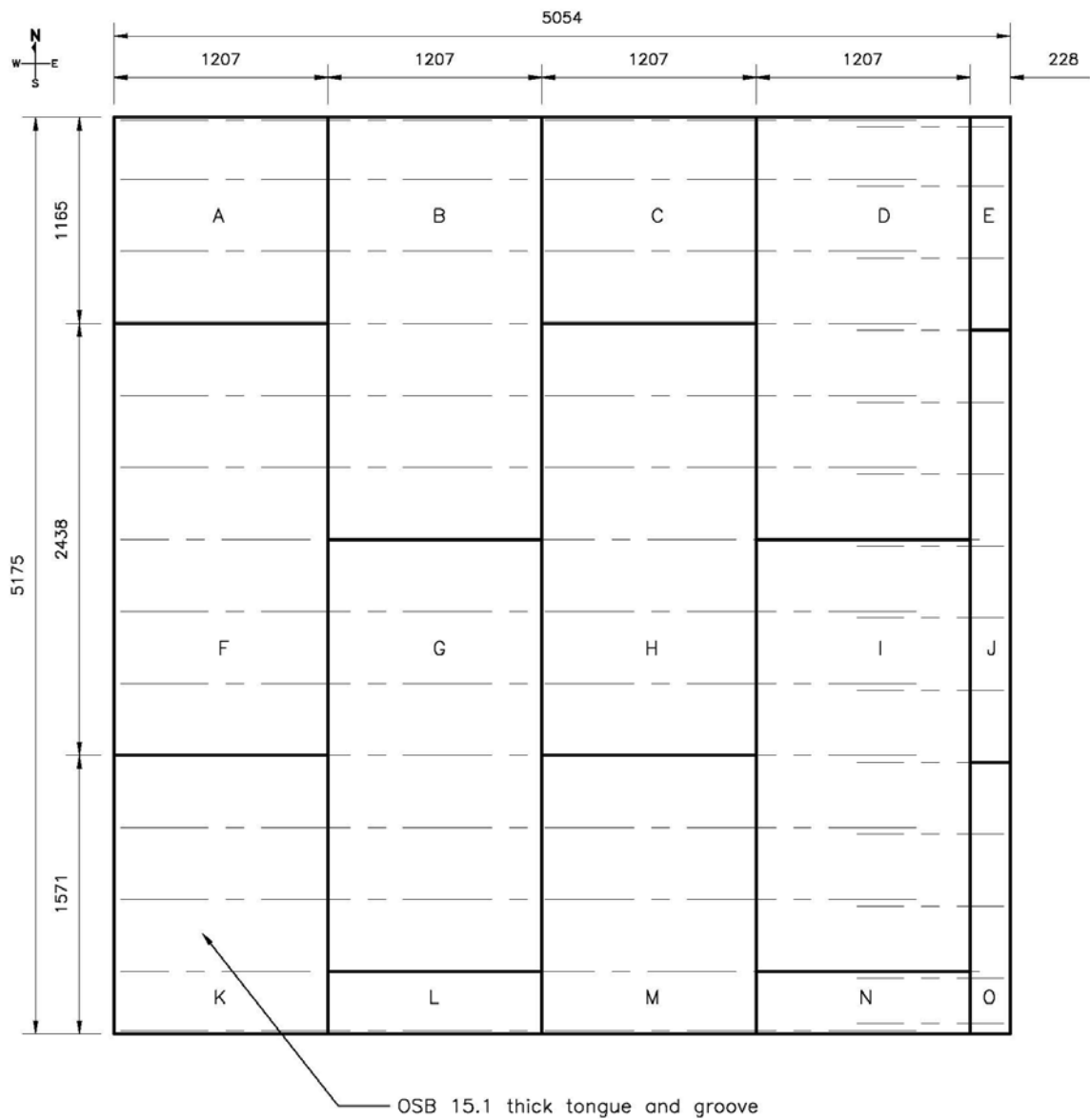


**Figure 15. Subfloor layout** (all dimensions in mm).

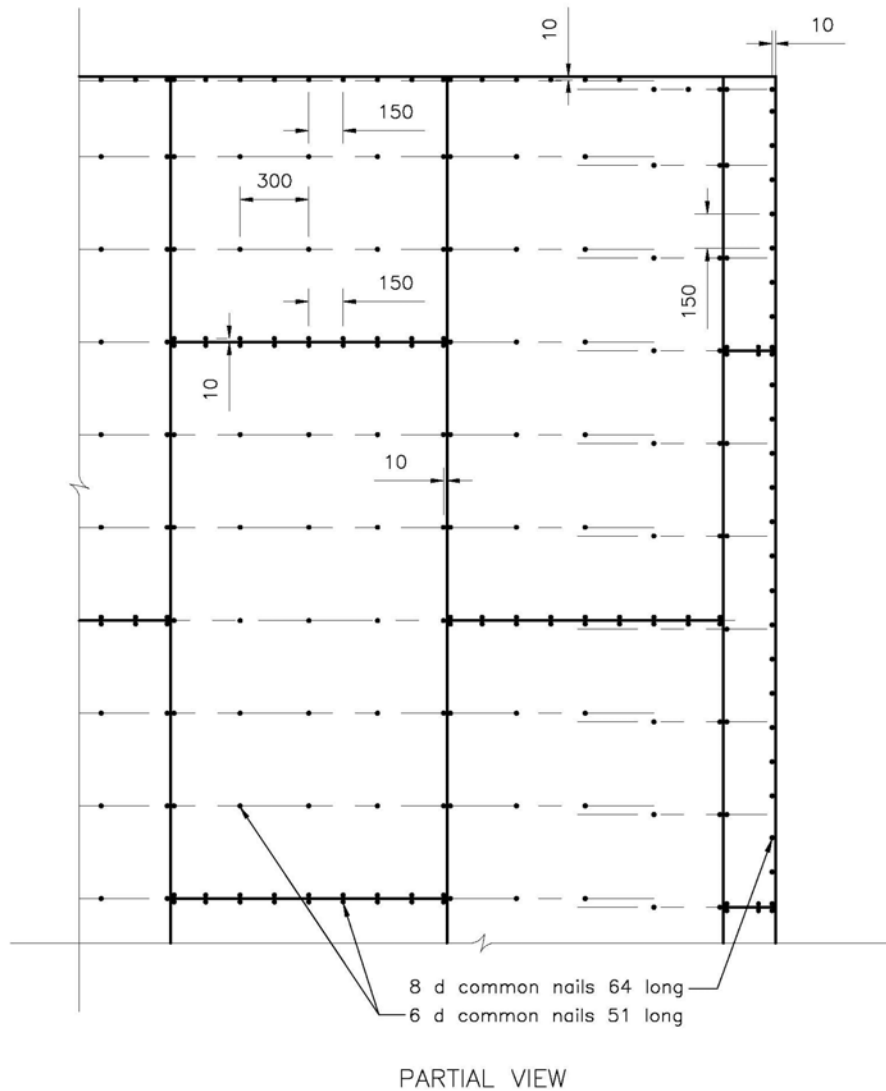


**Figure 16. Subfloor nail pattern and nail description** (all dimensions in mm).

## 2.8 Instrumentation of the Floor Assemblies

### 2.8.1 Temperatures in the Floor Assemblies

Ninety-seven Type K (20 gauge) chromel-alumel thermocouples, with a thickness of 0.91 mm, were used for measuring temperatures at a number of locations throughout each assembly. The thermocouple locations on the unexposed and exposed sides of the assemblies are shown in Figure 17 and Figure 18. These locations were chosen to monitor the conditions of the assembly at critical locations during the fire tests.

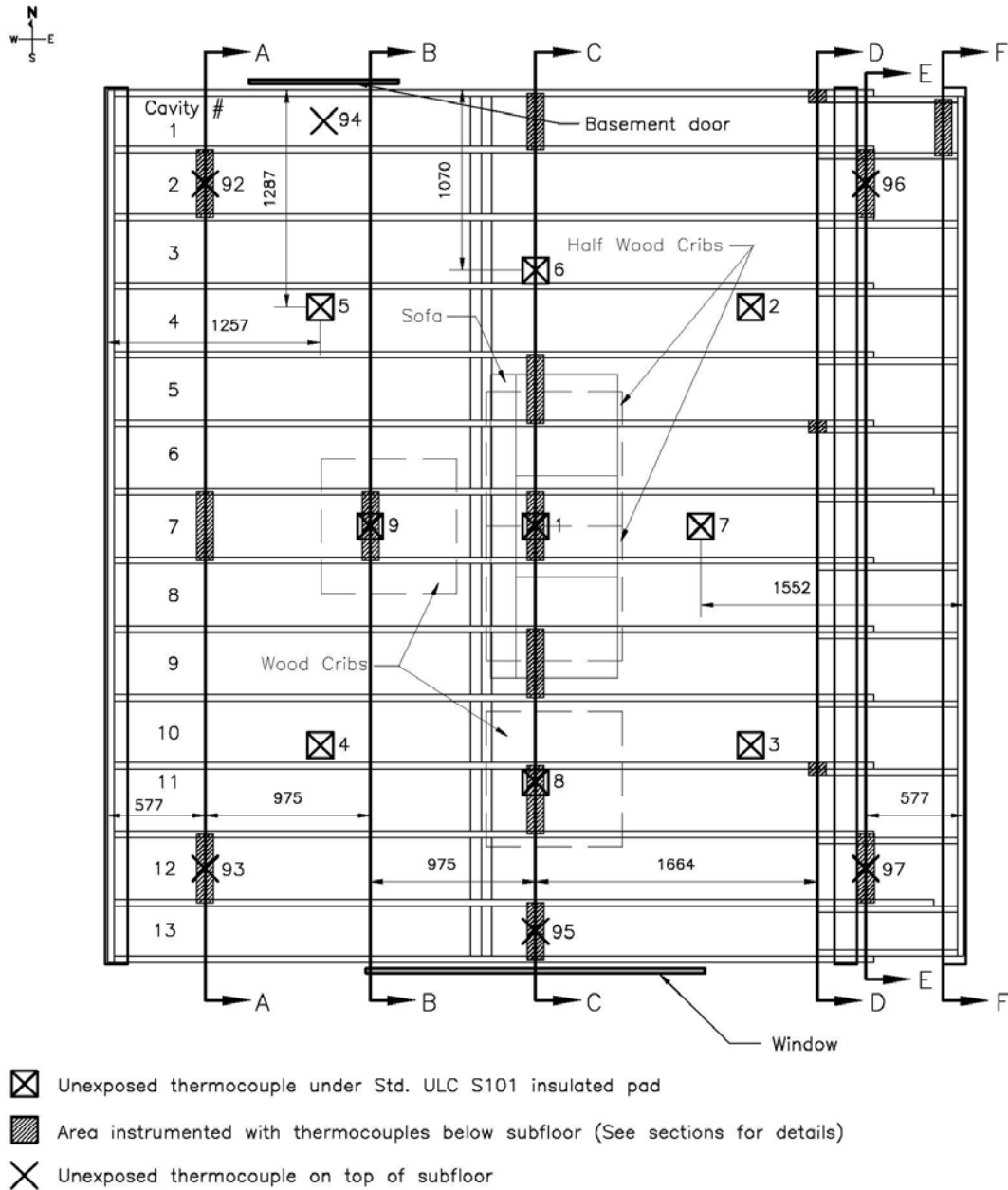


**Figure 17. Thermocouples locations** (all dimensions in mm).

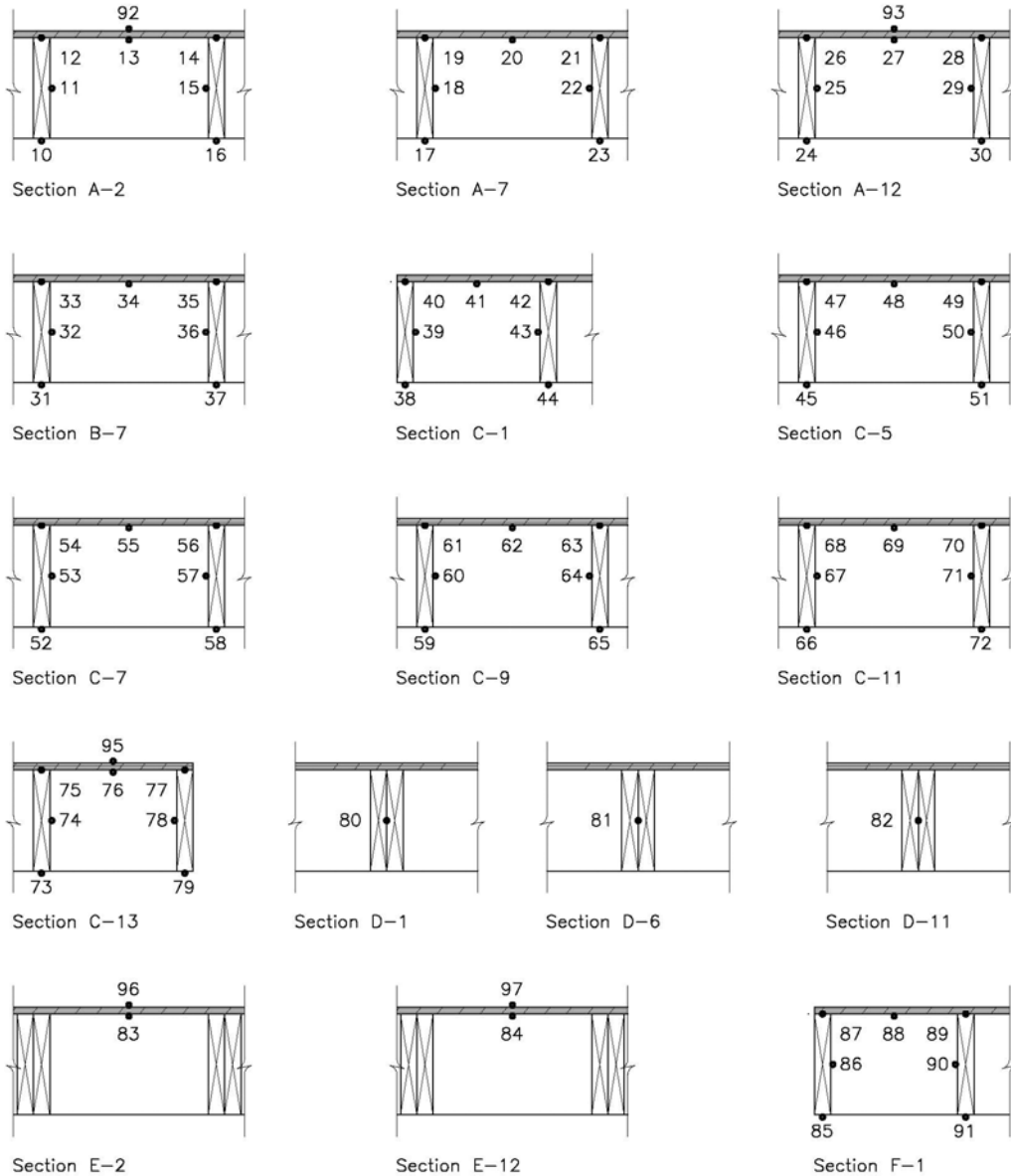


**Figure 18. Thermocouples locations reflecting the different sections shown in Figure 17**

## 2.8.2 Flame Penetration through the Floor Assemblies

Flame penetration through the floor assembly is considered to be an initial indicator of the impending failure of the assembly. For test UF-01, cameras on the first storey were used to observe the flames penetrating through the floor. However, the visibility during the test was too poor for the cameras to see the flame penetration; consequently, a device was developed and used for the remaining tests to better determine the time for flames to penetrate the floor. The special device consisted of a wire mesh placed at 3 locations on the unexposed surface of the floor assembly, specifically at three of the

tongue and groove joints, as shown in Figure 19. A detailed description of the device is provided in reference [8]

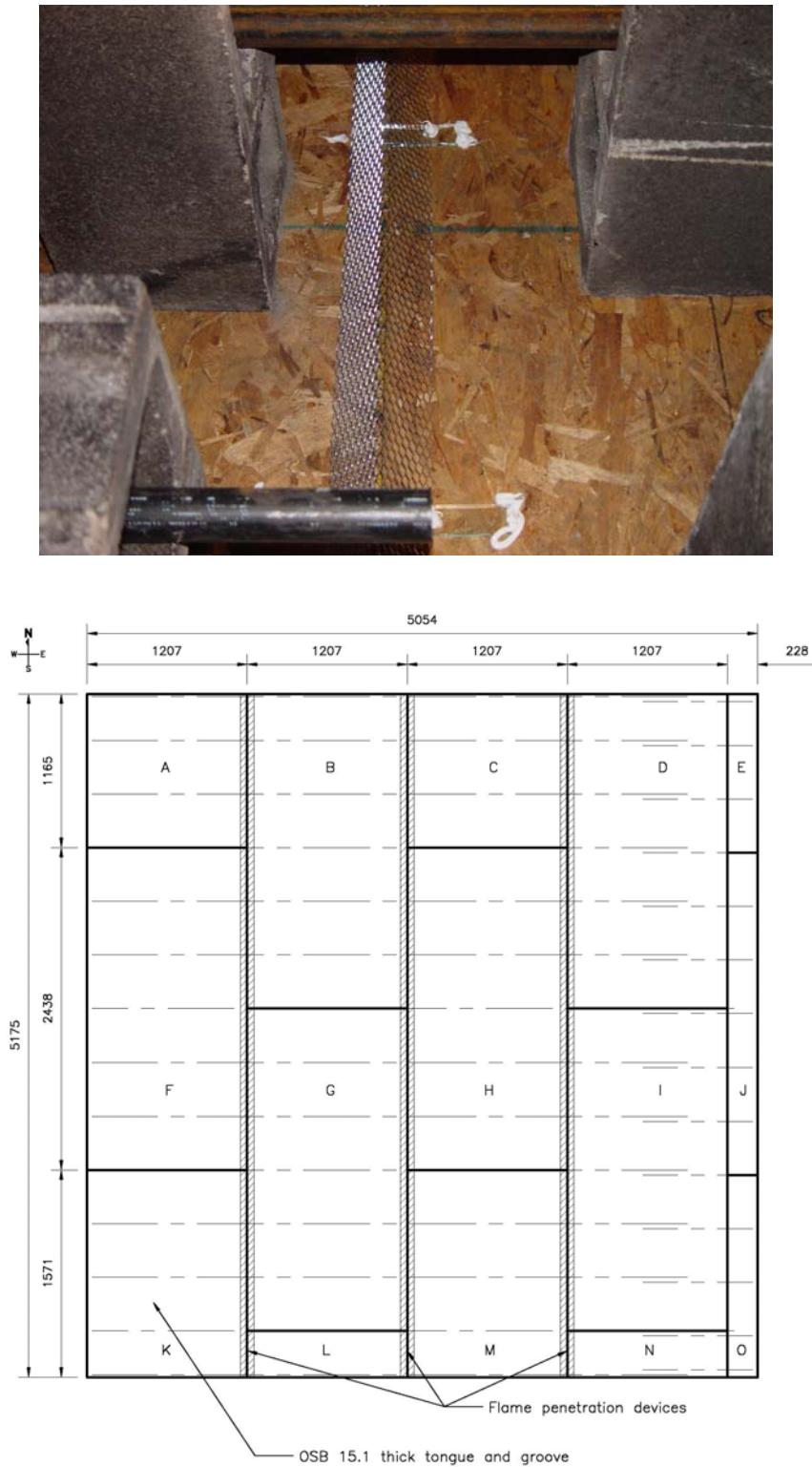


**Figure 19. Wire mesh device to detect flame penetration** (all dimensions in mm).

### 2.8.3 Deflection of the Floor Assemblies

The floor deflection was measured at 9 points. The measurement technique utilized 9 rods that were touching the tops of 9 concrete blocks placed on the unexposed surface of the floor assembly at the locations shown in Figure 20. This ensured that the downward movement of the subfloor was monitored during the fire exposure. The deflections were recorded using an electro-mechanical method described in Reference [9].

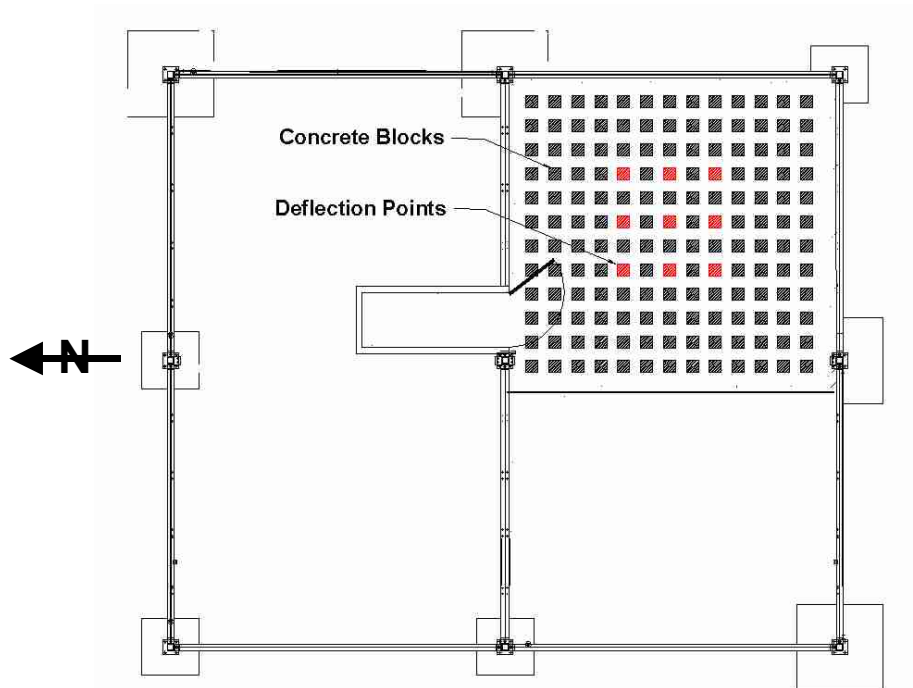


**Figure 20. Loading blocks and locations of the deflection measurement points on the unexposed side of the floor**

## 2.9 Loading of the Floor Assemblies

The load applied on the floor assemblies was equal to the self-weight (dead load) of the assembly plus an imposed load (live load) of 0.95 kPa (i.e., half of that prescribed by the NBCC [1] for residential occupancies, i.e., half of 1.90 kPa). The rationale to use this combination was based on the fact that in a fire situation, only part of the prescribed load is available. In fact, a number of international standards (Eurocode [10], New Zealand and Australian standards [11 and 12], and ASCE [13]) use a load combination similar to the one used in this study for fire design purposes. The total imposed load applied to the floor was equal to 0.95 kPa multiplied by the floor area; this is equivalent to approximately 25 kN.

The loading method consisted of 144 hollow concrete blocks (totalling 2490 kg) distributed uniformly on the floor as shown in Figure 20. The blocks were 190 x 190 x 390 mm (nominal 8" x 8" x 16") and weighed 17.3 kg each. To prevent the blocks from falling into the basement and causing any damage, a restraining system was designed using a series of pipes attached to beams on both ends, which were secured to the steel frame of the 3-storey house, as shown in Figure 21. The pipes were inserted through the hollow cores of the concrete blocks prior to the fire tests. The weight of the pipes was included in the total imposed load.

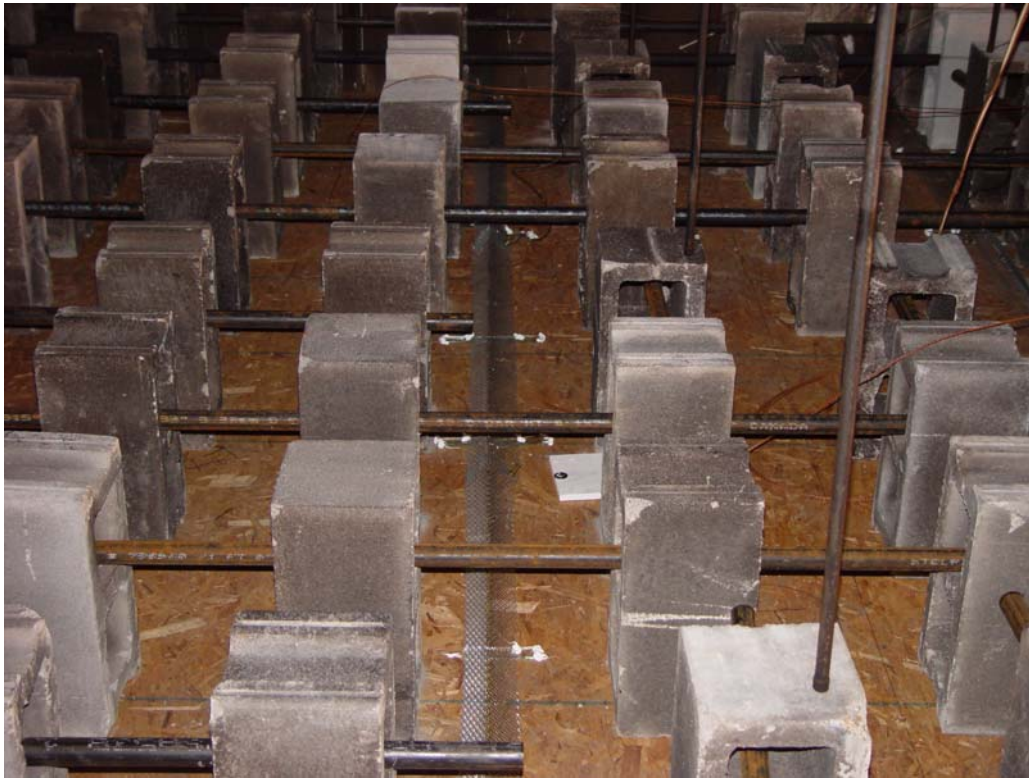


**Figure 21. Loading blocks restraining system**

Calculations of the maximum imposed loads (live load) that the floors were capable of supporting (based on the span used and production of maximum allowable bending stress/deflection, whichever applies, calculated in accordance with CAN/ULC-S101 standard [14]) indicate that these floors had a large strength reserve. The calculated reserves in %, based on comparison of the loading requirement with maximum imposed loads, which govern in this case, are shown in Table 1.

**Table 1. Reserve Live Load Capacity**

Test Number	Imposed load (kPa)	Maximum imposed load (kPa)		Reserve of live load capacity (governed by strength) (%)	Reserve of live load capacity (governed by deflection) (%)
		Strength	Deflection		
UF-01	0.95	4.28	2.83	78	66
UF-02	0.95	4.28	2.83	78	66

### **3 RESULTS OF THE TESTS**

#### **3.1 Recording of Results**

Compartments and floor assemblies were instrumented with smoke alarms, thermocouples, gas analyzers (CO, CO<sub>2</sub> and O<sub>2</sub>), smoke density instruments, pressure measurement instruments, and video cameras. The measurements of temperatures, gas concentrations, smoke density, and pressure were recorded at 5-second intervals using a Solotron data acquisition system.

In the following sections, discussions of the different recorded results are provided. Figures showing various quantities have been organized as follows:

- Figure 22 to Figure 36 show the test results for temperatures vs. time in the compartments, and at different openings (basement window opening, door opening to the basement, door opening to the outside), and at the top of the stairs (between the basement and first storey, and between the first and second storeys).
- Figure 37 and Figure 38 show the test results for temperatures vs. time on the unexposed side of the floor assemblies
- Figure 39 and Figure 40 show the test results for temperatures vs. time on the exposed side of the floor assemblies
- Figure 42 and Figure 43 show the test results for deflection vs. time on the unexposed side of the floor assemblies
- Figure 45 shows the results from the flame-sensing devices.
- Figure 46 to Figure 55 show the smoke and gas measurement results (CO, CO<sub>2</sub>, O<sub>2</sub> and optical density) and tenability conditions vs. time in the compartments
- Figure 56 and Figure 57 show the test results for the sequence of fire events in Tests UF-01 and UF-02.

Although velocity measurements were recorded at various openings during the experiments, they are not discussed in this report. However, these results may be useful for fire modeling purposes in the future.

#### **3.2 Observations and Recordings**

Table A 1 and Table A 2 show the test summary for UF-01 and UF-02, respectively. This includes a short description of the tests, the times for various events, and the detection times for all smoke alarms that operated. The tests were stopped after indications of either the structural or load-bearing failure of the floors.

#### **3.3 Time-temperature Curves at Different Locations**

##### **3.3.1 Temperatures in the Compartments**

In the following sections, the temperatures in the basement, first storey, and second storey are discussed. All thermocouple trees provided measurements at 0.4, 0.9, 1.4, 1.9 and 2.4 m above the floor level. Figure 22 to Figure 27 show these temperatures.

### 3.3.1.1 Basement level

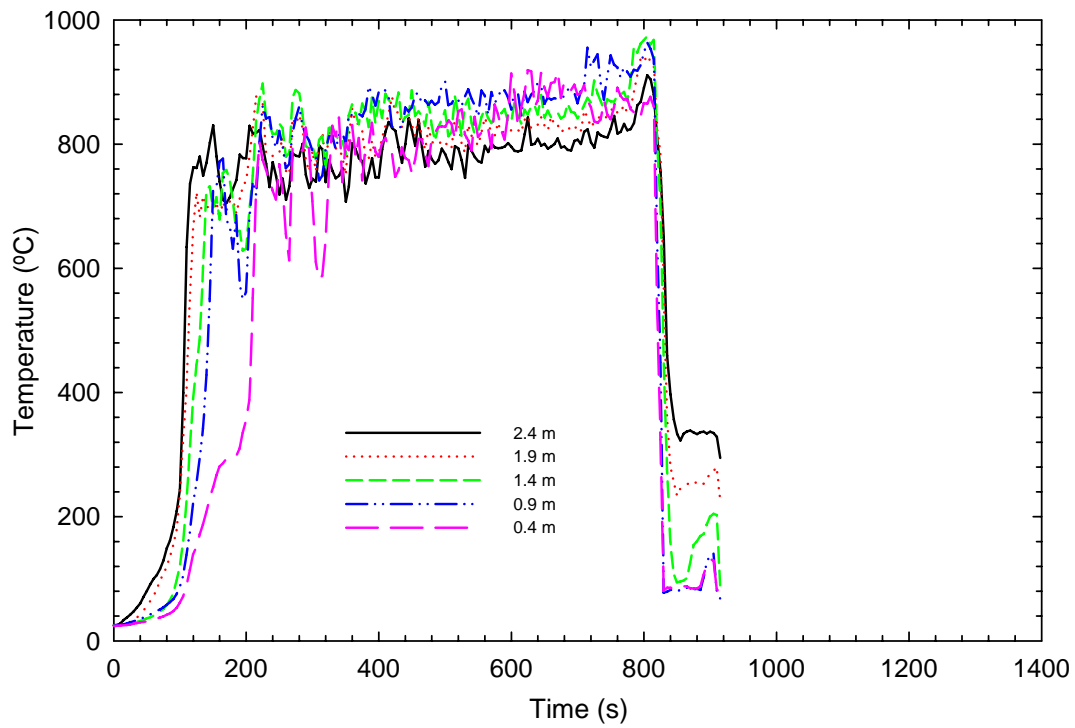
Figure 22 and Figure 23 (a, b, c, and d) show the temperatures in the basement fire compartment at the 4 room quarter points, southeast (SE), southwest (SW), northeast (NE) and northwest (NW), respectively.

In the case of UF-01 (open basement doorway), Figure 22, the temperatures rose to a maximum of 700 to 800°C in the first 120 s. The initial peak temperature was likely due to the high rate of heat release from the mock-up sofa near its peak burning rate. As shown in the figures, the initial temperature rise was faster at the 2.4 m height than the other heights because the hot smoke layer formed first at the ceiling and flames also impinged on the ceiling.

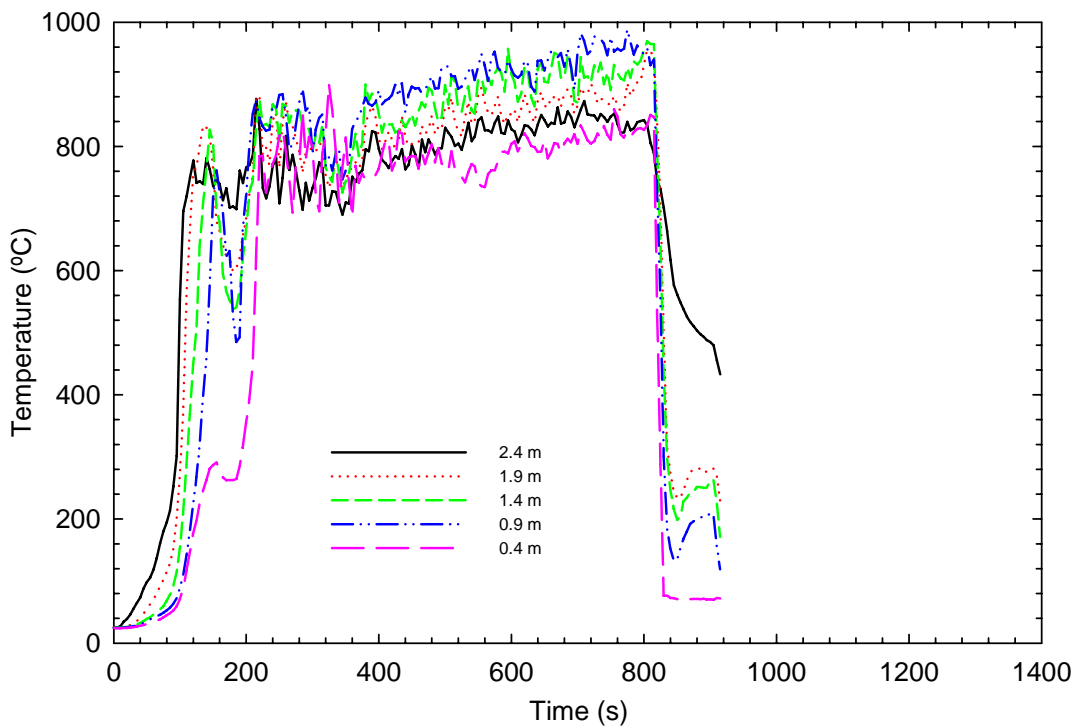
Just after the maximum temperature was reached, there was a slight decrease in temperatures likely due to the combined effect of opening the basement window at 105 s and the fact that a significant portion of the polyurethane foam component of the fuel package had been consumed. The temperatures decreased further after the exterior door was opened, which created a movement of air and smoke between the basement and first storey. The fresh air coming from the basement window also increased the combustion of the wood cribs and the exposed floor assembly, which caused the temperatures to begin increasing steadily again, reaching a maximum temperature of just under 1000°C.

During the fully-developed phase of the fire, temperatures were lower at the higher level likely due to flow stagnation at the surface and the conductive heat losses through the floor assembly. Finally, the temperatures started decreasing again just after 800 s when the blocks started falling through the floor and the fire was extinguished using sprinklers.

It should be noted that the first peak in the temperature (due to the mock-up sofa burning) was lowest in the case of the NE tree. This may be partially attributed to the fact that the NE corner was the least impacted by the fire, as it was farthest away from the fire source and that most of the hot gases were moving to the upper storeys through the SE to NW path.

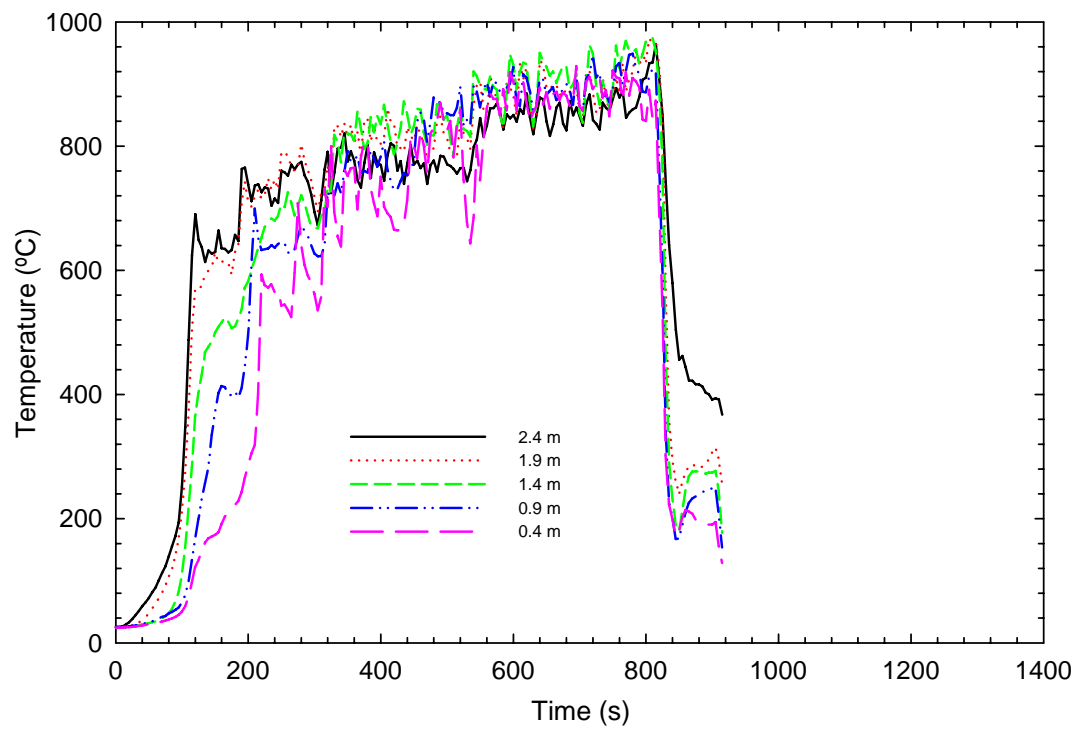


a) Basement SE quadrant

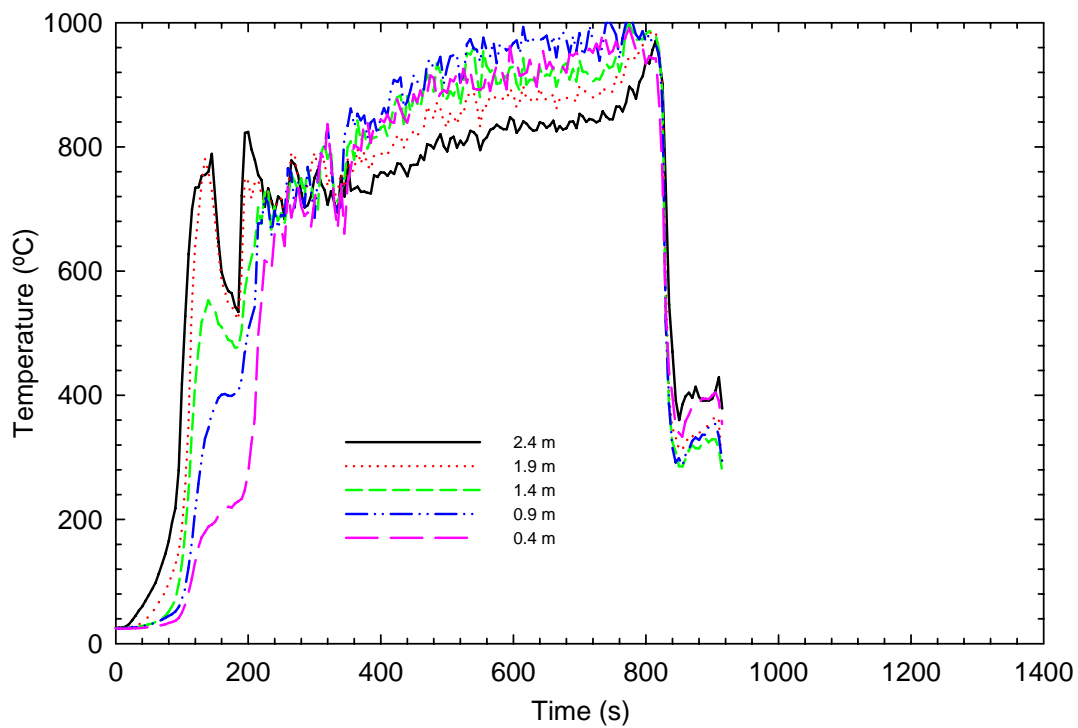


b) Basement SW quadrant

**Figure 22 (a and b). TC Trees in the basement for UF-01**



c) Basement NE quadrant

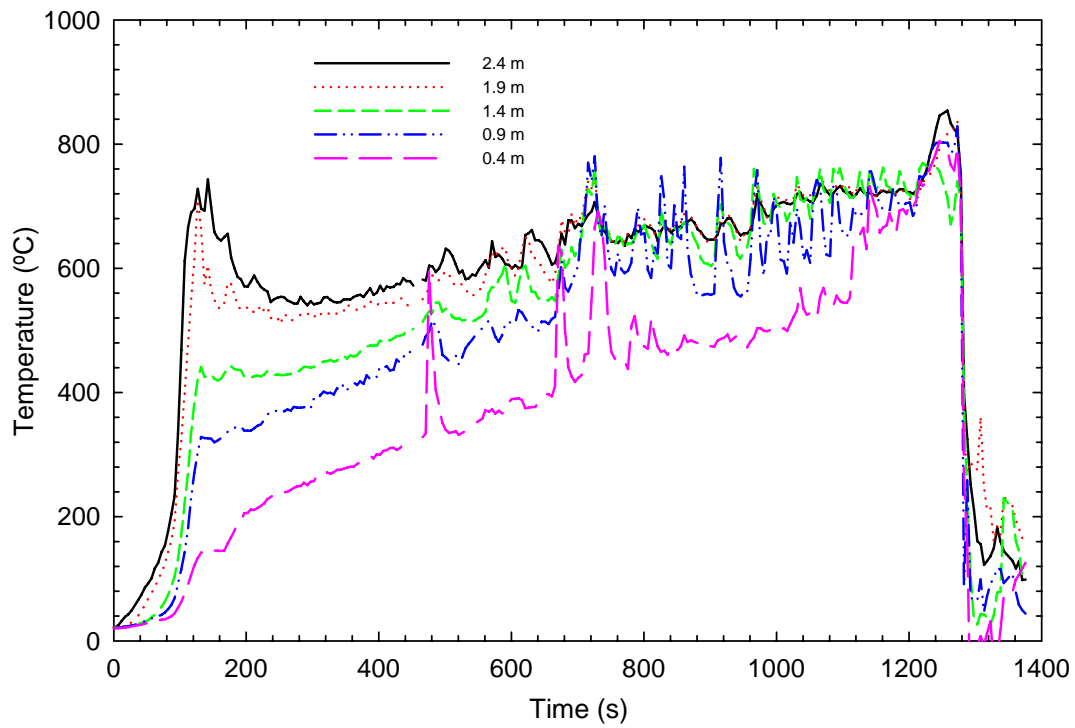


d) Basement NW quadrant

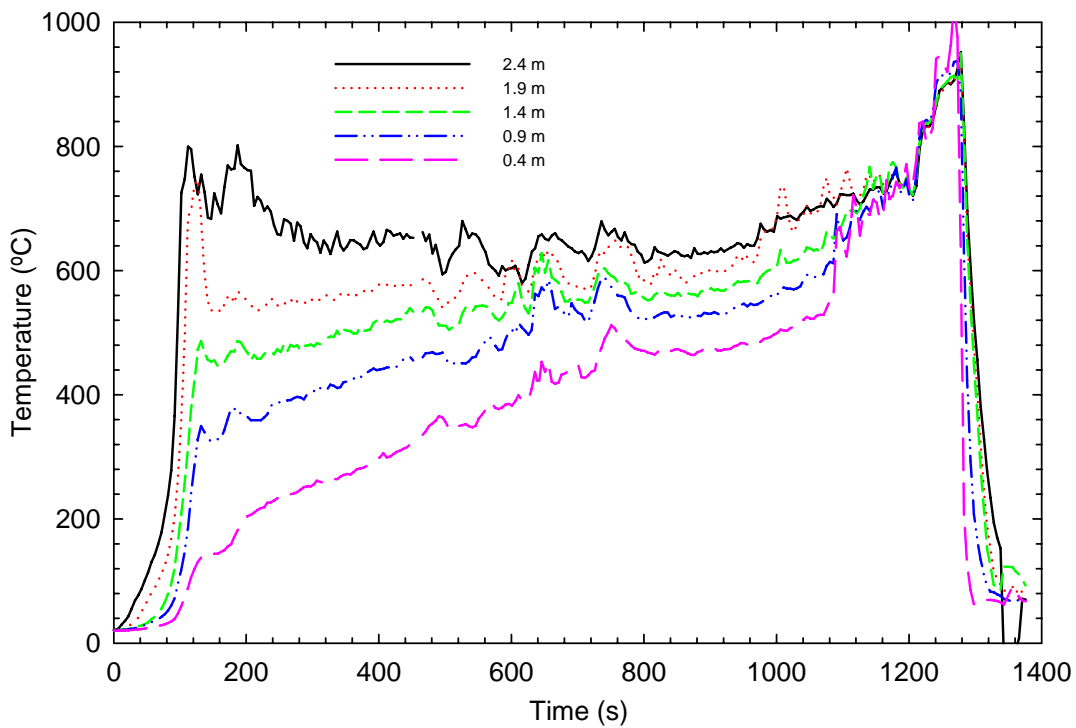
**Figure 22 (c and d). TC Trees in the basement for UF-01**

For the case UF-02 (wood joist floor - scenario with door closed), Figure 23, the trend was similar to UF-01. There was an initial steep increase in temperatures in the first 120 s followed by an appreciable decrease due to the combined effect of opening the basement window and depletion of the polyurethane foam component of the fuel package. A sustained gradual temperature rise followed as the wood crib fire increased. In this test, compared to the results in test UF-01, the temperatures at the different heights were more clearly distinguished from each other until very late in the fire. The peak temperature during the burning of the mock-up sofa was higher than the temperatures reached during the burning of the wood cribs and floor assembly during the first 1100 s. Beyond this time and close to 1200 s, the wood elements of the fuel package and floor assembly were burning intensely and the temperatures reached higher values (exceeding 750°C). After about 1200 s, the temperatures measured at the thermocouple tree locations showed the highest values. This may be due to the flames penetrating through the floor, creating holes, and allowing the air to increase the combustion in that region. The temperatures started decreasing around 1240 s when the blocks started falling through the floor and the test was terminated by extinguishing the fire using sprinklers.

For both UF-01 and UF-02, the combustion was dominated by the mock-up sofa during the first 120 to 180 s, while the wood cribs and floor assembly, including the subfloor, provided the fuel for combustion after this period. The duration of the fire was shorter for UF-01 compared to UF-02 because the availability of more air in Test UF-01 resulted in faster and more efficient combustion. For UF-02, combustion air was limited until late in the test.

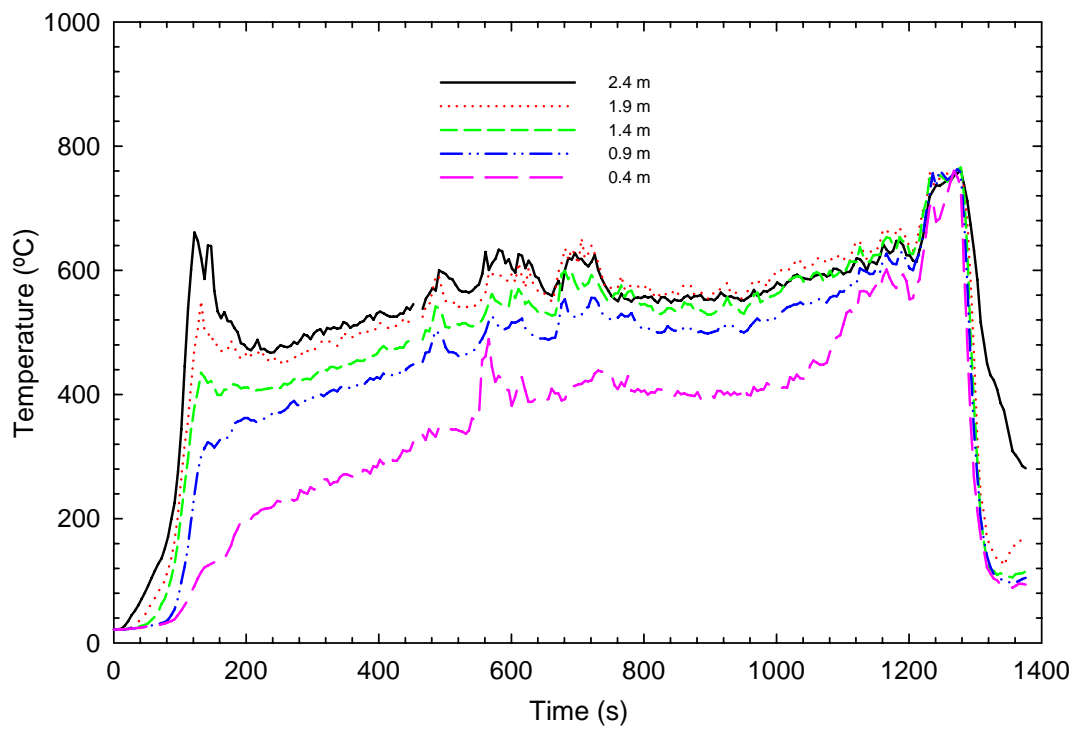


a) Basement SE quadrant

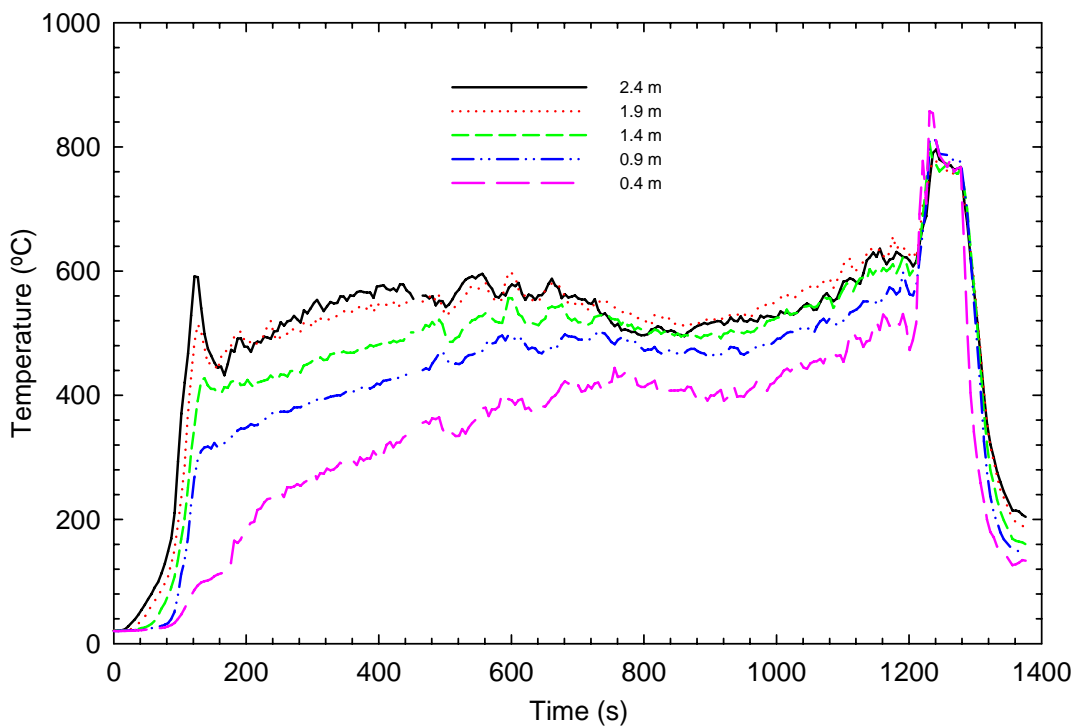


b) Basement SW quadrant

**Figure 23 (a and b). TC Trees in the basement for UF-02**



c) Basement NE quadrant



d) Basement NW quadrant

**Figure 23 (c and d). TC Trees in the basement for UF-02**

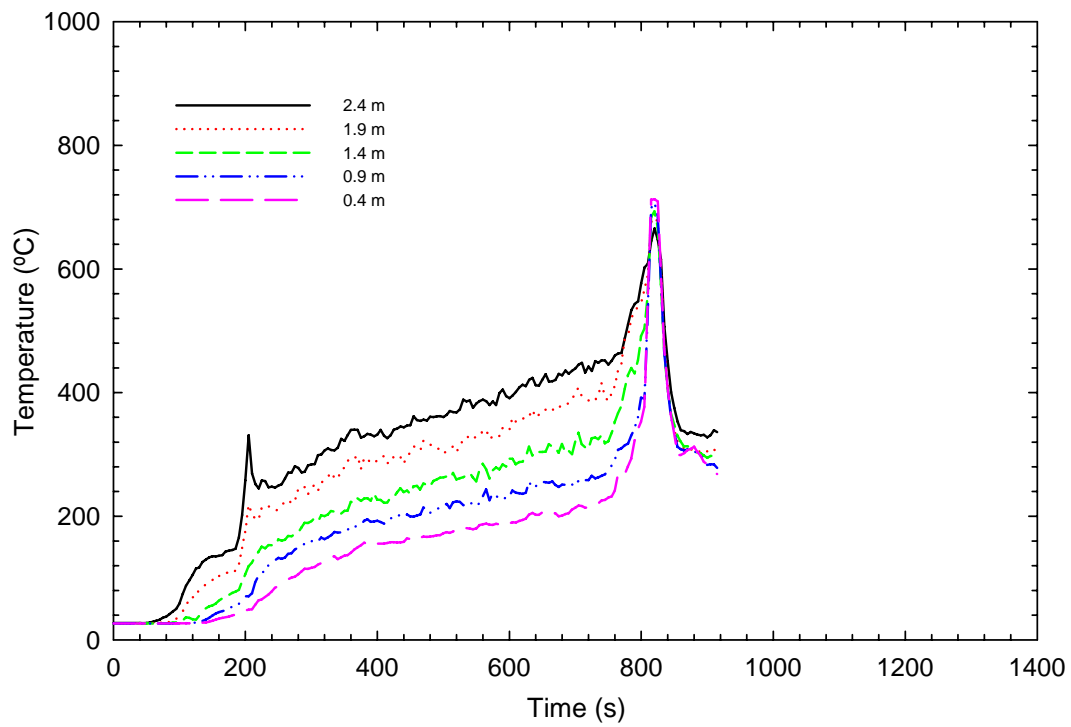
### 3.3.1.2 First storey

Figure 24 and Figure 25 (a, b, c and d) show the temperatures measured at the thermocouple tree locations in the first storey at the 4 compartment quarter points, SE, SW, NE and NW, respectively.

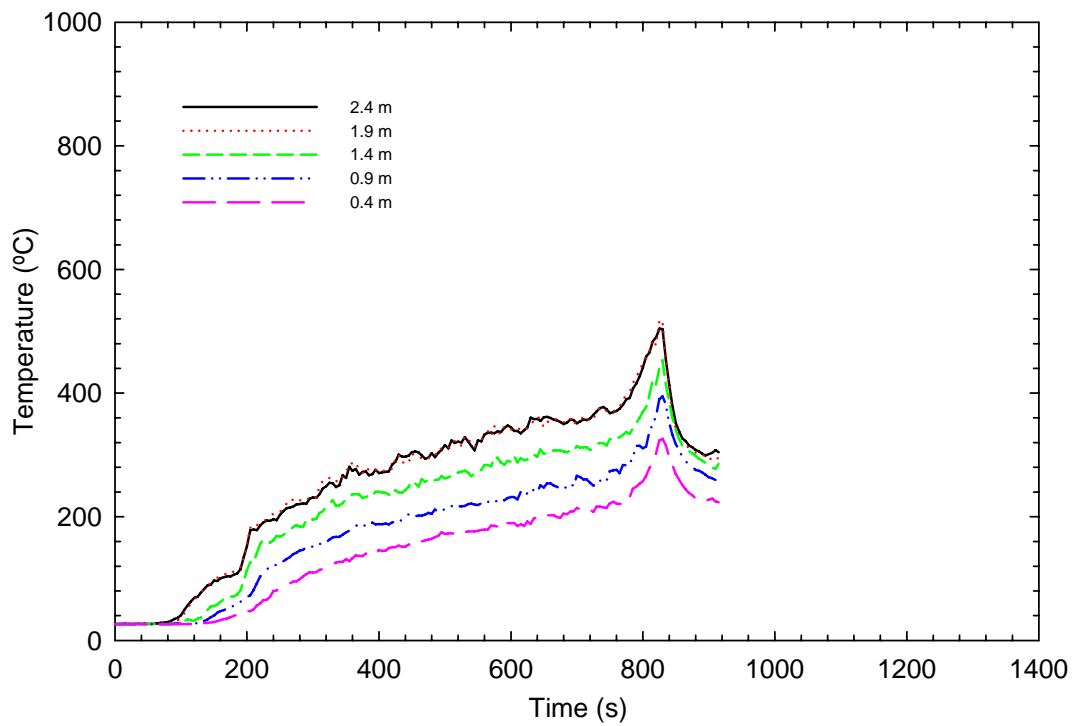
In the case of UF-01 (open basement doorway), Figure 24, the temperatures steadily increased due to the heating of the floor from below and from the hot gases and smoke migrating from the basement to the first storey through the stairway and the basement door opening. The highest temperatures were recorded at the SE thermocouple tree because the fire in the basement fire compartment was just underneath this tree. The temperatures measured at the other thermocouple trees were comparable. At around 760 s, there was a sharp increase in temperatures at the four room quarter points, an indication that flame had penetrated through the floor. The peak temperatures were 700, 500, 420 and 380°C for SE, SW, NE and NW, respectively. After about 830 s, the temperatures decayed because of the extinguishment of the fire.

In the case of UF-02 (closed basement doorway), Figure 25, the temperatures increased very slowly mainly because the doorway was closed and the only source of heat being through the floor assembly from below. The migration of the hot gases and smoke to the first storey did not start until late in the test when openings started forming in the floor or from the burning of the basement door. The highest temperatures were recorded at the SE tree because the fire in the basement was positioned just under the location of this thermocouple tree. The temperatures measured at the other three thermocouple tree locations were comparable. At around 1160 s, all the trees showed a sharp increase in temperatures, which may be an indication that flames had penetrated through the floor. The peak temperatures were 850, 620, 640 and 400°C for SE, SW, NE and NW, respectively. After about 1240 s, the test was terminated; consequently the temperatures started decaying because of the extinguishment of the fire.

The temperatures recorded in the first storey for test UF-02 were much lower before flame penetration occurred than those recorded in UF-01. After flame penetration, temperatures in UF-02 showed a very sharp increase compared to UF-01. The peak values were also higher for UF-02 than UF-01.

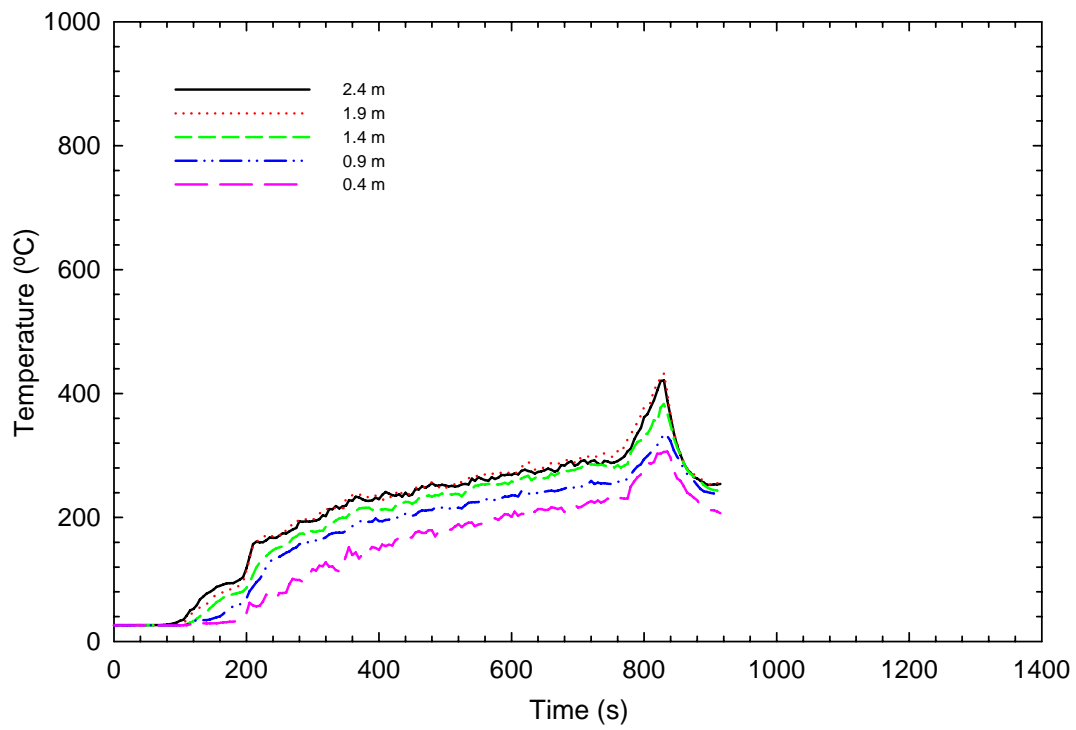


a) First Storey SE quadrant.

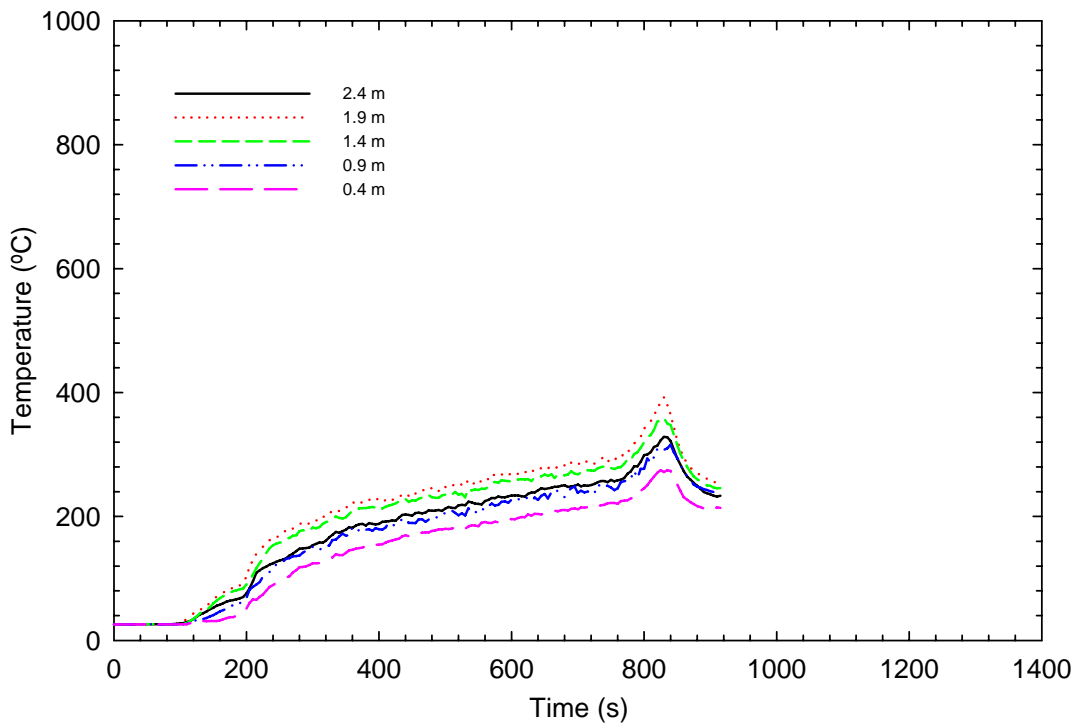


b) First Storey SW quadrant.

**Figure 24 (a and b). TC trees in the first storey for UF-01**

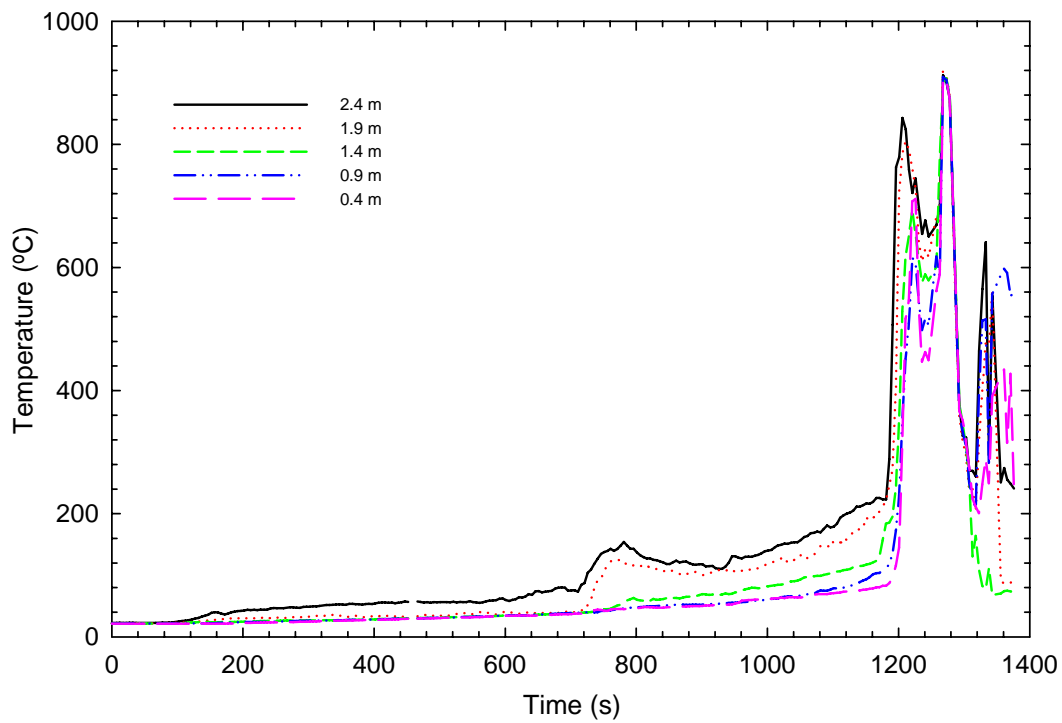


c) First Storey NE quadrant

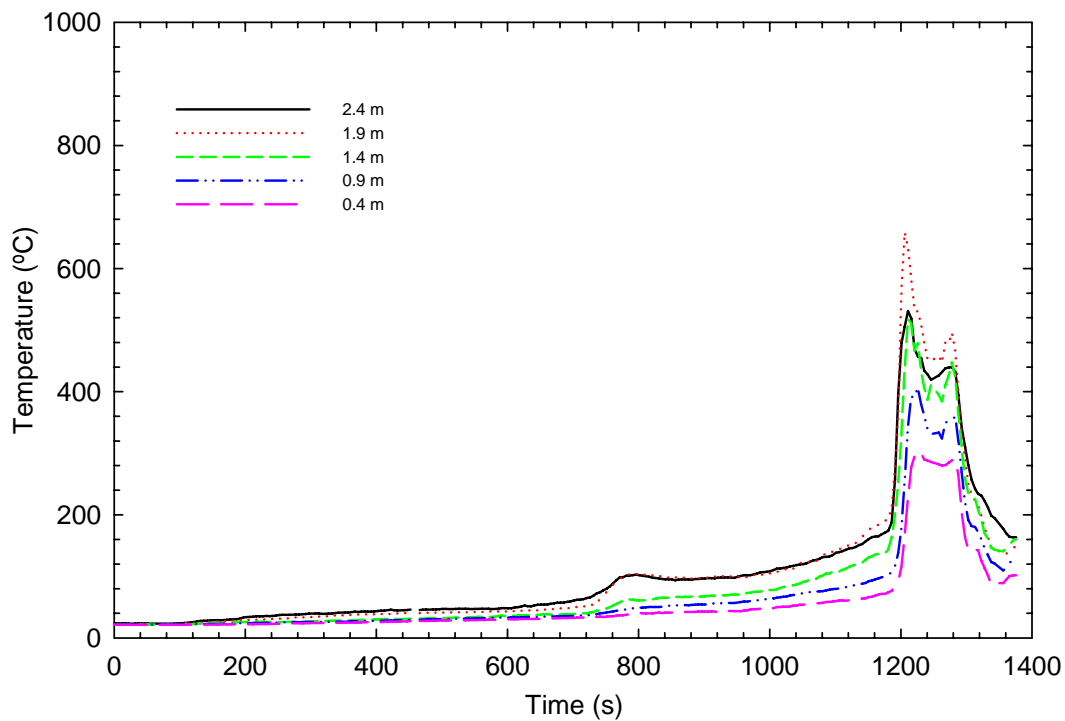


d) First Storey NW quadrant

**Figure 24 (c and d). TC trees in the first storey for UF-01**

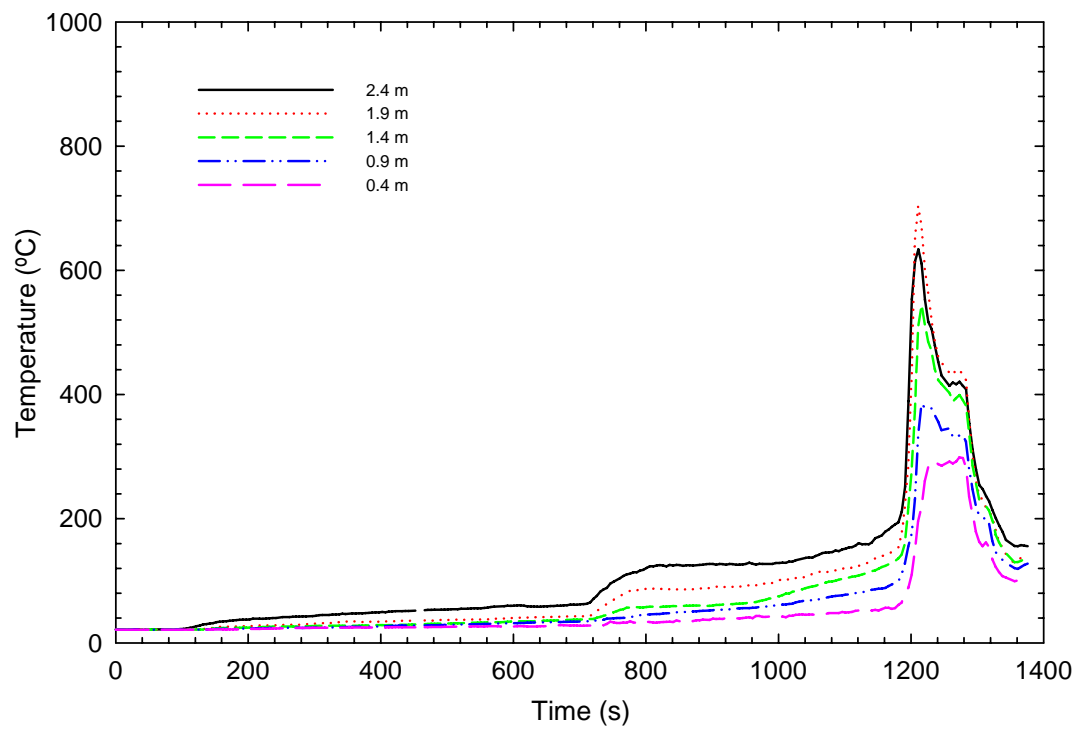


a) First Storey SE quadrant

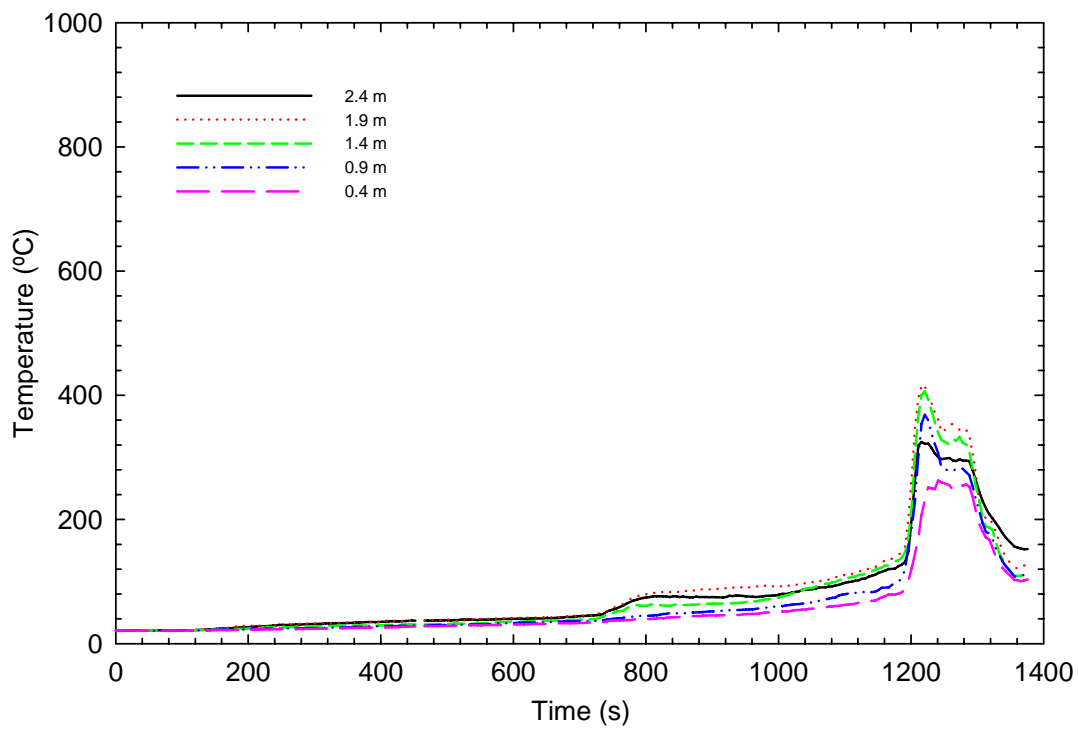


b) First Storey SW quadrant

**Figure 25 (a and b). TC trees in the first storey for UF-02**



c) First Storey NE quadrant



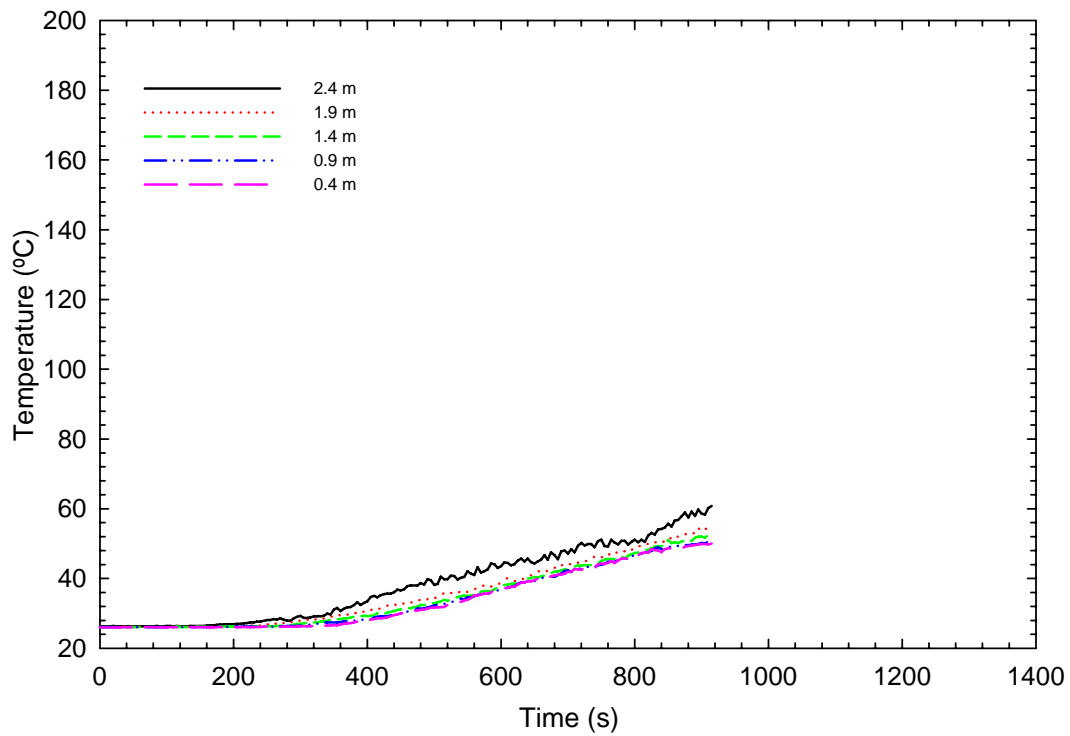
d) First Storey NW quadrant

**Figure 25 (c and d). TC trees in the first storey for UF-02**

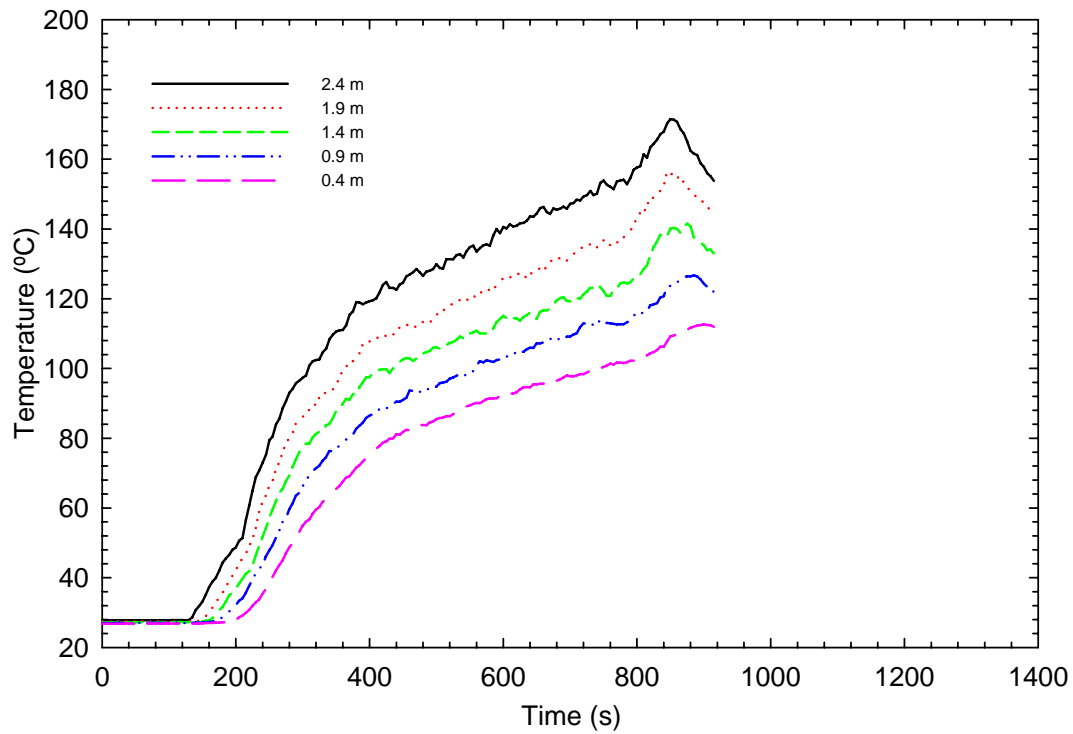
### 3.3.1.3 Second storey

Figure 26 (a) and Figure 26 (b) show the temperatures in the SE and SW bedrooms, respectively for Test UF-01. The door to the SE bedroom was closed while the door to the SW bedroom was open. Ambient temperature was measured for about the first 120 s. After this, the temperatures, at different heights within the room, started increasing. This increase was greater for the SW bedroom than the SE bedroom because more of the migrating hot gases and smoke entered the SW bedroom since the door was open. Smoke entered the SE bedroom mainly through gaps around the door. Maximum temperatures of about 60 and 170°C were reached at the 2.4 m height above the floor level for the SE and SW bedrooms, respectively. For the SW bedroom, the temperatures decreased after the extinguishment of the fire was initiated.

Figure 27 (a) and Figure 27 (b) show the temperatures in the SE and SW bedrooms, respectively for Test UF-02. The door to the SE bedroom was closed while the door to the SW bedroom was open. Ambient temperature was measured for about the first 800 s for the SE bedroom and 200 s for SW bedroom. After these times, the temperatures, at different heights within the rooms, started increasing. This increase was faster for the SW bedroom than the SE bedroom because more migrating hot gases and smoke entered the SW bedroom since the door was open. The smoke entered the SE bedroom mainly through gaps around the door. Maximum temperatures of about 50 and 165°C were reached at 2.4 m height above the floor level for the SE and SW bedrooms, respectively. For the SW bedroom, the temperatures showed a sudden increase around 1200 s, which may be due to flame penetrating into the first storey through the burning floor and the door to the basement, and then they started decaying after the extinguishment of the fire was initiated.

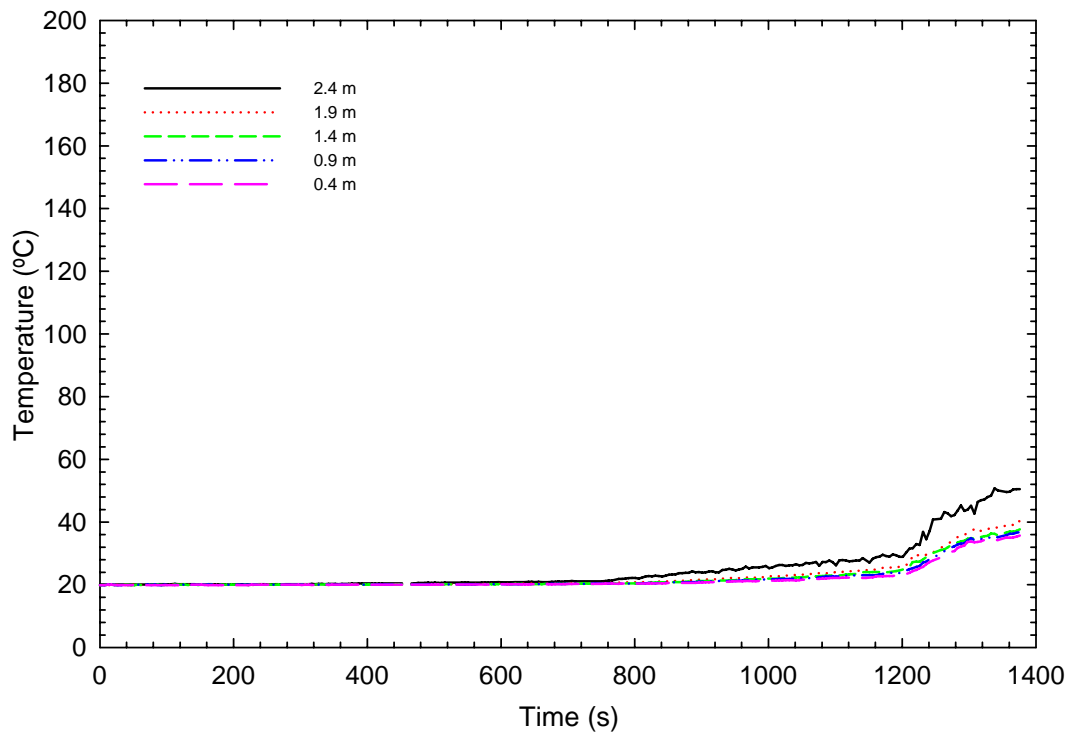


a) Second Storey SE bedroom

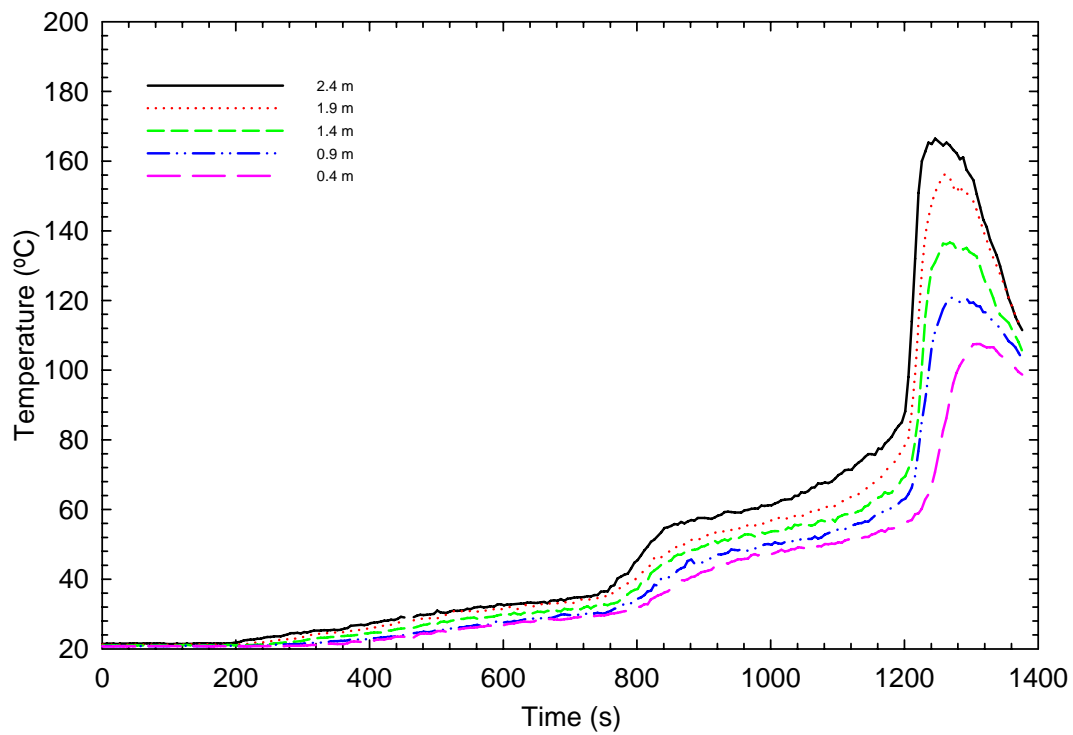


b) Second Storey SW bedroom

**Figure 26. TC trees in the second storey bedrooms for UF-01  
(SE bedroom: door closed; SW bedroom: door open)**



a) Second Storey SE bedroom



b) Second Storey SW bedroom

**Figure 27. TC trees in the second storey bedrooms for UF-02  
(SE bedroom: door closed; SW bedroom: door open)**

### 3.3.2 Temperatures at the Window in the Basement

Five thermocouples were located in the basement window opening. Three were located along the vertical centreline of the opening, 125 mm from the bottom, 250 mm from the bottom and 375 mm from the bottom, respectively. The remaining two thermocouples were located 375 mm up from the bottom of the opening and 500 mm in from each side of the opening.

Figure 28 and Figure 29 show the temperatures recorded at the basement window for Test UF-01 and Test UF-02, respectively. For both UF-01 and UF-02, the temperatures increased to 600°C in the first 110 s. The window was opened after 105 s and 97 s, for UF-01 and UF-02, respectively, when the temperature reached 300°C at the thermocouples. After 120 s, due to air entering and smoke exiting the basement through the window, the temperatures varied depending on whether or not the flames were touching the thermocouples (the bottom TC was probably below the neutral plane).

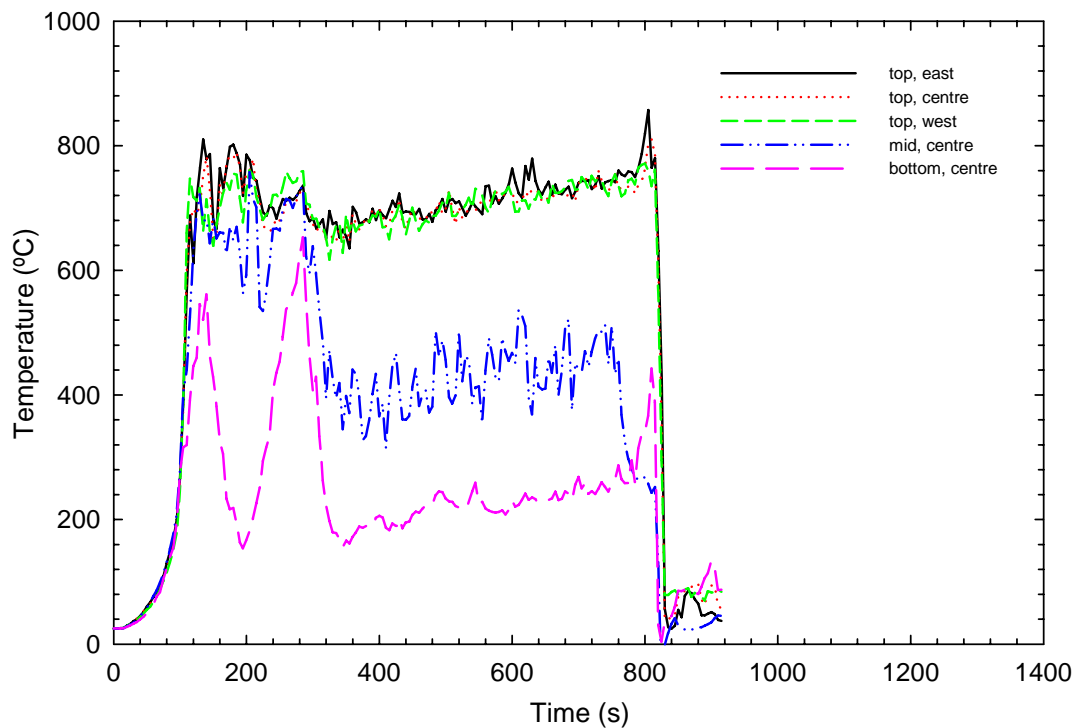


**Figure 28. Temperatures at the window in the basement for UF-01**

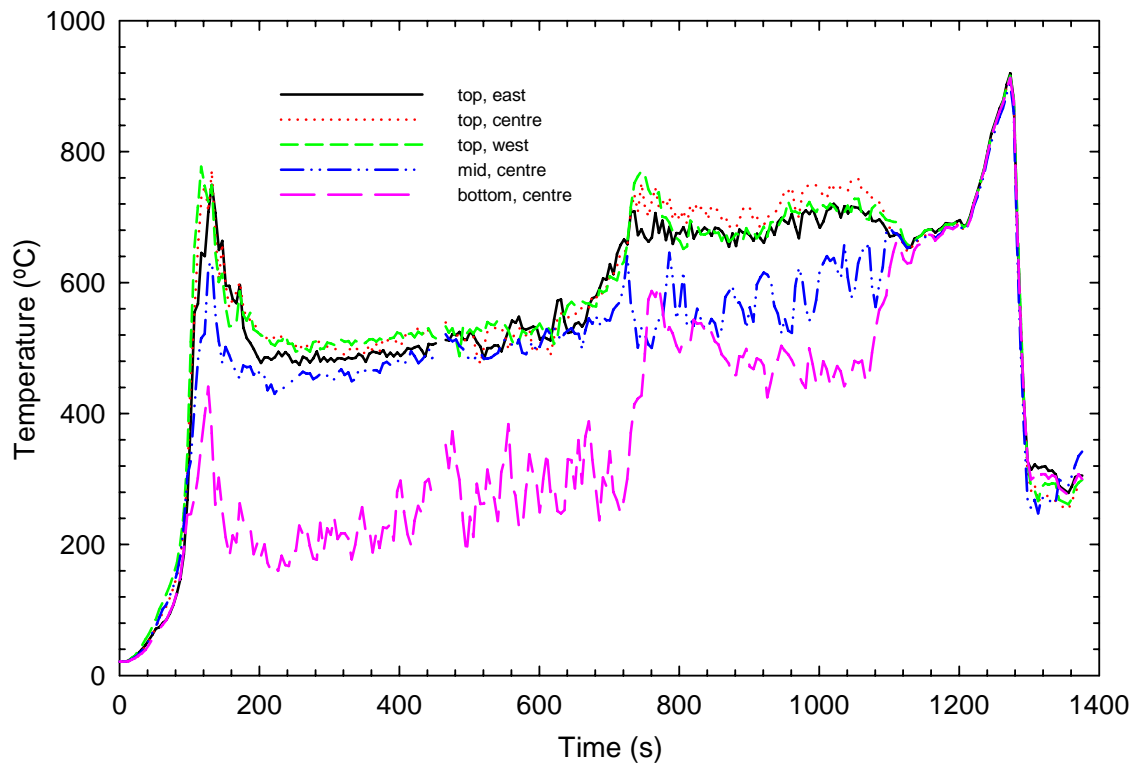


**Figure 29. Temperatures at the window in the basement for UF-02**

### 3.3.3 Temperatures at the Doorway to the Basement

The temperature at the doorway to the basement was measured for Test UF-02 only, since this test was conducted with the closed basement doorway. Figure 30 shows the temperatures of the exposed side [basement side] of the door at the centre and at three heights: 0.9, 1.4 and 1.9 m. The temperatures increased in the first 180 s to a maximum of about 200°C (due to rapid hot gas build up in the staircase opening), then there was a gradual increase to about 400°C between 200 and 800 s. The increase continued at a lower rate until 1200 s reaching a temperature of about 500°C. Just after 1200 s, the temperatures increased to a maximum 800°C at 1280 s. The last increase is an indication of the burning of the door when flames started penetrating through the burning floor and exposing the door on its initially unexposed side. The decay after 1280 s was due to the extinguishment of the fire.

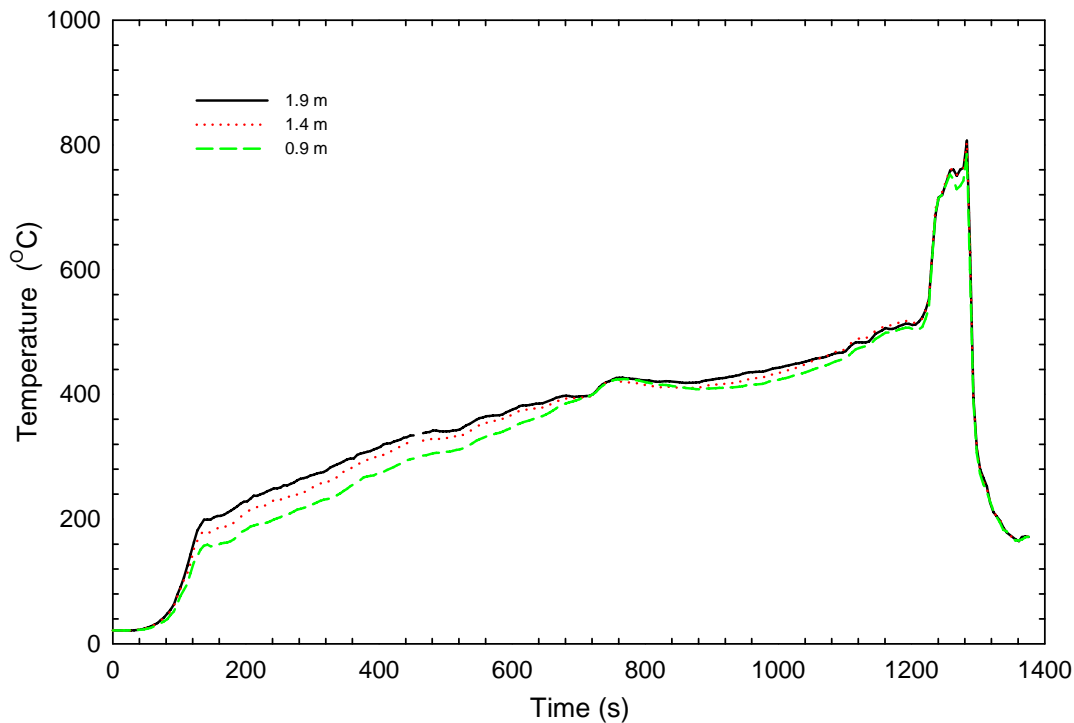
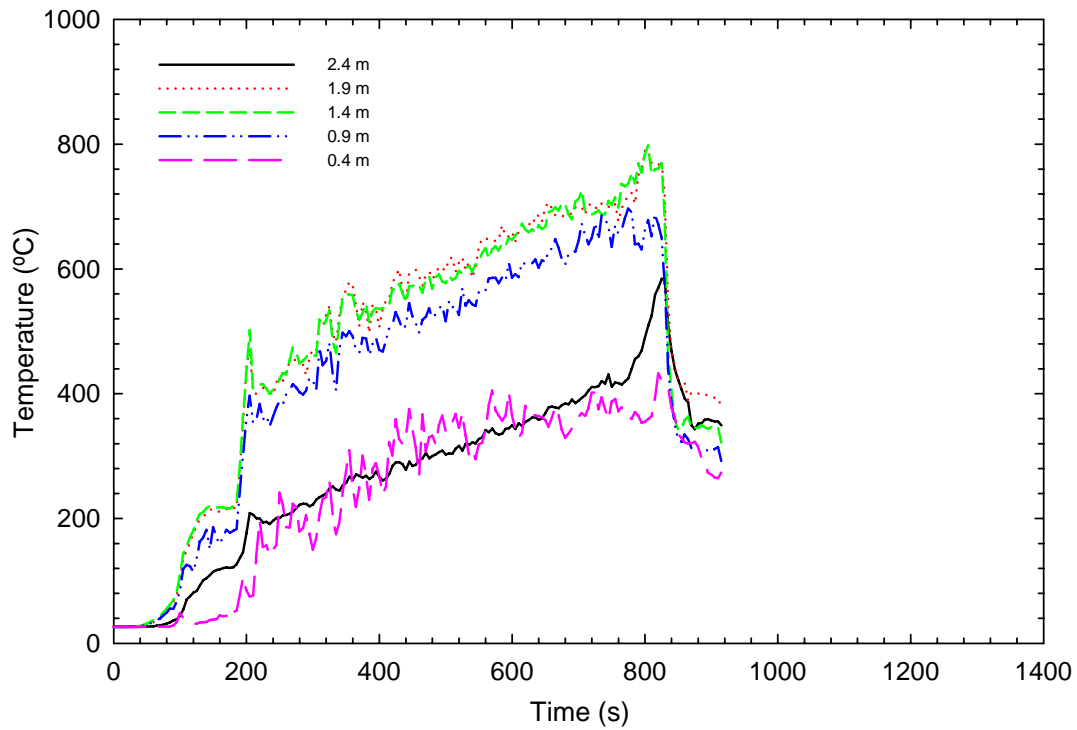


**Figure 30. Temperatures at the exposed side [basement side] of the basement door for Test UF-02**

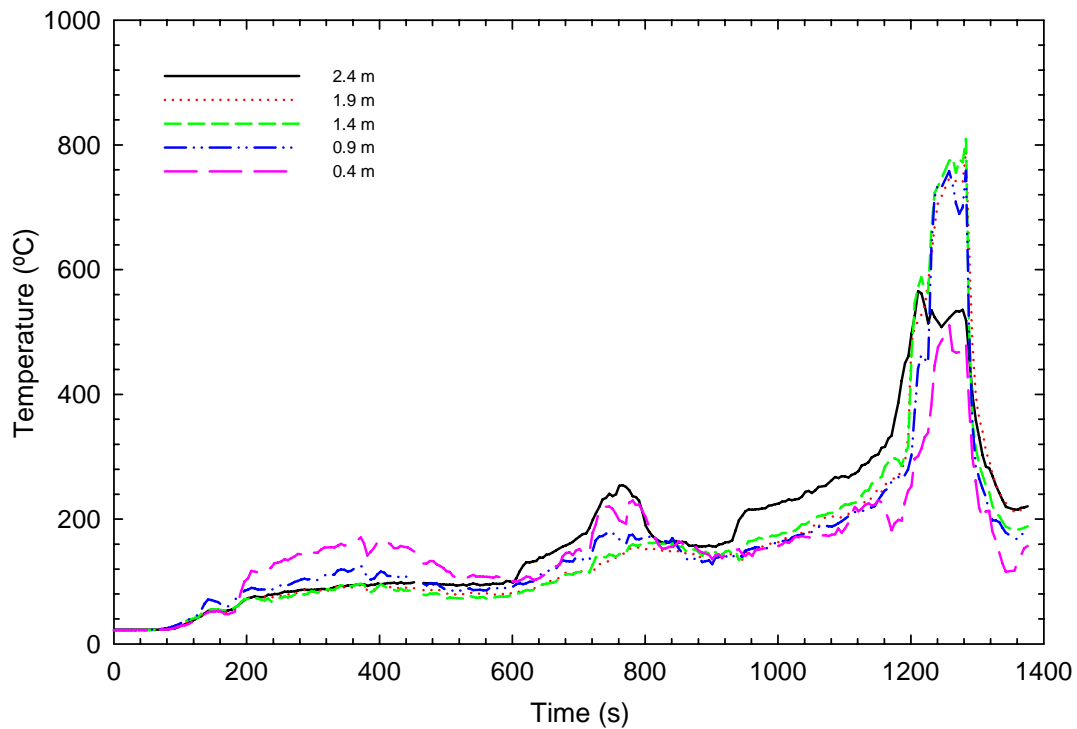
#### 3.3.4 Temperatures on the First Storey at the Top of the Stairs from the Basement

Figure 31 shows the temperatures at the top of the stairs on the first storey at different heights for Test UF-01. The conditions remained at ambient temperature for about the first 80 s. After this, temperatures, at different heights, started increasing due to the migration of hot gases and smoke from the basement to the upper storeys. A maximum temperature of about 800°C was reached at both 1.9 and 1.4 m heights but not at the 2.4 m level, probably indicating that cooler air was entering into the basement at both the upper level and lower level of the doorway. The temperatures started decaying around 800 s after the extinguishment of the fire was initiated.

Figure 32 shows the temperatures at the top of the stairs on the first storey at different heights for Test UF-02. The conditions remained at ambient temperature for about the first 120 s. After this time, the temperatures, at different heights, started increasing very gradually due to the migration of hot gases and smoke through gaps around the floor assembly. The temperatures showed a sudden increase at about 1200 s, which may be related to flame penetrating into the first storey through the burning floor, and then they started decaying around 1240 s after the extinguishment of the fire was initiated. A maximum temperature of about 800°C was reached.



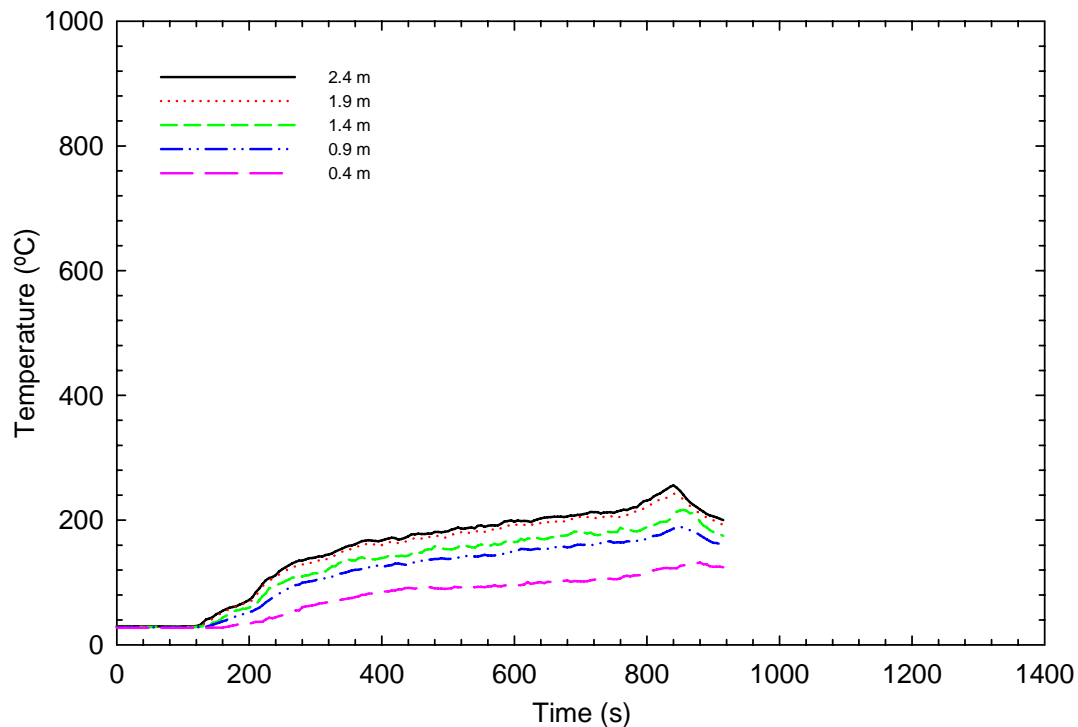
**Figure 31. Temperatures on the first storey at the top of the stairs from the basement for Test UF-01**



**Figure 32. Temperatures on the first storey at the top of the stairs from the basement [unexposed side of basement door] for Test UF-02**

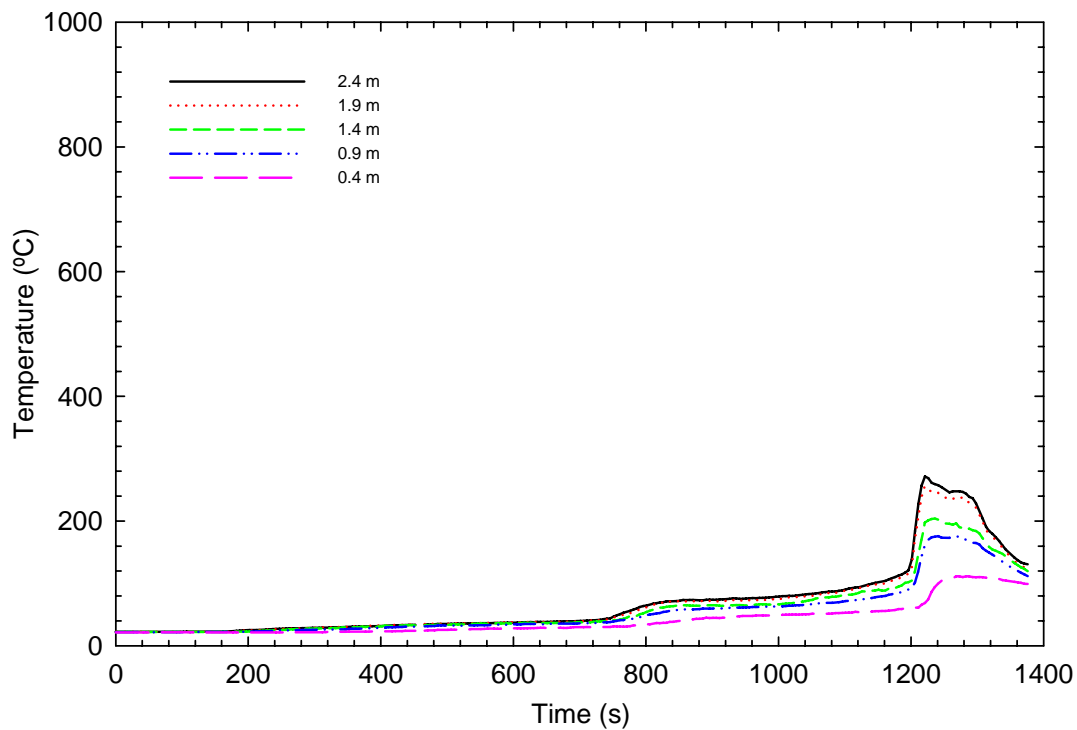
### 3.3.5 Temperatures on the Second Storey at the Top of the Stairs

Figure 33 shows the temperatures at the top of the stairs on the second storey at different heights for Test UF-01. The conditions remained at ambient temperature for about the first 120 s. After this, temperatures, at different heights, started increasing due to the migration of hot gases and smoke from the basement to the upper storeys. A maximum temperature of about 255°C was reached at the 2.4 m height. The temperatures started decaying around 840 s after the extinguishment of the fire was initiated.



**Figure 33. Temperatures on the second storey at the stairs for UF-01**

Figure 34 shows the temperatures at the top of the stairs on the second storey at different heights for Test UF-02. The trend was similar to the results for UF-01, but the temperatures measured during Test UF-02 were lower in the first 800 s. The conditions remained at ambient temperature for about the first 200 s. After this time, the temperatures, at different heights, started increasing very gradually due to some migration of hot gases and smoke mainly through gaps around the floor assembly. A maximum temperature of about 280°C was reached at the 2.4 m height. The temperatures showed a sudden increase at about 1200 s, which may be related to flame penetrating into the first storey through the burning floor, and then they started decaying around 1240 s after the extinguishment of the fire was initiated.



**Figure 34. Temperatures on the second storey at the stairs for UF-02**

### 3.3.6 Temperatures at the Outside Doorway on the First Storey

Figure 35 and Figure 36 show the temperatures at the exterior doorway on the first storey for UF-01 and UF-02, respectively. Ambient temperature was measured for about the first 120 s and 160 s for UF-01 and UF-02, respectively. After these times, the temperatures started increasing reaching 140°C at 220 s in Test UF-01 and 60°C at 800 s in Test UF-02 due to smoke and hot fire gases exiting through the open exterior door (smaller increase in temperature in Test UF-02 with the closed basement doorway). Then they reached 260°C at 760 s and 130°C at 1180 s for UF-01 and UF-02, respectively. Just after 760 s for UF-01 and 1180 for UF-02, there was a sharp increase in temperatures (due probably to flame penetration through the floor producing more radiation and hot gases in the vicinity of the exterior door). The maximum temperatures reached were about 350°C at 830 s for UF-01 and 530°C at 1210 s for UF-02. The temperatures started decaying around 840 s and 1210 s for UF-01 and UF-02, respectively, after the extinguishment of the fire was initiated.

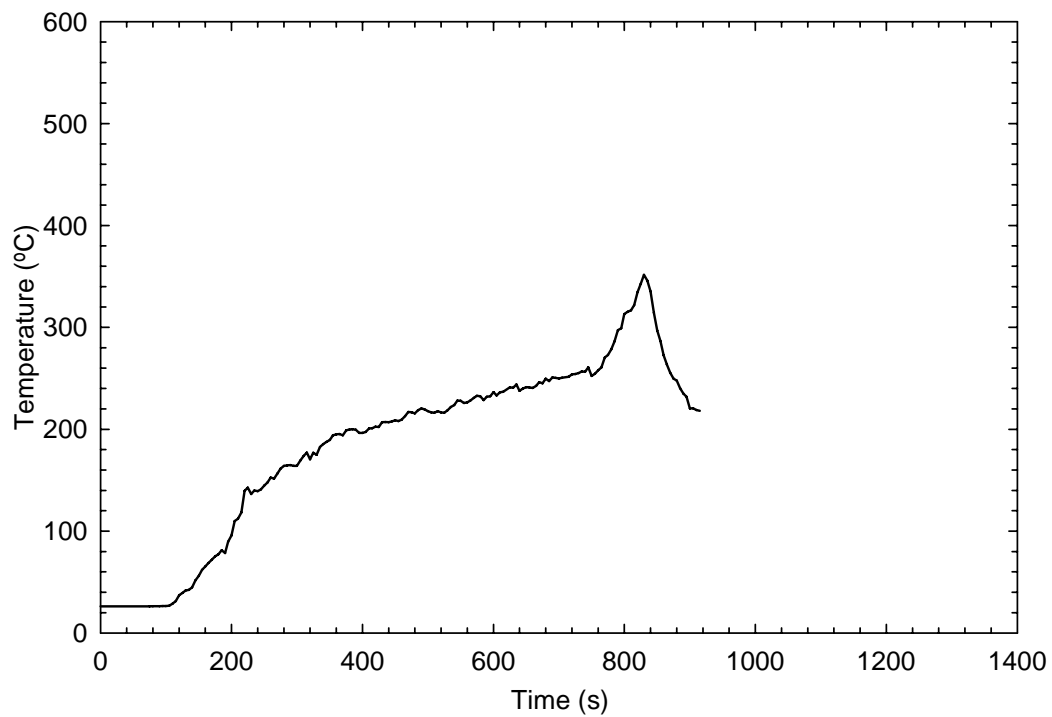


**Figure 35. Temperatures at the outside doorway on the first storey for UF-01**

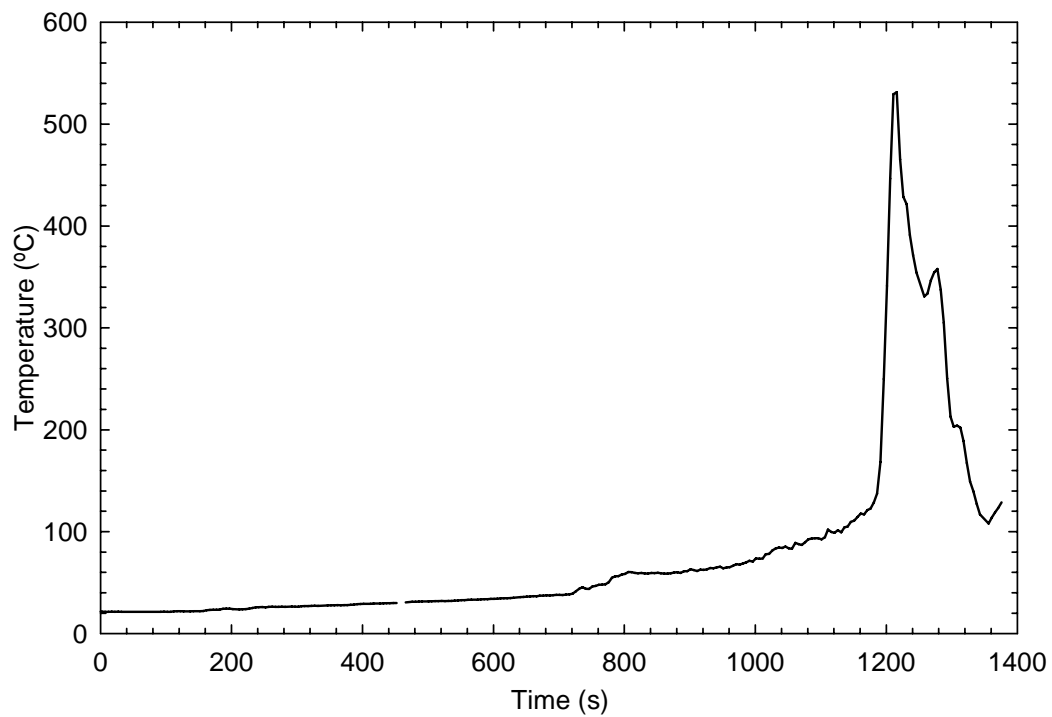


**Figure 36. Temperatures at the outside doorway on the first storey for UF-02**

### 3.3.7 Temperatures on the First Storey on the Unexposed Side of the Floor Assemblies

#### 3.3.7.1 Test UF-01

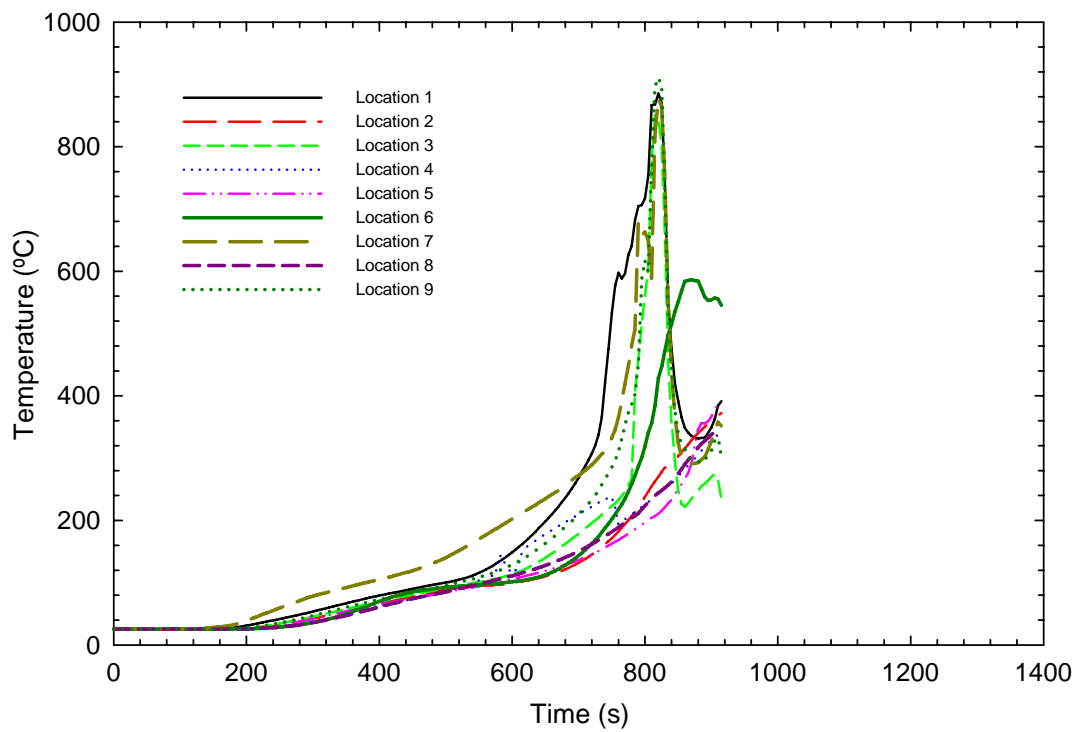
Figure 37 (a and b) show the temperatures measured by thermocouples (TCs) No. 1 to 9 and No. 92 through 97 located on the unexposed side (top) of the OSB subfloor in the floor assembly (see Figure 17 and Figure 18).

For TCs 1 to 9, the temperatures remained at ambient temperature for the first 200 s. After this, the temperatures increased gradually until 600 s; thereafter, the temperatures show a faster rate of increase especially for locations 1, 7 and 9. This faster increase in temperature rise was due to the critical positioning of the thermocouples. TC1 was located just above the position of the mock-up sofa, TC 7 was located above the fuel package at a joint in the floor and TC 9 was positioned just above the location of one of the wood cribs.

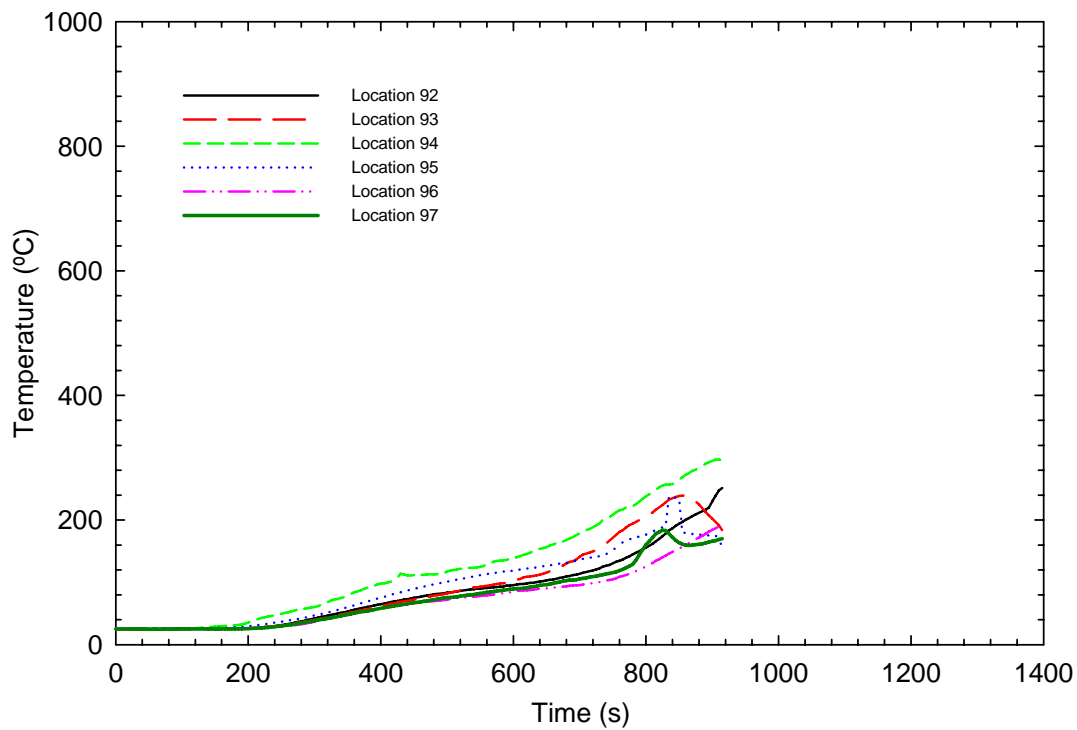
After 730 s, the temperatures at locations 1, 7 and 9 increased from 300°C to 900°C within 80 s. This is likely an indication that flames penetrated through the subfloor at these locations. The temperatures measured at locations 3 and 6 show a rapid increase shortly after the increase at locations 1, 7 and 9, which indicates that the floor was being breached at many locations around 800 s. This time corresponds to the time when there was a sharp increase in temperatures measured at the thermocouple tree in the SE region on the first storey (see Figure 24 (a)). Subsequently, the temperatures decreased during the extinguishment of the fire.

TCs No. 1 to 9 that were covered with insulated pads were closer to those areas of the floor assembly that were directly over the fire source; while the bare TCs No. 92 to 97 were around the perimeter of the floor assemblies. The temperatures measured with the bare TCs 92 to 97 were lower than those measured with the TCs covered by insulated pads.

It is worth mentioning that under standard fire test conditions (CAN/ULC-S101 and ASTM E 119 tests) [14], temperatures on the unexposed faces of specimens measured with uncovered TCs are always lower than those measured by TCs covered with insulated pads. In the standard tests [14], on the basis of temperature, floor failure is defined as a temperature rise of 140°C above ambient temperature for the average of the nine padded thermocouples or a temperature rise of 180°C above ambient temperature at any single point (padded thermocouple) on the unexposed side.



a) Unexposed TCs under insulated pad on top of subfloor



b) Bare TCs on unexposed (top) side of the subfloor

**Figure 37. Temperatures at the unexposed side of subfloor for UF-01**

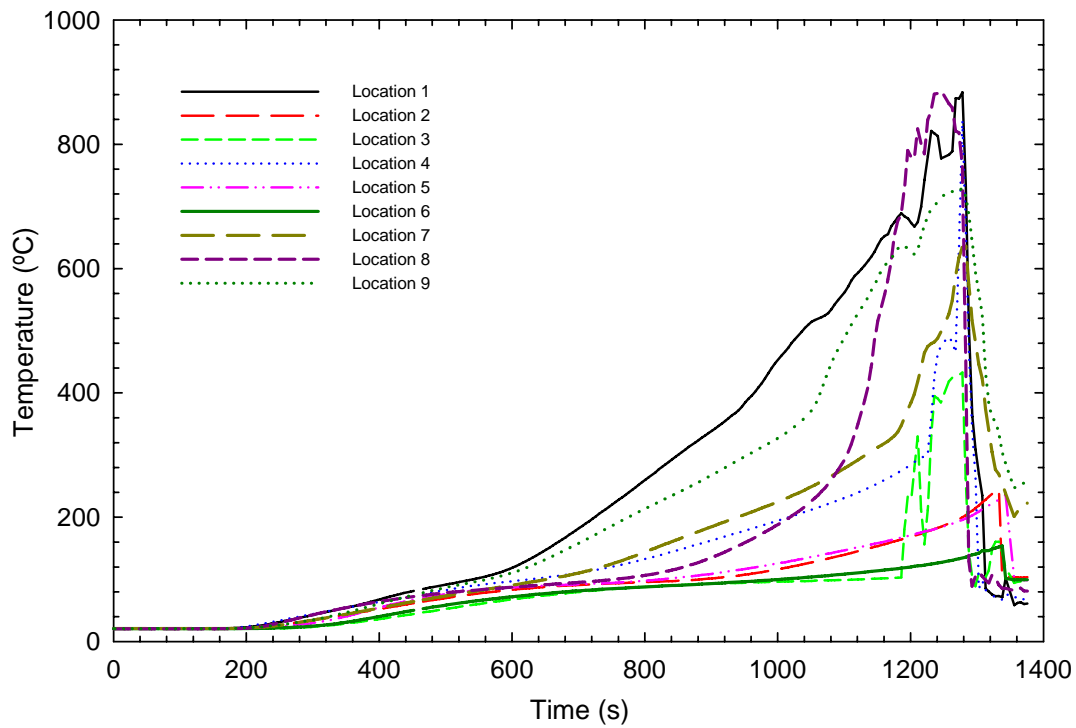
### 3.3.7.2 Test UF-02

Figure 38 (a and b) show the temperatures measured by thermocouples No. 1 to 9 and No. 92 through 97 located on the unexposed side (top) of the OSB subfloor in the floor assembly (see Figure 17 and Figure 18).

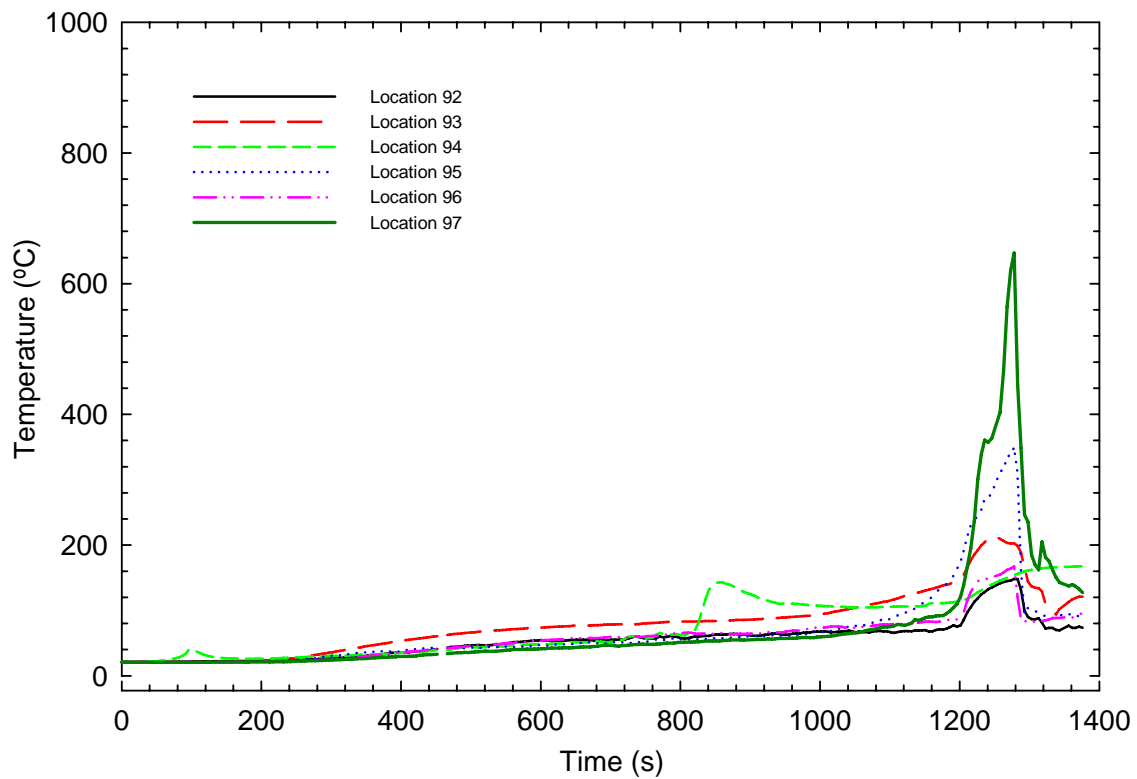
For TCs 1 to 9, the temperatures remained at ambient temperature for the first 200 s. After this, the temperatures increased gradually until 600 s; thereafter, the temperatures show a faster rate of increase especially for locations 1 and 9. This faster temperature rise was due to the critical positioning of the thermocouples. TC1 was located just above the position of the mock-sofa and TC 9 was positioned just above the location of one of the wood cribs.

At around 1080 s, the temperatures at locations 1, 7, 8 and 9 increased to maximum temperatures of 880°C. The temperature at location 4 shows a similar trend but only after 1200 s. This is an indication that around 1100 s, flames started penetrating through the floor at the above-mentioned locations and probably others as the floor was breached. The temperatures measured at locations 2, 5 and 6 do not show the same sharp increase in temperatures and the maximum values reached at these points were 240, 240 and 160°C, respectively. This indicated that the north part of the floor was not being penetrated by the flames as much as the south and central portions of the floor. This could be attributed to the fact most of the fuel was in the south and central parts of the basement and that openings were formed in these areas to allow air and smoke to move between the basement and the door to the outside since the door to the basement was closed.

The times, corresponding to flames penetrating the floor, were comparable to those recorded using the flame-sensing devices and the time at which there was a sharp increase in temperatures at the thermocouple tree in the SE region on the first storey (see Figure 25 (a)). Subsequently, the temperatures decreased during the extinguishment of the fire.



a) Unexposed TCs under insulated pad on top of subfloor



b) Bare TCs on unexposed (top) side of the subfloor

**Figure 38. Temperatures at the unexposed side of subfloor for UF-02**

### 3.3.8 Temperatures on the Exposed Side of the Floor Assemblies

The location of each grouping of thermocouples is identified by the Section label (A, B, C, D, E and F) and the joist space shown on Figure 17 and Figure 18. For example, C-1 is the group of thermocouples located along Section C in Joist Cavity 1.

For the thermocouple groupings within the joist cavities with seven thermocouples at each section, the individual thermocouples are identified as follows: bottom of north joist (Bot WJ North (1)), mid-height of north joist (Mid WJ North (2)), between the north joist and the subfloor (SF/WJ North (3)), on the subfloor mid-distance between the two joists (SF/Cav (4)), between the south joist and the subfloor (SF/WJ South (5)), mid-height of south joist (Mid WJ South (6)) and bottom of south joist (Bot WJ south (7)).

The temperatures on the exposed side of the floor assembly were measured at a number of locations distributed in such a way as to learn, as much as possible, the effect of the fire on the floor assemblies. As shown in Figure 17 and Figure 18 (Location of Thermocouples), in most of the locations (Sections A, B, C and F), seven thermocouples were installed: 2 at the bottom of two adjacent joists, 2 in the cavity at mid-height of the two joists, 2 between the subfloor and the two joists, and 1 in the cavity at the subfloor at mid-distance between the 2 joists. For Section D, the thermocouples were installed at mid-height of the interface of the overlapped joists. Section E had only 1 thermocouple in the cavity at the subfloor at mid-distance between the 2 overlapped joists.

#### 3.3.8.1 Test UF-01

Figure 39 (a) to Figure 39 (l) show the temperatures measured by the thermocouples located on the exposed side of the floor for Test UF-01. For all the locations with 7 thermocouples (A-2, A-7, A-12, B-7, C-1, C-5, C-7, C-9, C-11, C-13, and F-1), in almost every case the trend was similar with a sharp increase in temperatures for all the exposed thermocouples in the first 120 s to 160 s. For the thermocouples located at the interface between the top of a joist and the subfloor (SF/WJ), the temperature rise in most cases was relatively slow and gradual due to the shielding of the thermocouples by the joists. When the temperatures for SF/WJ North (3) and SF/WJ South (5) show a temperature increase, which is sudden in some cases (the case of B-7, C-1 (SF/WJ South (5) only), C-5, C-7, C-11, C-13 and F-1), it is an indication that gaps were forming between the top of the joists and the subfloor at these points and that the thermocouples were being exposed to the hot gases from the fire. For SF/WJ North (3) at C-1, the increase in temperature was much earlier (similar to exposed thermocouples), which might be due to the existence of a large enough gap between the top of the joist and the subfloor prior to the start of the test to allow early fire exposure.

The increase in temperature happened at different times for the different locations. The difference in time between the two SF/WJ (North and South) thermocouples is partly due to the view factor relative to the burning fuel package. In some cases, the bulk of the fuel package was 'positioned' South of the thermocouple grouping. Consequently, the thermocouple at top of the North joist experienced a greater heat insult from both the convective and radiative effects from the burning fuel. For the thermocouple groupings with the bulk of the fuel package located to the North, the reverse effect occurred.

Of particular mention is Section C-9 where the temperatures at SF/WJ North (3) and SF/WJ South (5) reached the same peak values as the temperatures at the exposed thermocouples in the first 100 s. This is an indication that gaps due to structural movement and charring of the wood at the interface of the joists and subfloor occurred much earlier at this location than other locations as it was directly above the mock-up sofa and very close to the wood cribs.

For the exposed thermocouples, the highest peak temperature (880°C) was recorded at Section C-7 (located at about the centre of the basement and directly over the burning mock-up sofa). In most cases, there was a drop in temperature measured by the exposed thermocouples just after about 160 s, which may be attributed to the fresh air coming from the open basement window and also the opening of the outside door at 180 s. The decrease in temperature lasted only about 60 s and then the temperatures either stayed almost constant or started increasing again.

The almost constant temperatures were recorded for sections B7, C-7, C-9, C-11 and C-13, which were close to the fire and the intensely burning items (mock-up sofa and cribs). This may be attributed to the fact the temperatures at these locations peaked in the initial 160 s, reaching values of approximately 800°C and could not go beyond these values due to limited air supply. The highest temperatures after 180 s were recorded at locations C-7 and C-9.

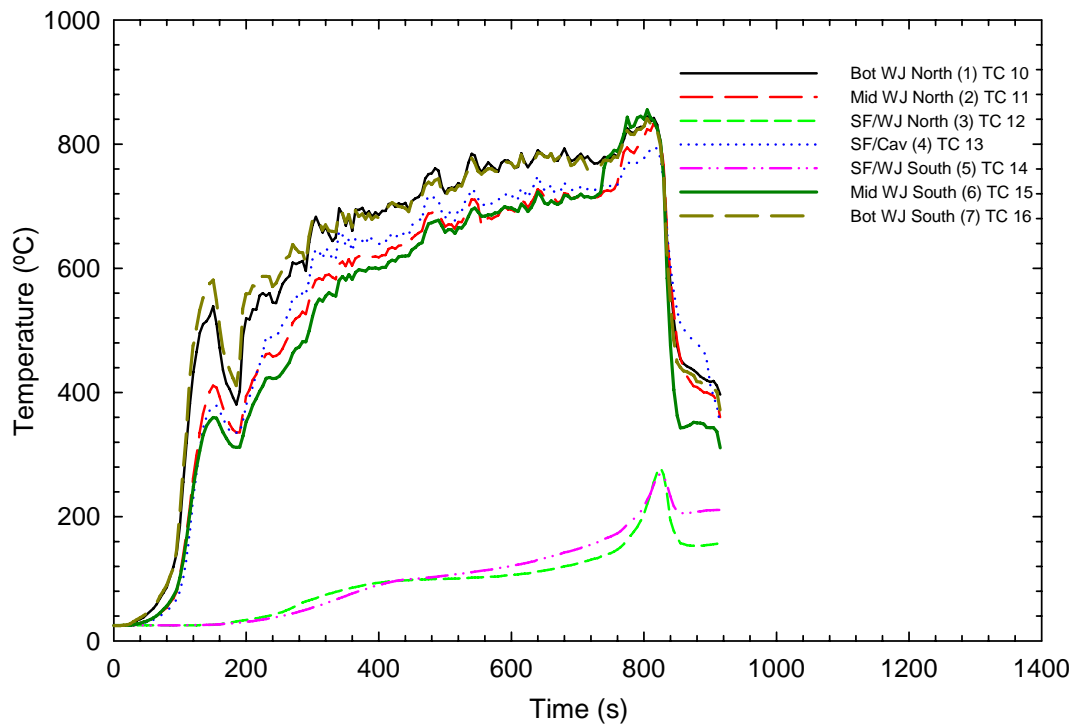
The exposed thermocouples at some locations showed a temperature increase after the decrease at 160 s (A-2, A-7, A-12, C-5). This was probably due to the fact that the temperatures at these locations had not reached their peak values as they were farther away from the burning fuel.

There were cases where there was no obvious drop in the temperature at 160 s (C-1 and F-1) and this is because these locations were not in the proximity of the fuel package and thus had limited radiative impact from the fuel.

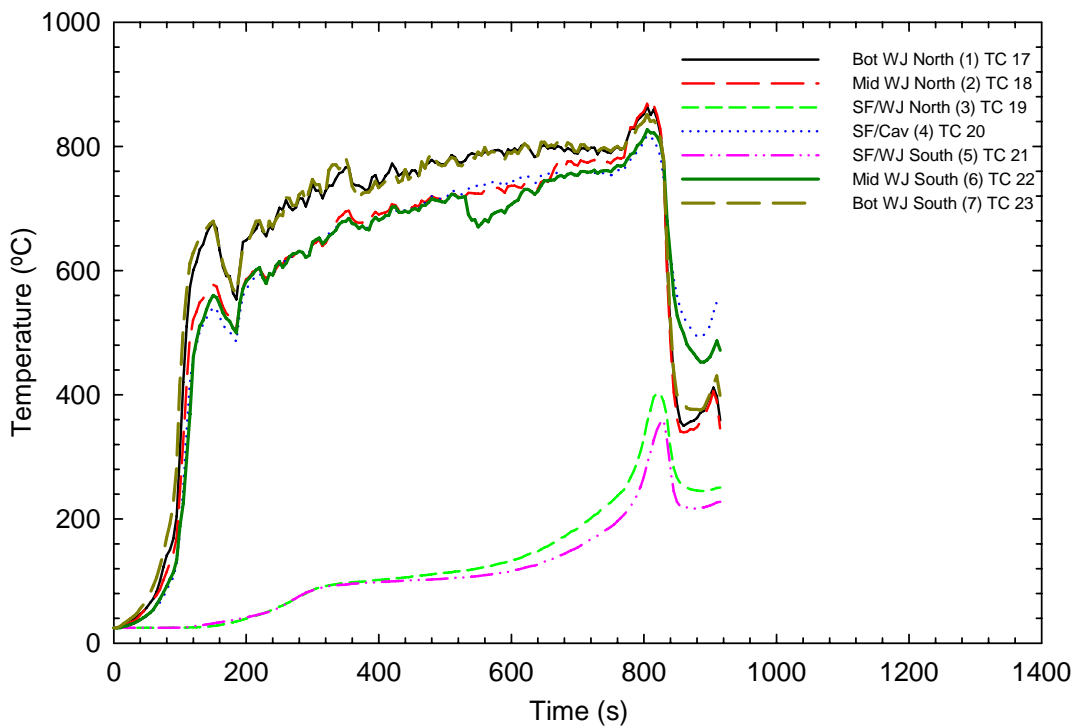
The temperature measured at SF/Cav (4) at Section C-7 seems anomalous compared to the other thermocouples exposed in the cavity. It is possible that the thermocouple at this location was partially shielded, by other components of the structure, from the flames when the joists started deflecting.

For Sections D and E, point D-1, E-2 and E-12 have the same trend as the exposed thermocouples in section F (away from the fire), while points D-6 and D-11 behave in similar fashion as the exposed thermocouples in Sections C5 and C11.

At approximately 760 s, the temperatures at the different locations show a slight increase probably because the flames penetrated the floor and allowed more fresh air to enter and slightly more burning to occur in the basement. The temperatures started to decrease around 820 s after the extinguishment of the fire was initiated.

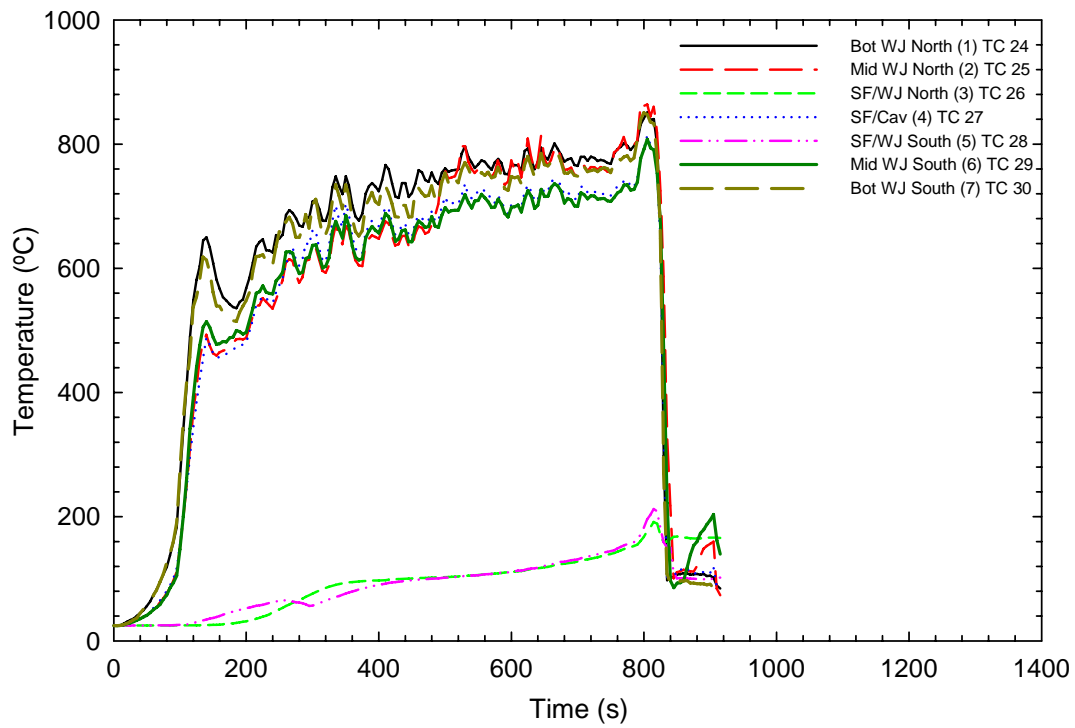


a) Thermocouples in cavity A-2

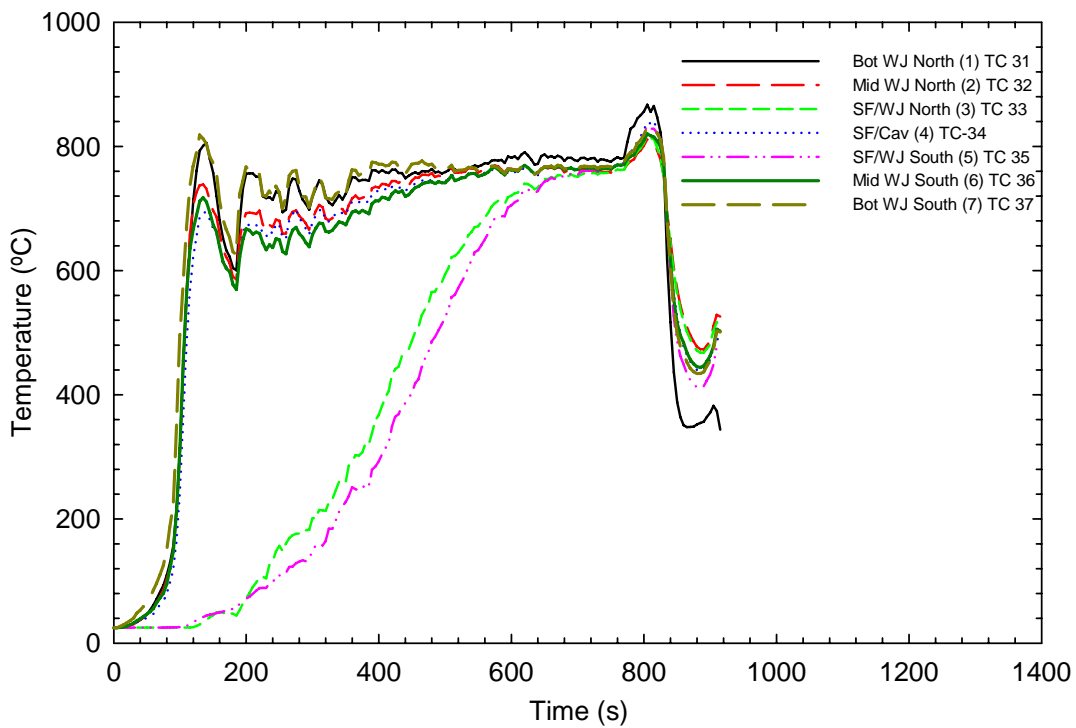


b) Thermocouples in cavity A-7

**Figure 39 (a and b). Temperatures at the exposed side for UF-01**

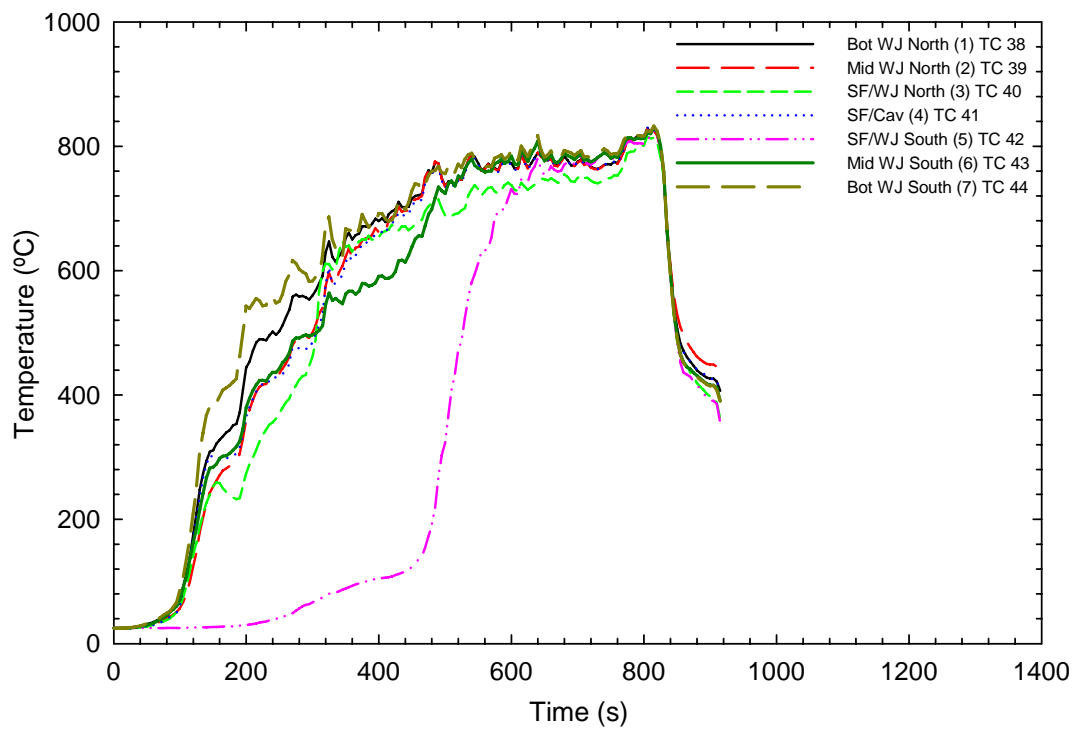


c) Thermocouples in cavity A-12

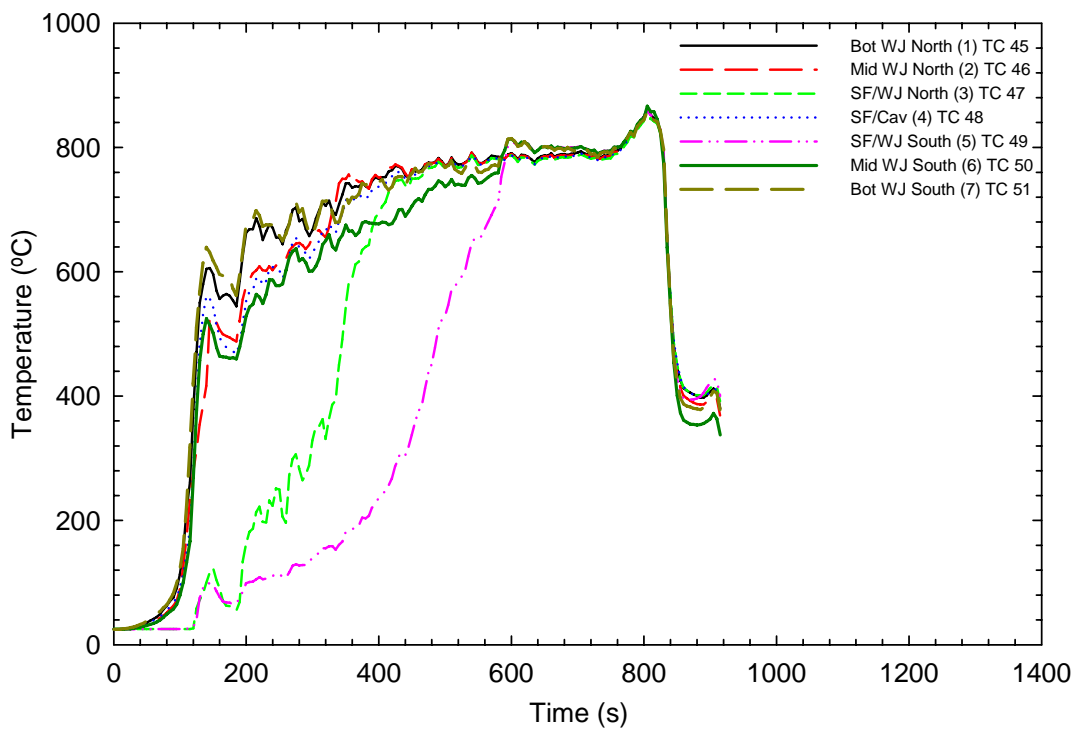


d) Thermocouples in cavity B-7

**Figure 39 (c and d). Temperatures at the exposed side for UF-01**



e) Thermocouples in cavity C-1



f) Thermocouples in cavity C-5

**Figure 39 (e and f). Temperatures at the exposed side for UF-01**

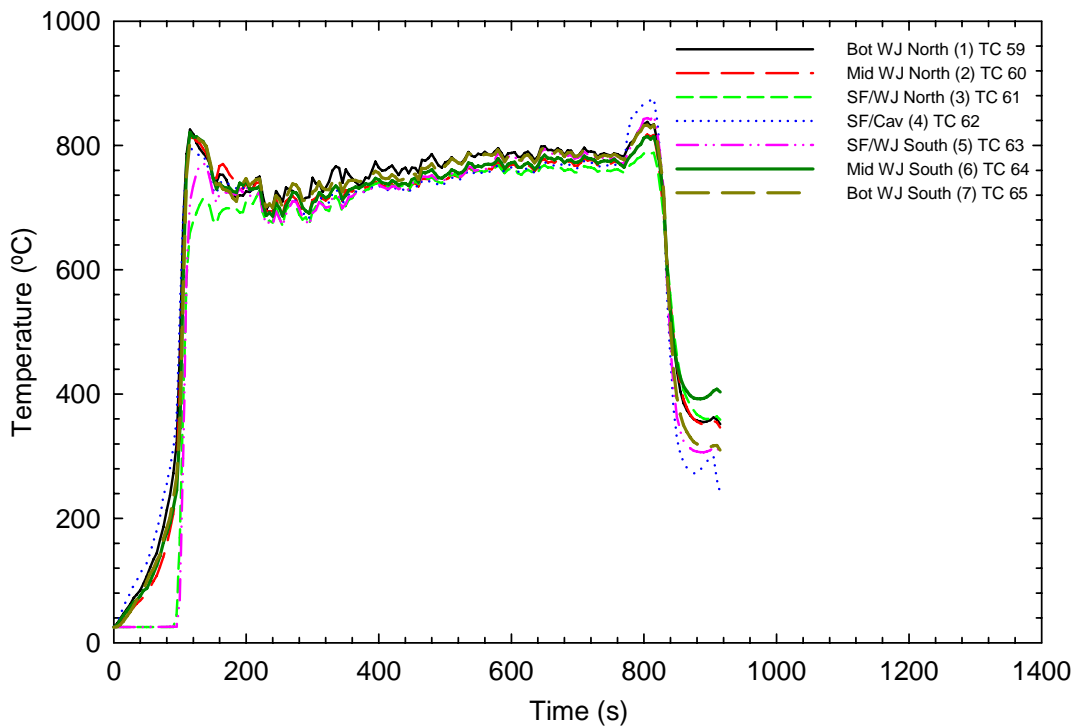
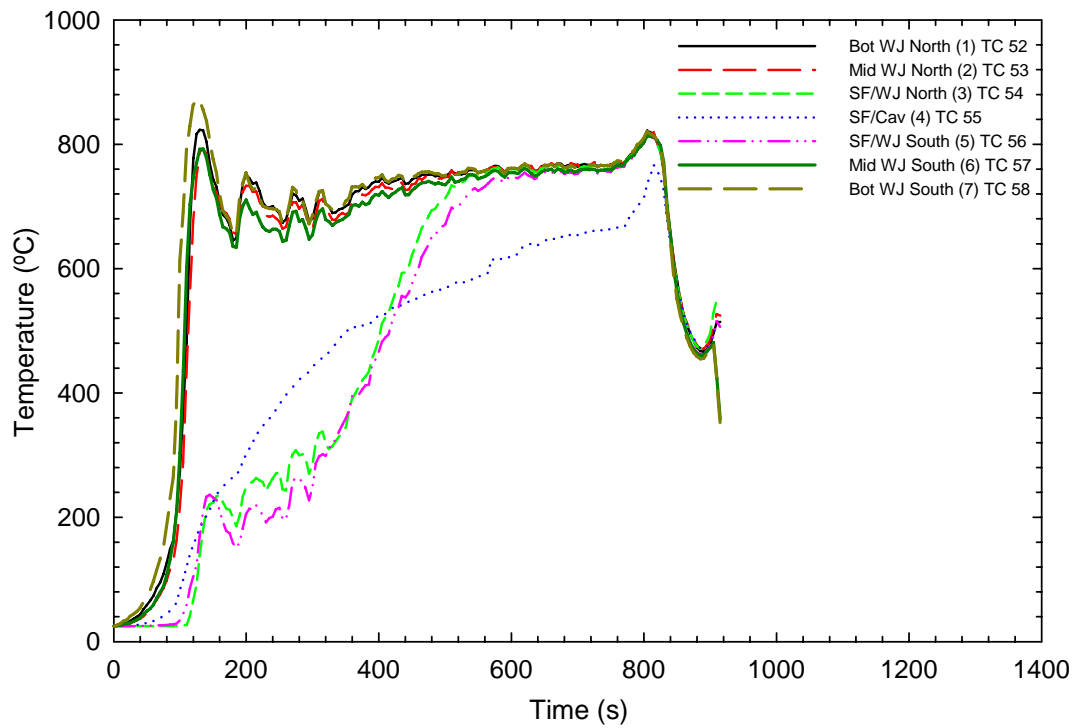
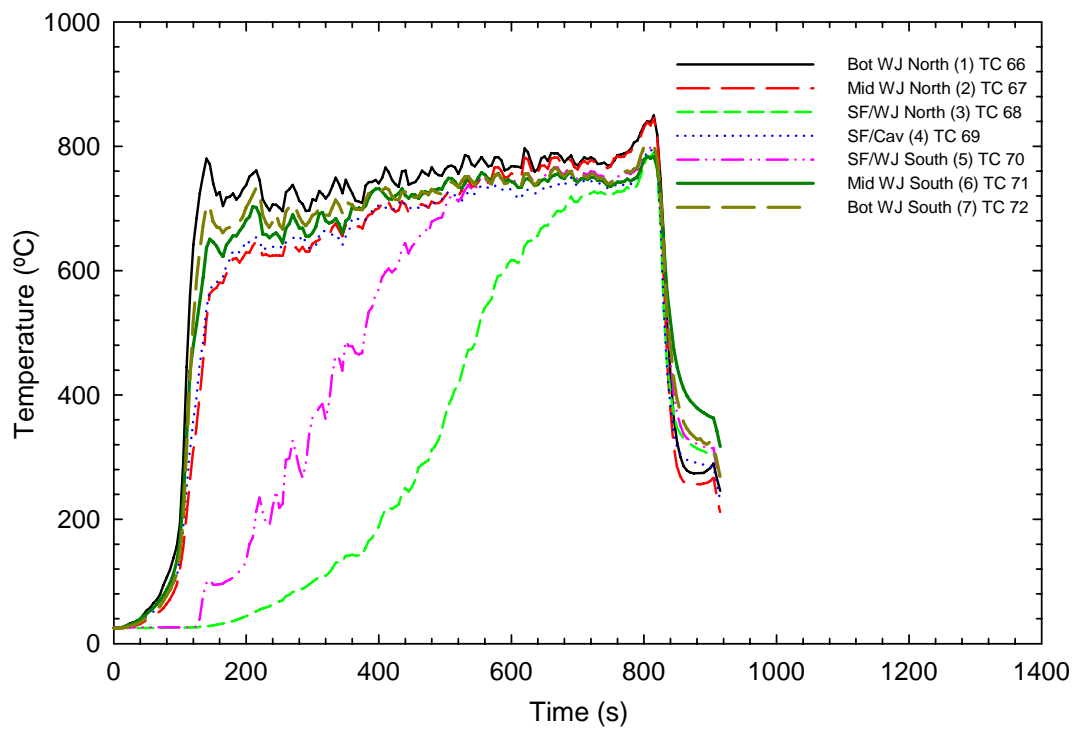
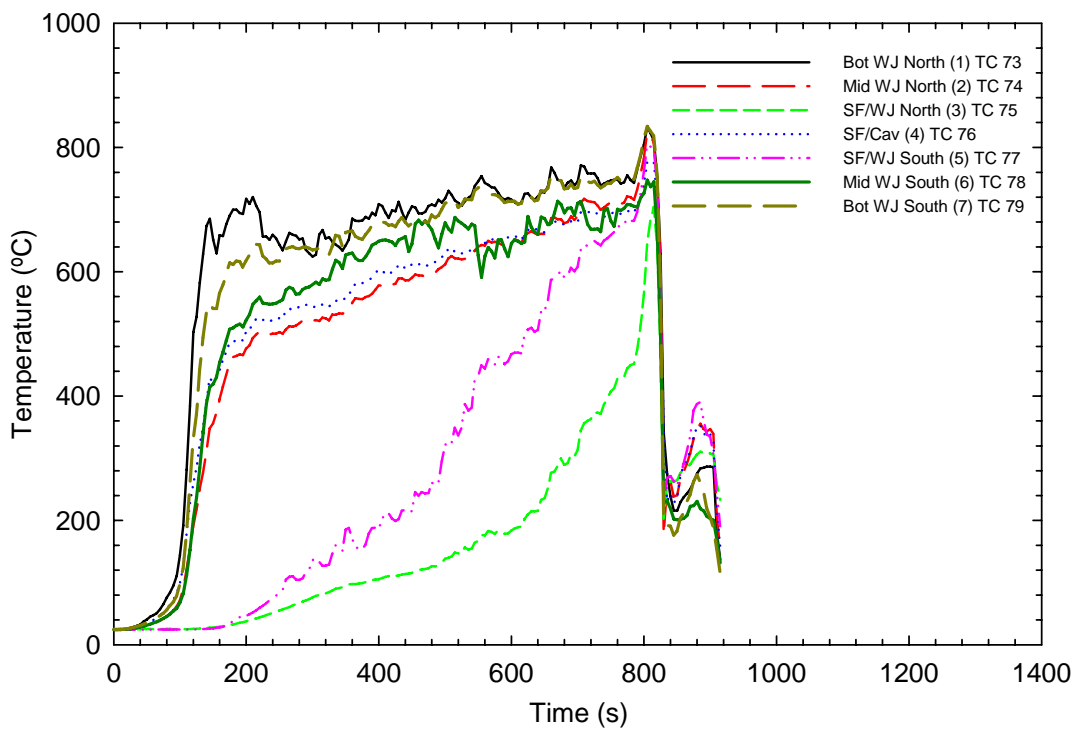


**Figure 39 (g and h). Temperatures at the exposed side for UF-01**

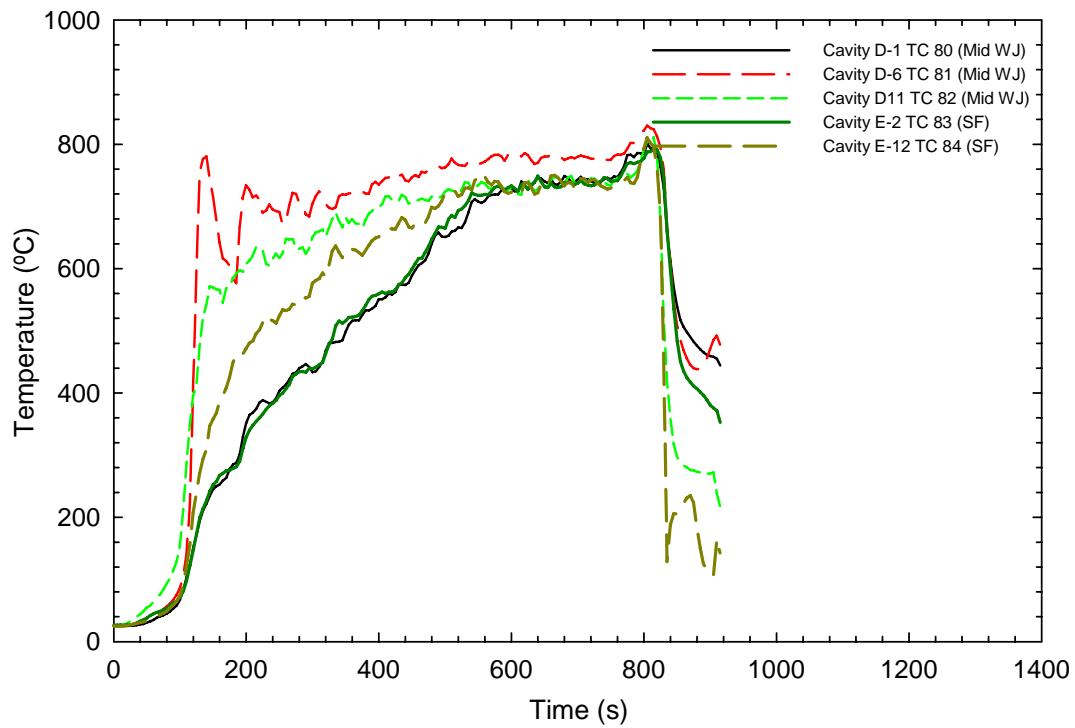


i) Thermocouples in cavity C-11

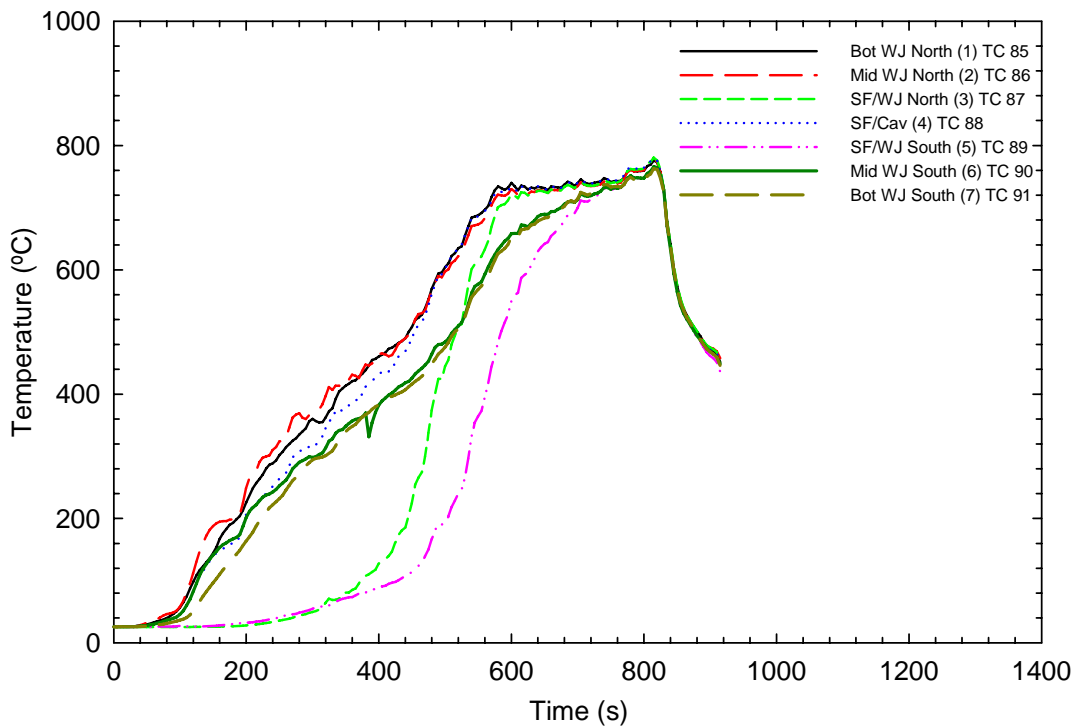


j) Thermocouples in cavity C-13

**Figure 39 (i and j). Temperatures at the exposed side for UF-01**



k) Thermocouples in cavities D-1, D-6, D-11, E-2 and E-12



l) Thermocouples in cavity F-1

**Figure 39 (k and l). Temperatures at the exposed side for UF-01**

### 3.3.8.2 Test UF-02

Figure 40 (a) to Figure 40 (l) show the temperatures measured by the thermocouples located on the exposed side of the floor for Test UF-02. For all the locations with 7 thermocouples (A-2, A-7, A-12, B-7, C-1, C-5, C-7, C-9, C-11, C-13, and F-1), in almost every case the trend was similar with a sharp increase in temperatures for all the exposed thermocouples in the first 120 s to 160 s. For the thermocouples located at the interface between the top of a joist and the subfloor (SF/WJ), the temperature rise in most cases was relatively slow and gradual due to the shielding of the thermocouples by the joists. When the temperatures at the SF/WJ North (3) and SF/WJ South (5) show a temperature increase, which was sudden in some cases (the case of B-7, C-7, C-11 and C-13), it is an indication that gaps were forming between the top of the joists and the subfloor at these locations allowing flames and hot gases into the gap. The increase in temperature happened at different times for the different locations.

There was very little difference between the two SF/WJ (North and South) thermocouples, which may be partly due to the small effect of the view factor relative to the burning fuel package, due to the increased amount of smoke in the fire compartment, because of limited ventilation.

Of particular mention is Section C-9 where the temperatures at SF/WJ North (3) and SF/WJ South (5) reached the same peak values as the other exposed points in the first 100 s. This is an indication that gaps due to structural movement and charring of the wood at the interface of the joists and subfloor occurred much earlier at this location than other locations as it was directly above the mock-up sofa and very close to the wood cribs. Section C-7 shows a similar behaviour to that of C-9, but there was a slight time delay for SF/WJ North (3) and SF/WJ South (5) to reach the same temperatures as the exposed thermocouples.

The temperature measured at Bot WJ South (7) at Section C-7 seems anomalous compared to the other thermocouples exposed in the cavity. It is possible that the thermocouple at this location was partially shielded, by other components of the structure, from the flames when the joists started deflecting.

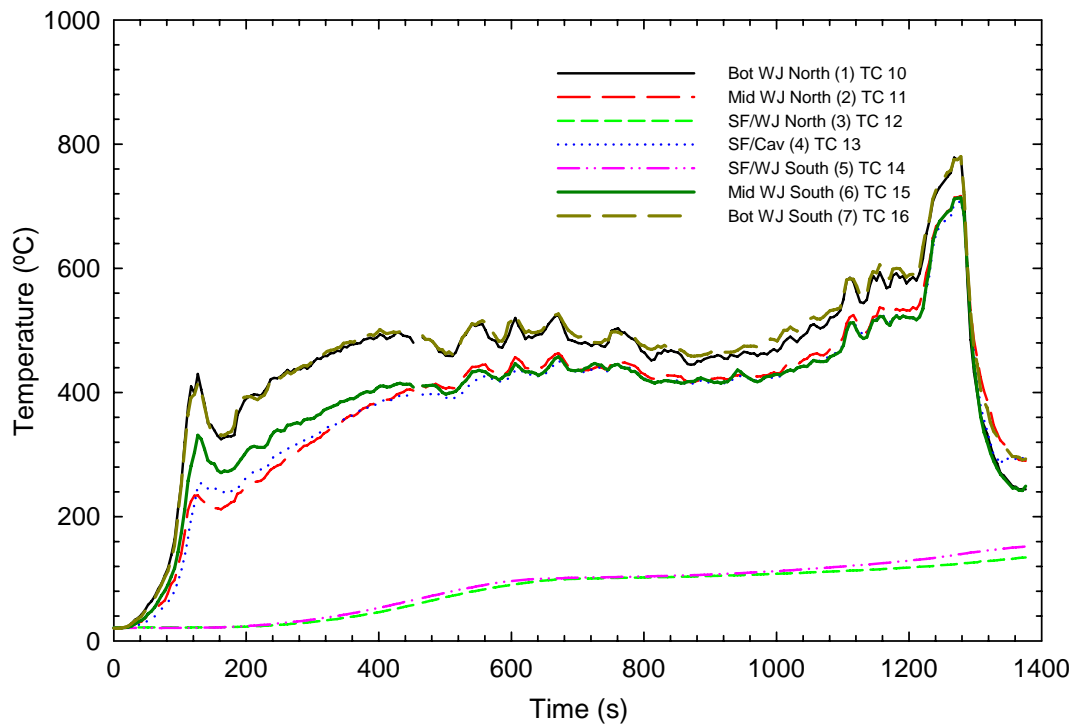
For the exposed thermocouples, the highest initial peak temperature (800°C) was recorded at Section C-9 (located directly over the burning mock-up sofa and the wood cribs).

In most cases, there was a drop in temperature just after 160 s, which may be attributed to the addition of fresh air coming from the opened basement window. The decrease in temperature lasted only about 60 s and then the temperatures either stayed constant or started increasing again. After about 500 s, there was a noticeable temperature drop and then a subsequent rise for a period of 200 s, which may be attributed to the floor being breached at some of these locations and allowing fresh air to enter from the first storey to the basement and enhancing the fuel burning in the basement. The section on “flame penetration” indicates that flames started penetrating the first storey around 600 s. This was the case for sections A-2, A-7, B-7, C-5, C-7, C-9, C-11 and C-13.

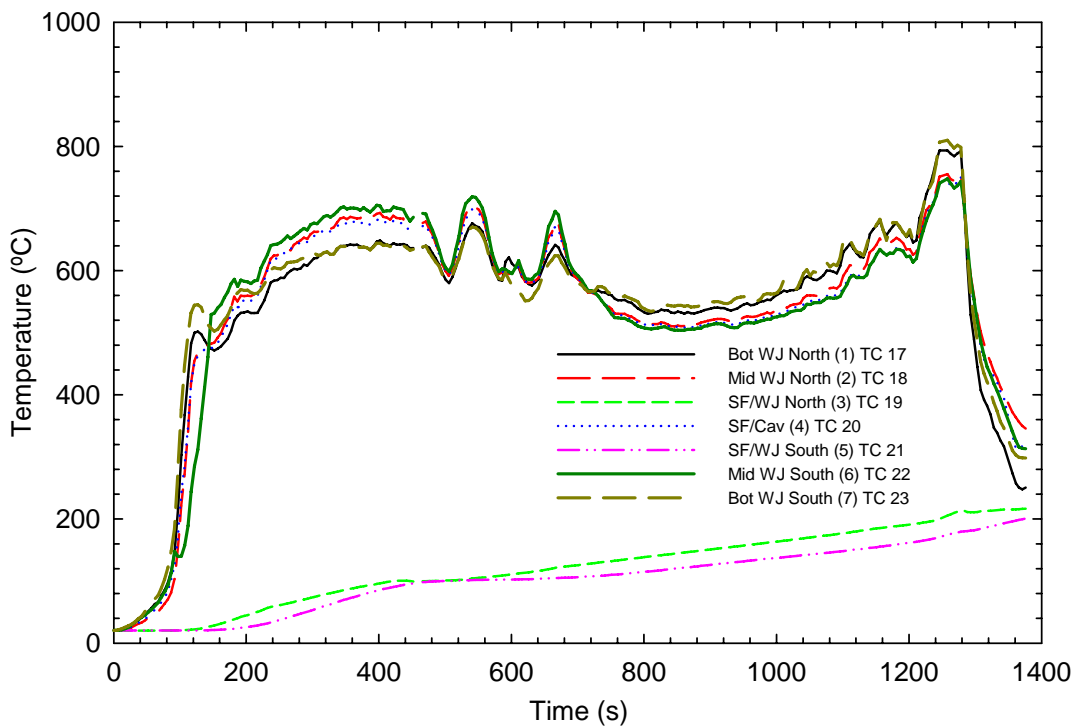
There were cases where there was no obvious decrease in temperature (C-1 and F-1). These locations were not close to the fuel package and thus had limited radiative impact from the fuel.

For sections D and E, point D-1 and E-2 have the same trend as the exposed thermocouples in section F (away from the fire), while points D-6, D-11 and E-12 behave in similar fashion as the exposed thermocouples in section A.

At approximately 1200 s, the temperatures at the different locations show a sharp increase probably because the flames penetrated the floor and allowed more fresh air to enter into the basement. The section on “flame penetration” indicates that flames started to penetrate into the first storey around 1160 s. In the case of A-2, A-7 and A-12, the temperatures at the SF/WJ North (3) and SF/WJ South (5) show no substantive increase in temperatures, indicating that the joists at these locations remained tightly fitted (no gaps) to the subfloor for the duration of the test. The temperatures started to decrease around 1280 s after the extinguishment of the fire was initiated.

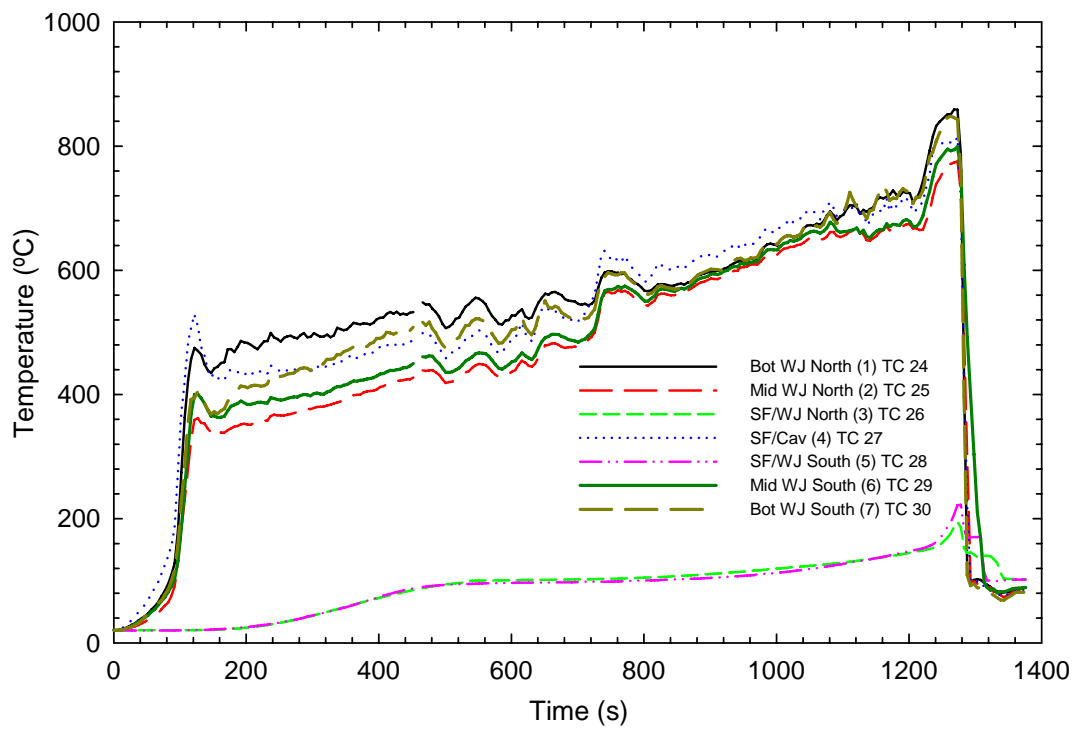


a) Thermocouples in cavity A-2

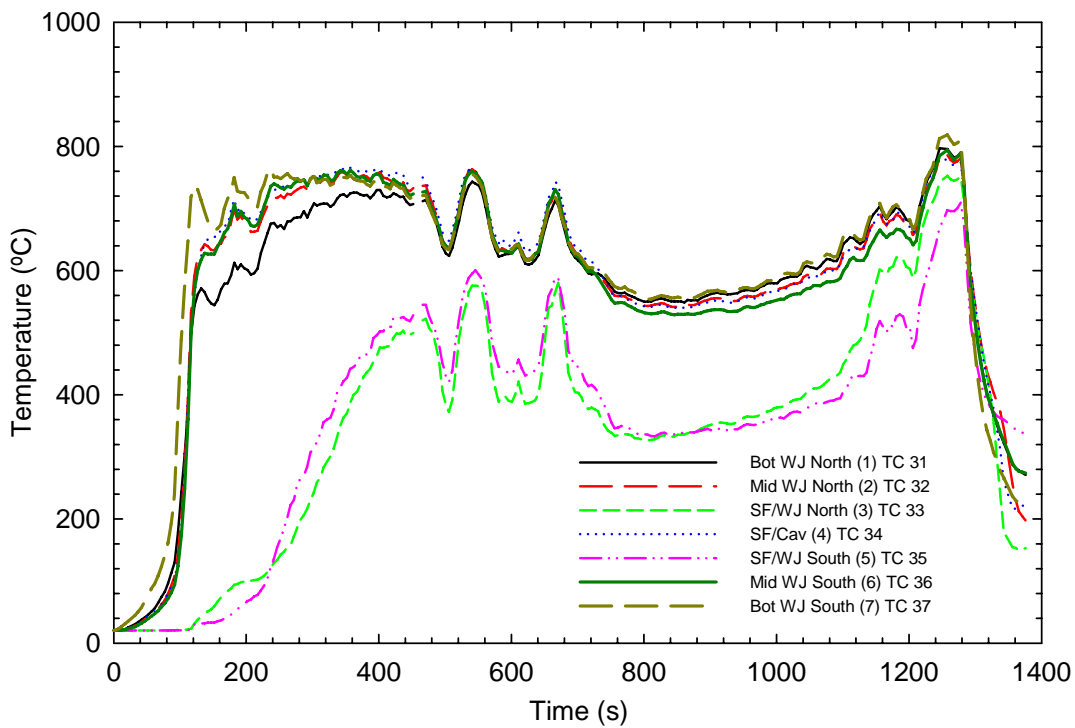


b) Thermocouples in cavity A-7

**Figure 40 (a and b). Temperatures at the exposed side for UF-02**

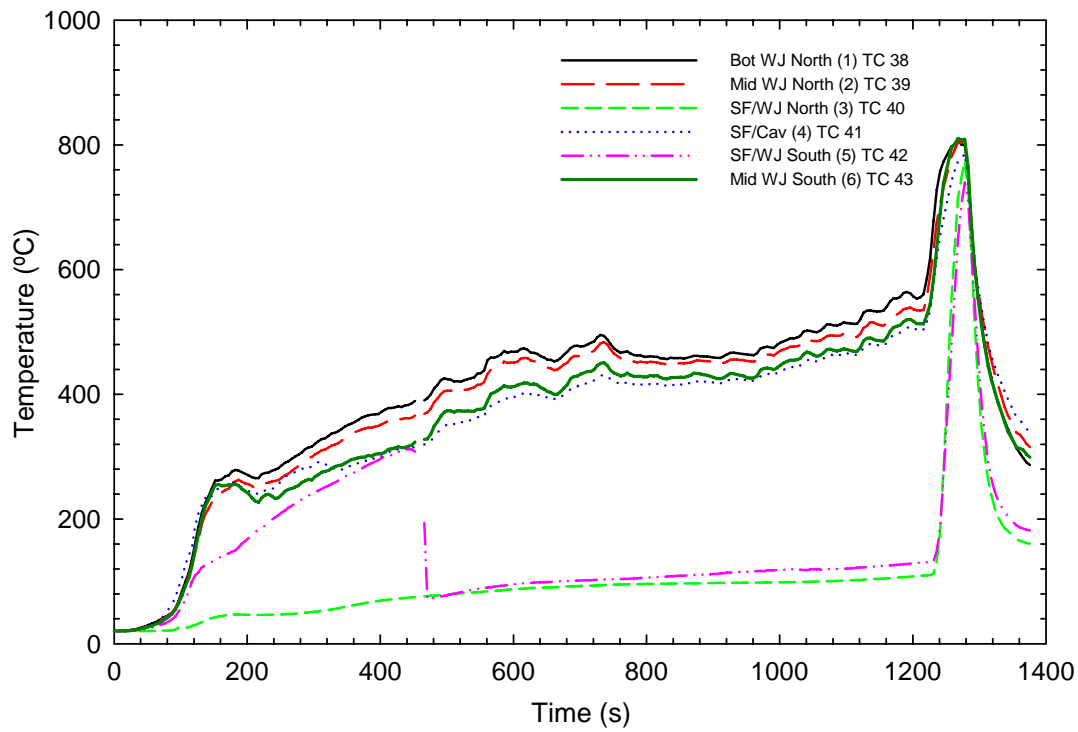


c) Thermocouples in cavity A-12

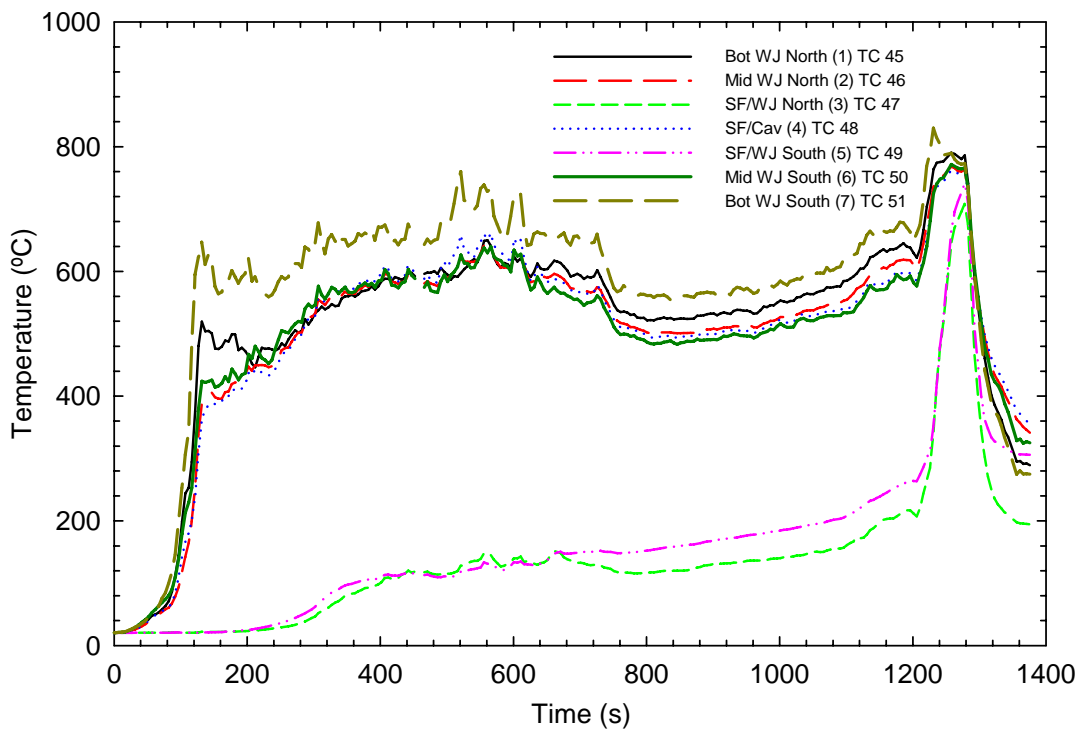


d) Thermocouples in cavity B-7

**Figure 40 (c and d). Temperatures at the exposed side for UF-02**



e) Thermocouples in cavity C-1



f) Thermocouples in cavity C-5

**Figure 40 (e and f). Temperatures at the exposed side for UF-02**

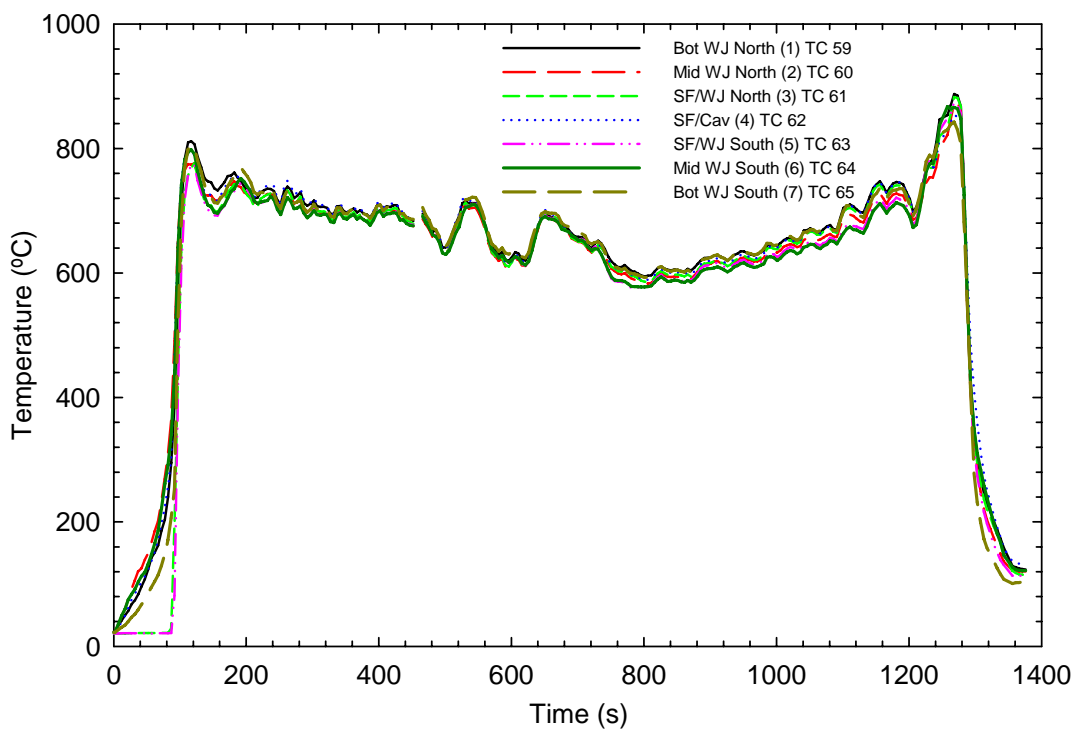
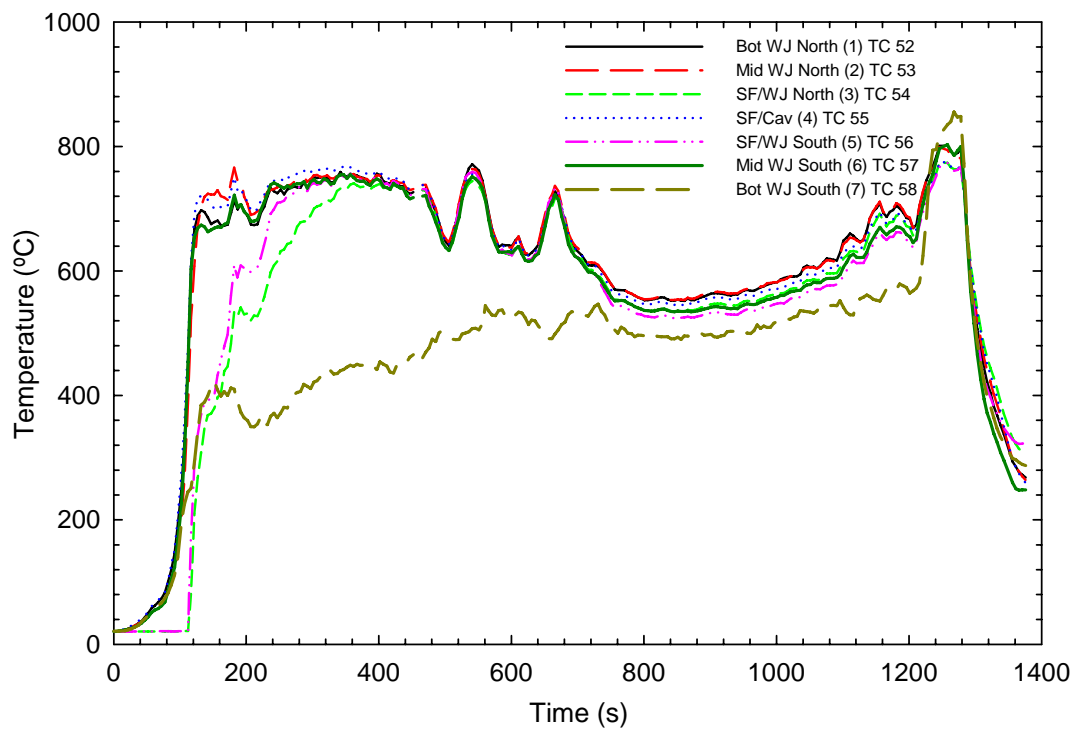
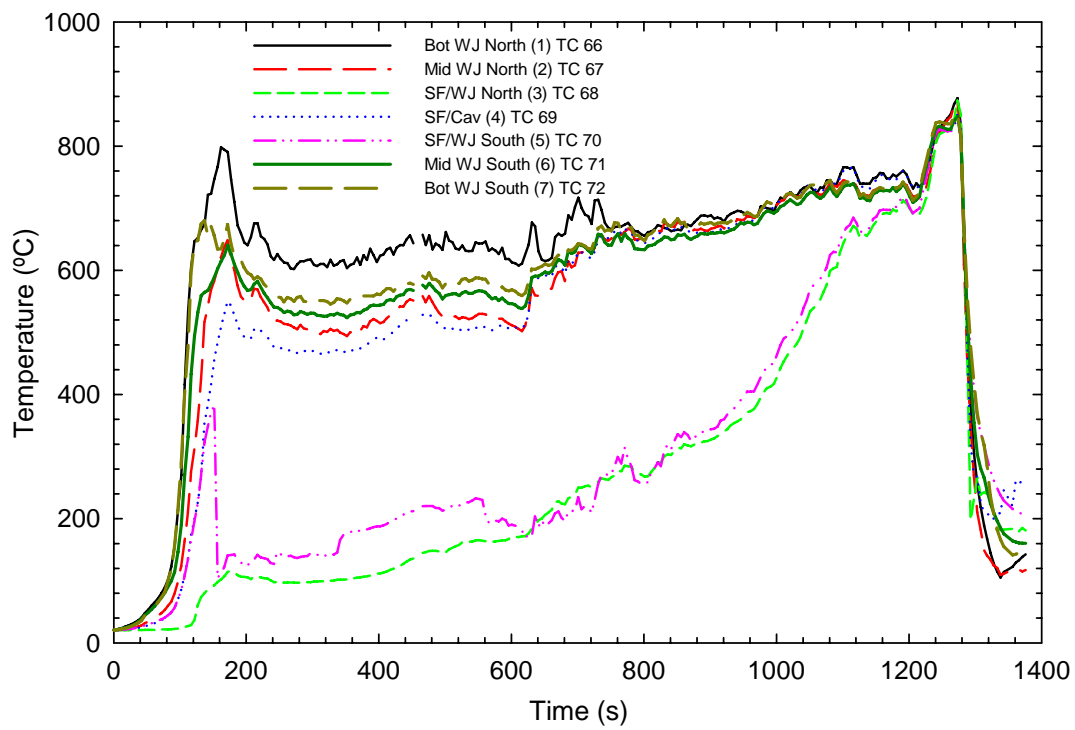
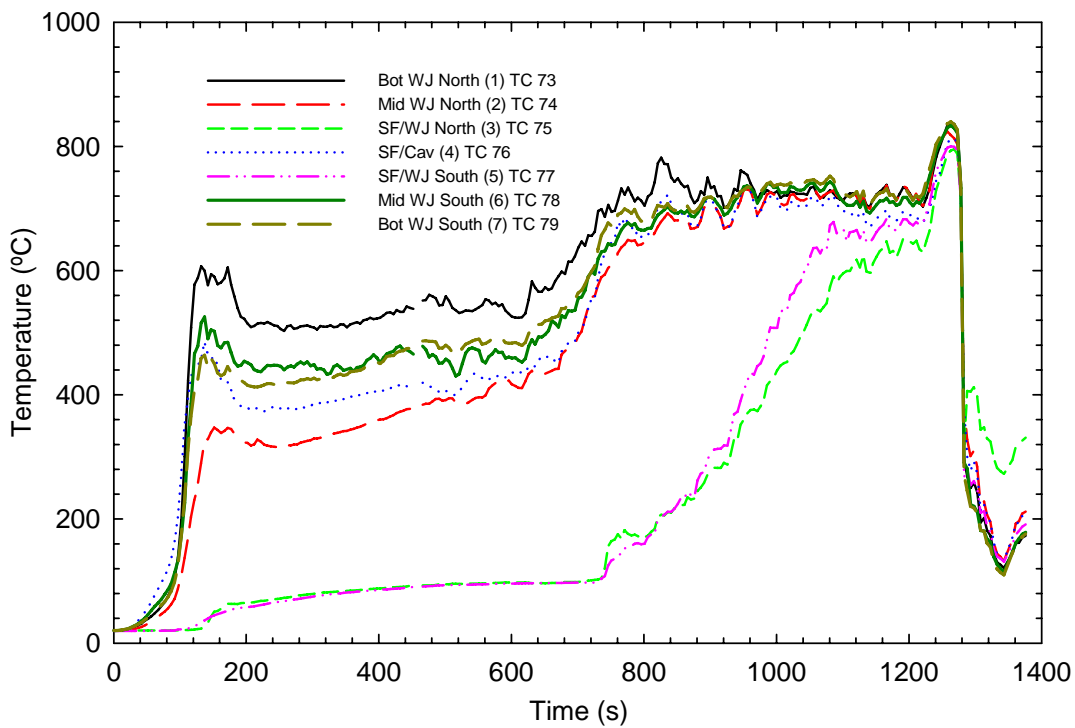


**Figure 40 (g and h). Temperatures at the exposed side for UF-02**

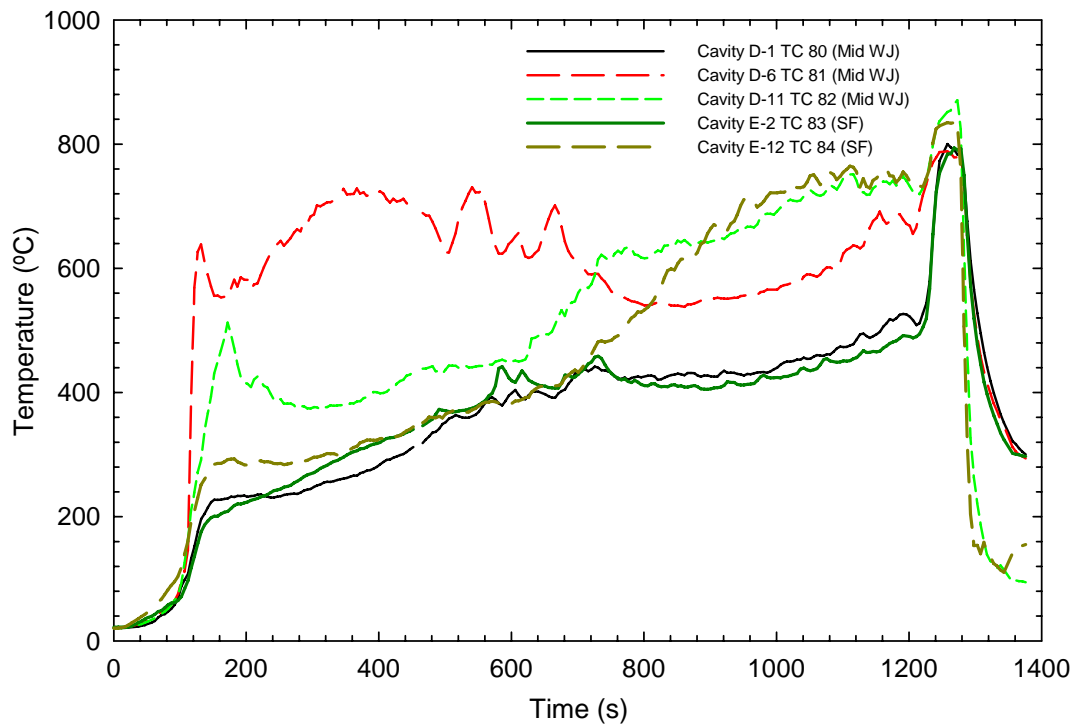


i) Thermocouples in cavity C-11

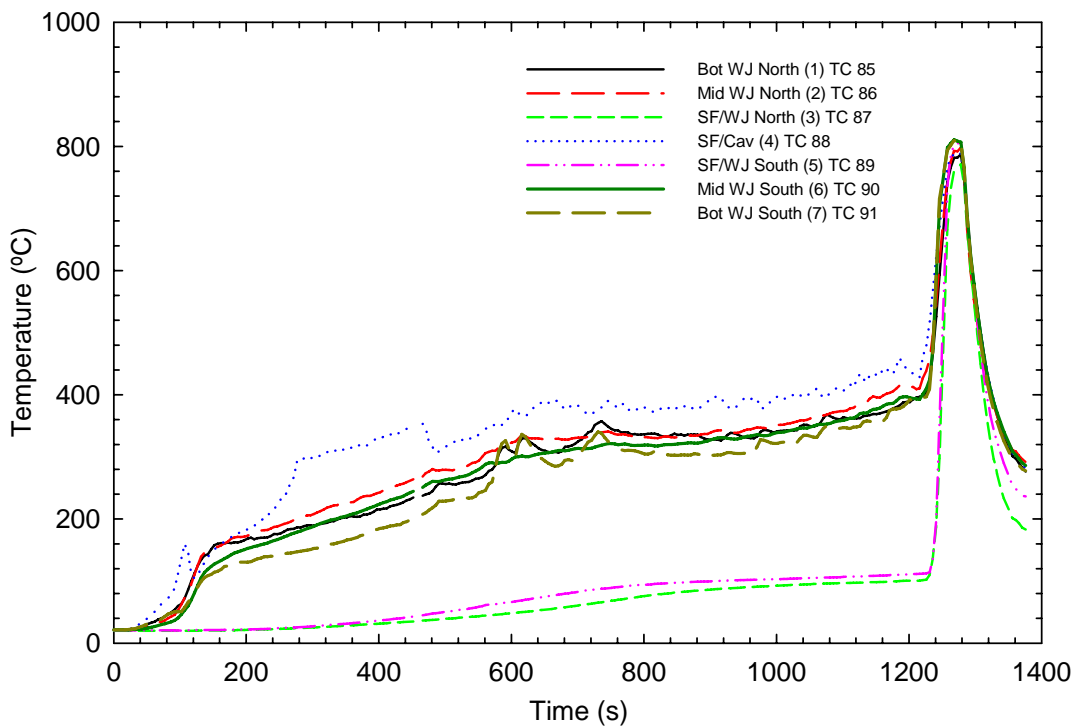


j) Thermocouples in cavity C-13

**Figure 40 (i and j). Temperatures at the exposed side for UF-02**



k) Thermocouples in cavities D-1, D-6, D-11, E-2 and E-12



l). Thermocouples in cavity F-1

**Figure 40 (k and l). Temperatures at the exposed side for UF-02**

### 3.4 Deflection Measurements Results and Structural Performance

Figure 41 shows the 9 deflection measurement points; Figure 42 and Figure 43 show the measurement results (as well as explained previously; see also Figure 11 for the joist closest to the deflection points). The points of measurement were chosen as they were located in the middle of the fire compartment just above the fire load where the impact of the fire on the structural integrity of the floor assembly was anticipated to be the greatest. Some measurement points were aligned with one of the joists, while the other row was positioned between joists.

#### 3.4.1 For Test UF-01

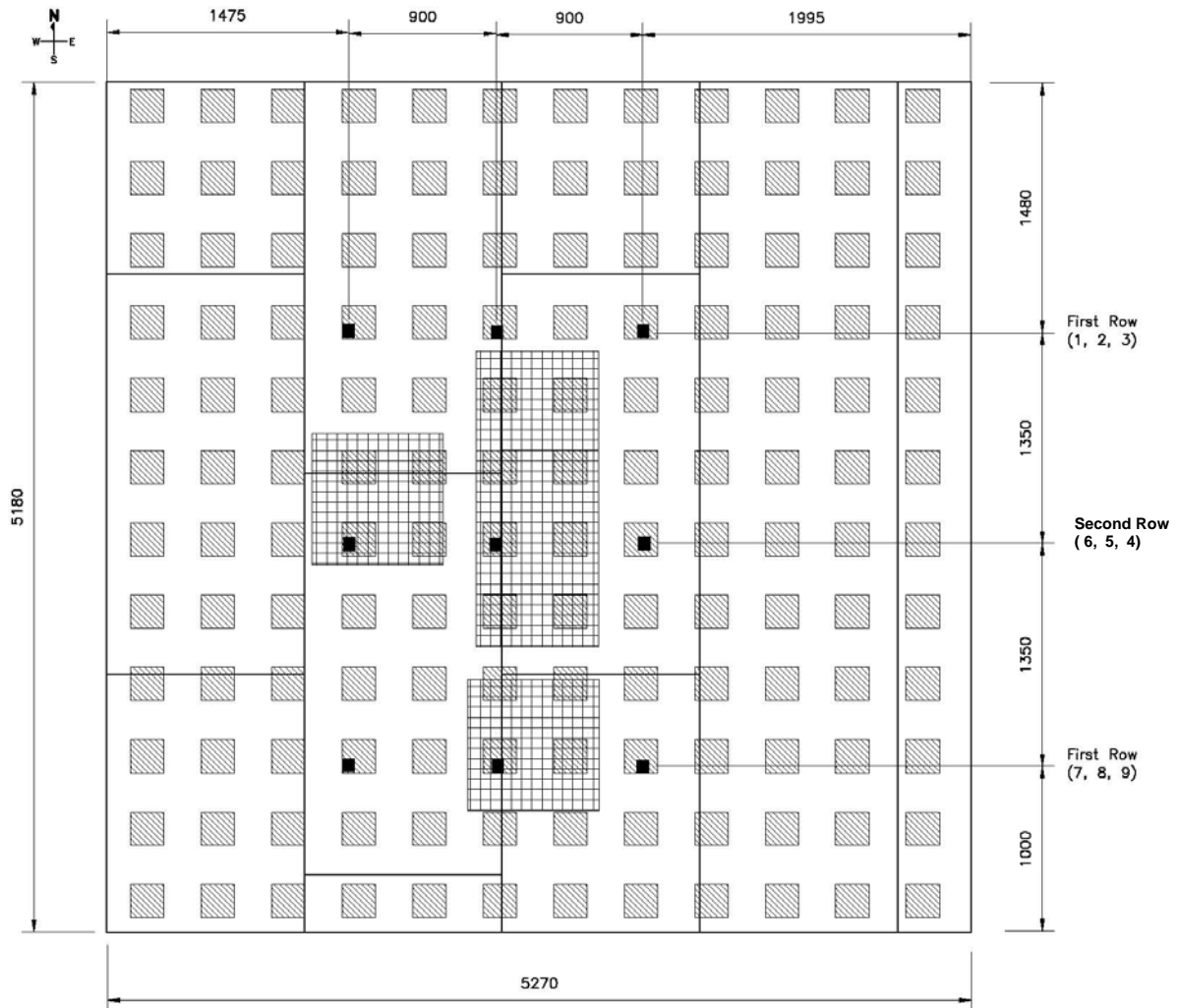
Figure 42 (a) shows the deflections measured in the first row (1, 2, and 3). Up to 400 s, the deflections were very small. After this time, the deflections increased at a relatively moderate rate, reaching a total of 75 to 80 mm after about another 400 s. The sharp increase in deflection close to 800 s is an indication that the floor assembly was deflecting at a high rate, which resulted in the blocks being dislodged and falling over. Visual observations through the window opening in the fire room also indicated that the blocks started falling through the subfloor around this time.

After 800 s, all the deflections were constant, which is an indication that the rods had reached their maximum gauge length and were not touching the concrete blocks (post test observations confirmed that the rods were hanging in the air). The times corresponding to the sharp increase in deflection and probable fall through of the blocks were 800 s, 795 s and 790 s for points 1, 2 and 3, respectively..

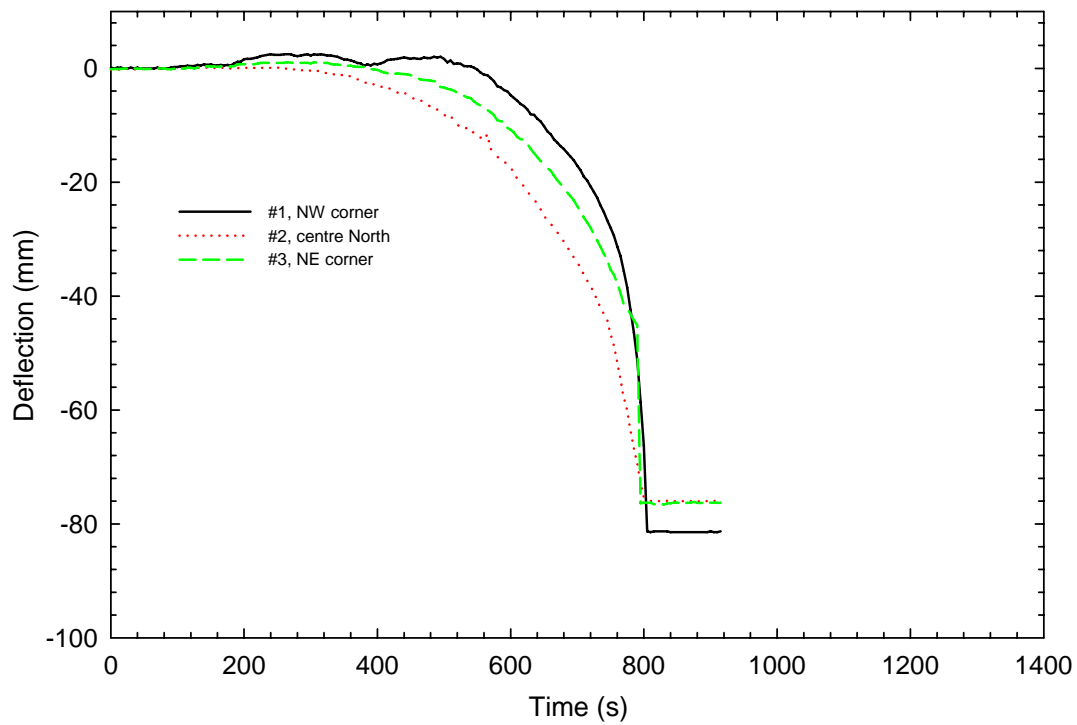
Figure 42 (b) shows the deflections measured in the second row (4, 5, and 6). Up to 300 s, the deflections were very small. After this time, the deflections increased at a relatively moderate rate, especially after 400 s, reaching a total of 75 to 85 mm after about another 450 s. For point No. 4, Figure 42 (b) shows that the deflection went straight down after reaching 50 mm at a time of 755 s. This was followed by a constant deflection after 755 s. For points No. 5 and 6, after 750s, the deflections were constant. This indicates that the rods had reached their maximum gauge length and were not touching the concrete blocks (post test observations confirmed that the rods were hanging in the air). The sharp increase in deflection close to 750 s is an indication that the floor assembly was deflecting at a high rate, which resulted in the blocks being dislodged and falling over. Visual observations through the rough window opening in the fire room also indicated that the blocks started falling through the subfloor around this time. The times corresponding to the sharp increase in deflection and probable fall through of the blocks are 755s, 740 s and 760 s for points 4, 5 and 6, respectively.

Figure 42 (c) shows the deflections measured in the third row (7, 8, and 9). Up to 400 s, the deflections were very small. After this time, the deflections increased at a relatively moderate rate, especially after 400 s, reaching a total of 75 to 83 mm after about another 400 s. At about 575 s, the deflections measured at the three locations show a sudden but brief downward movement, which may be explained by the sagging of the OSB subfloor between the joists. The rate of deflection was subsequently comparable to that for the other rows (located directly over the joists) but, like the others, the deflection continued to increase. At approximately 775 s, all the deflections were constant, which is an indication that the rods had reached their maximum gauge length and were not

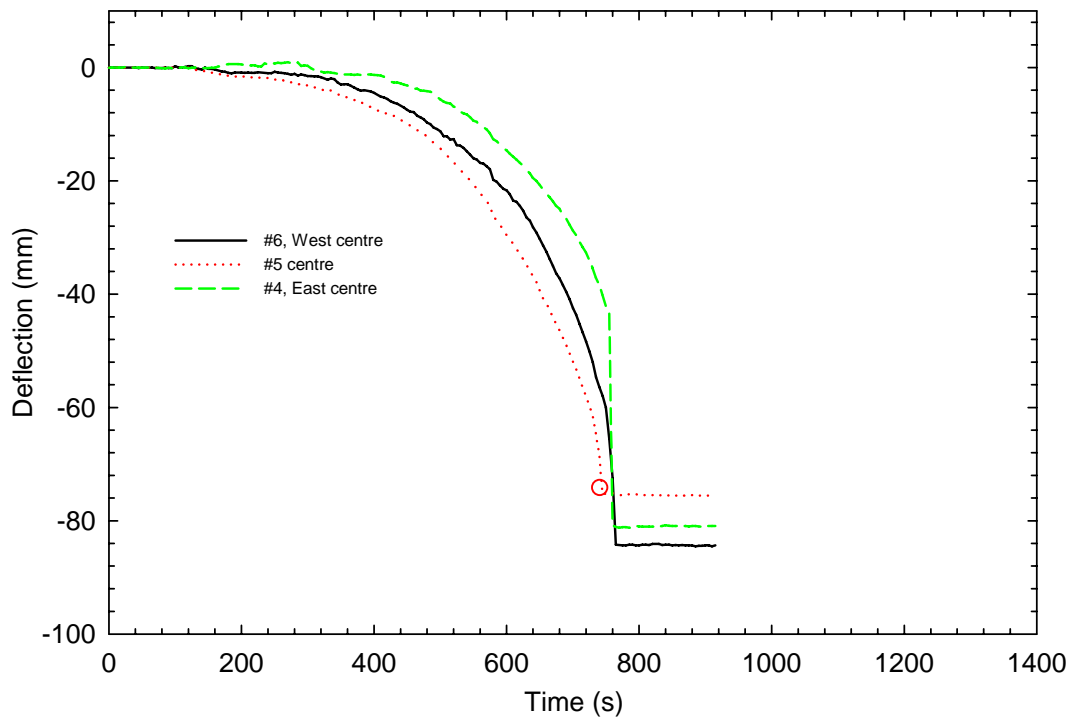
touching the concrete blocks (the after test observations confirmed that the rods were hanging in the air). The sharp increase in deflection close to 755 s is an indication that the floor assembly was deflecting at a high rate, which resulted in the blocks being dislodged and falling over. Visual observations through the rough window opening in the fire room also indicated that the blocks started falling through the subfloor around this time. The times corresponding to the sharp increase in deflection and probable fall through of the blocks are 785 s, 775 s and 785 s for points 7, 8 and 9, respectively. The time of terminating the test was 820 s.



**Figure 41. Deflection points measured (all dimensions in mm)**

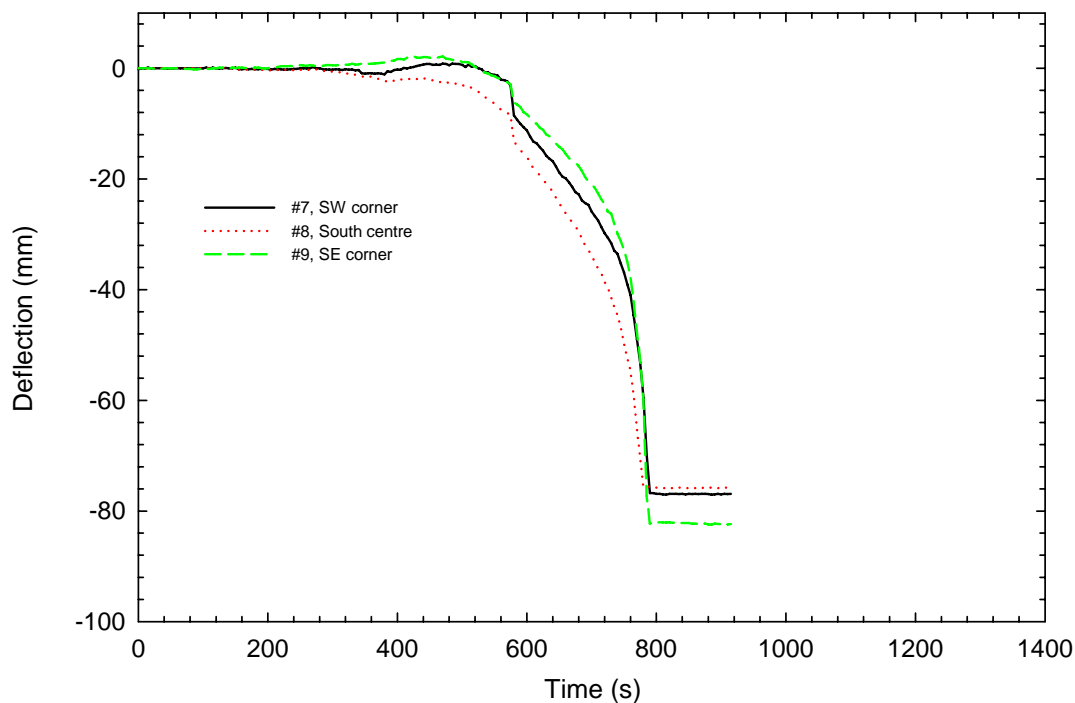


a) Floor Deflection, for Row 1, Joist E-1



b) Floor Deflection, for Row 2, Joist H-1

**Figure 42 (a and b). Deflection measurements for rows 1, 2 and 3 for UF-01**



c) Floor Deflection, for Row 3, Joist K-1

**Figure 42 (c). Deflection measurements for rows 1, 2 and 3 for UF-01**

### 3.4.2 For Test UF-02

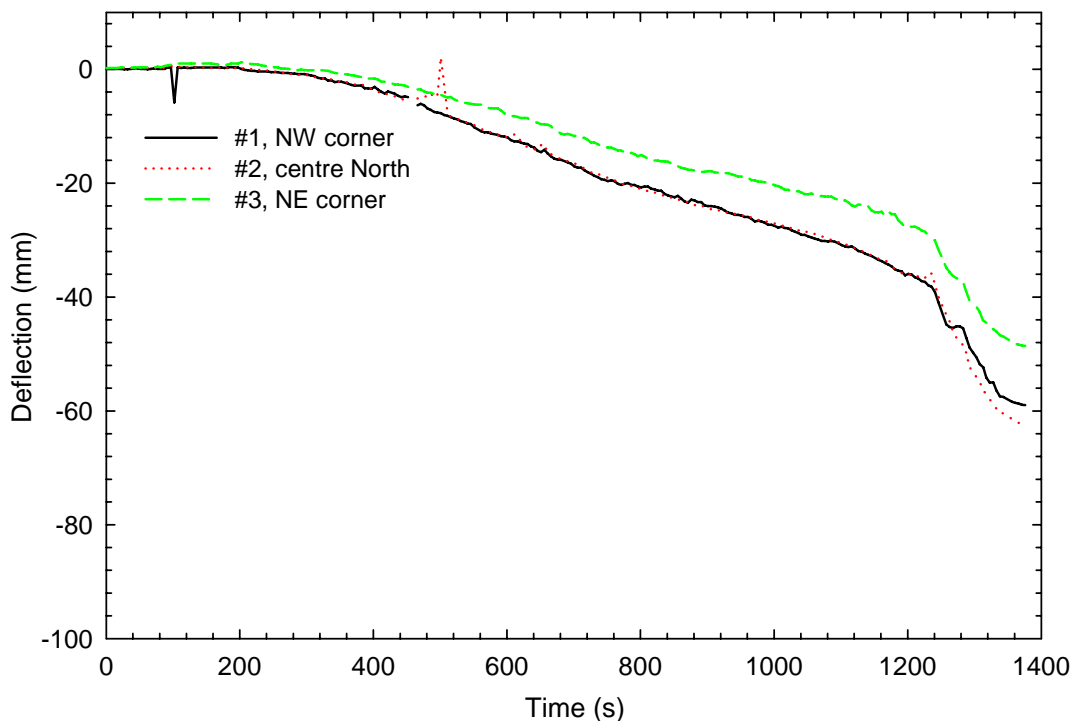
Figure 43 (a) shows the deflections measured in the first row (1, 2, and 3). Up to 400 s, the deflections were very small. After 400 s, the deflections increased at a relatively slow rate and reached 40, 40 and 24 mm for points 1, 2 and 3, respectively, at about 1250 s. After this time, the deflections increased at a faster rate reaching 59, 63 and 49 mm for points 1, 2 and 3, respectively, at about 1380 s. Figure 43 (a) shows that unlike Figure 42 (a, b and c), there was no constant deflection measured prior to the end of the test for points 1, 2 and 3. This observation is an indication that the blocks on top of which these rods were resting had not fallen into the basement before the end the test. It may also indicate that part of the north side of the floor was still able to carry the blocks at the end the test, probably due to the fire exposure to the joists and subfloor being less severe in that region of the fire room (See Figure 44 for this observation)

Figure 43 (b) shows the deflections measured in the second row (4, 5, and 6). Up to 300 s, the deflections were very small. After this time, the deflections increased at a relatively moderate rate, especially after 400 s, reaching a total of 80 to 85 mm after an additional 800 s. For point No. 4, Figure 43 (b) shows that the deflection went straight down after reaching 40 mm at a time of 1200 s. This was followed by a constant deflection after 1200 s. For points No. 5 and 6, after 1230s, the deflections were constant. This indicates that the rods had reached their maximum gauge length and were not touching the concrete blocks (post test observations confirmed that the rods were hanging in the air). The sharp increase in deflection after 1200 s is an indication

that the floor assembly was deflecting at a high rate, which resulted in the blocks being dislodged and falling over. Visual observations through the window opening in the fire room also indicated that the blocks started falling through the subfloor around this time. The times corresponding to the sharp increase in deflection and probable fall through of the blocks are 1200, 1230 s and 1240 s for points 4, 5 and 6, respectively.

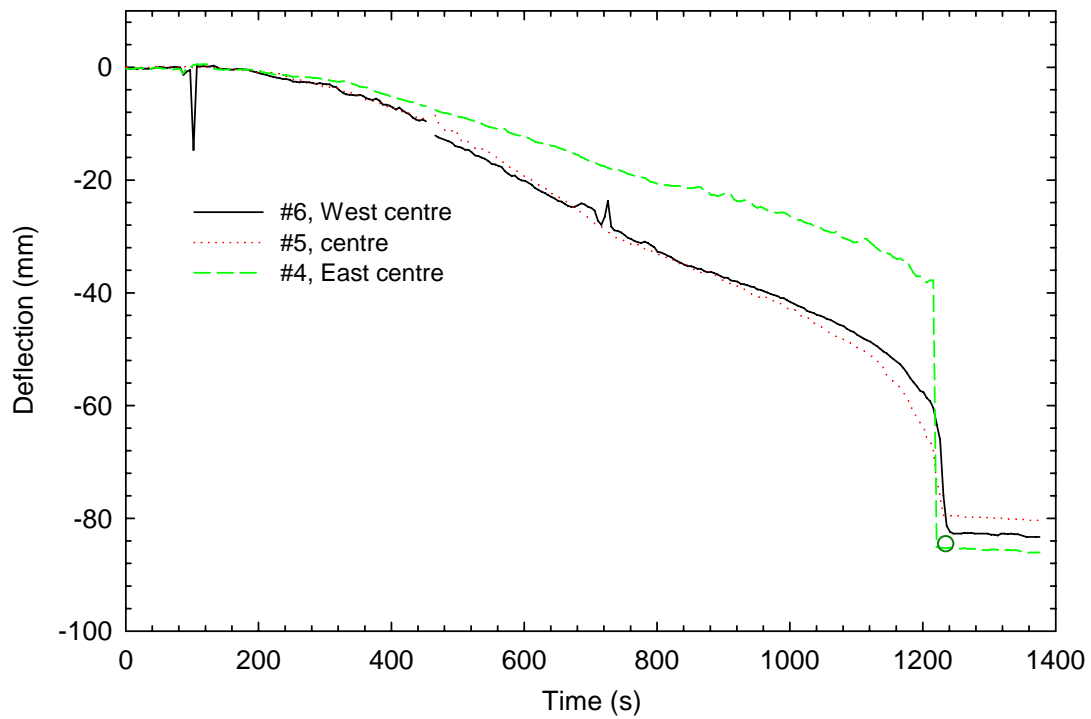
Figure 43 (c) shows the deflections measured in the third row (7, 8, and 9). Up to 300 s, the deflections were very small. After this time, the deflections increased at a relatively moderate rate, which increased somewhat after 1080 s, reaching a total of 81 to 92 mm at about 1200 s. At approximately 1200 s, all the deflections were constant, which is an indication that the rods had reached their maximum gauge length and were not touching the concrete blocks (post test observations confirmed that the rods were hanging in the air). The sharp increase in deflection after 1200 s is an indication that the floor assembly was deflecting at a high rate, which resulted in the blocks being dislodged and falling over. Visual observations through the window opening in the fire room also indicated that the blocks started falling through the subfloor around this time. The times corresponding to the sharp increase in deflection and probable fall through of the blocks are 1220 s, 1200 s and 1220 s for points 7, 8 and 9, respectively. The time of terminating the test was 1280 s.

A comparison of the two tests (UF-01 and UF-02) show that the scenario with the door closed results in a less severe fire impact, consequently the loadbearing capacity of the joists and subfloor was extended, which, in turn, delayed the deflection of the floor and therefore the structural failure of the burning floor. The shortest time to reach the maximum deflection in each test (740 s for UF-01 and 1200 s for UF-02) was taken as the time after which the floor structure would be no longer usable for egress.

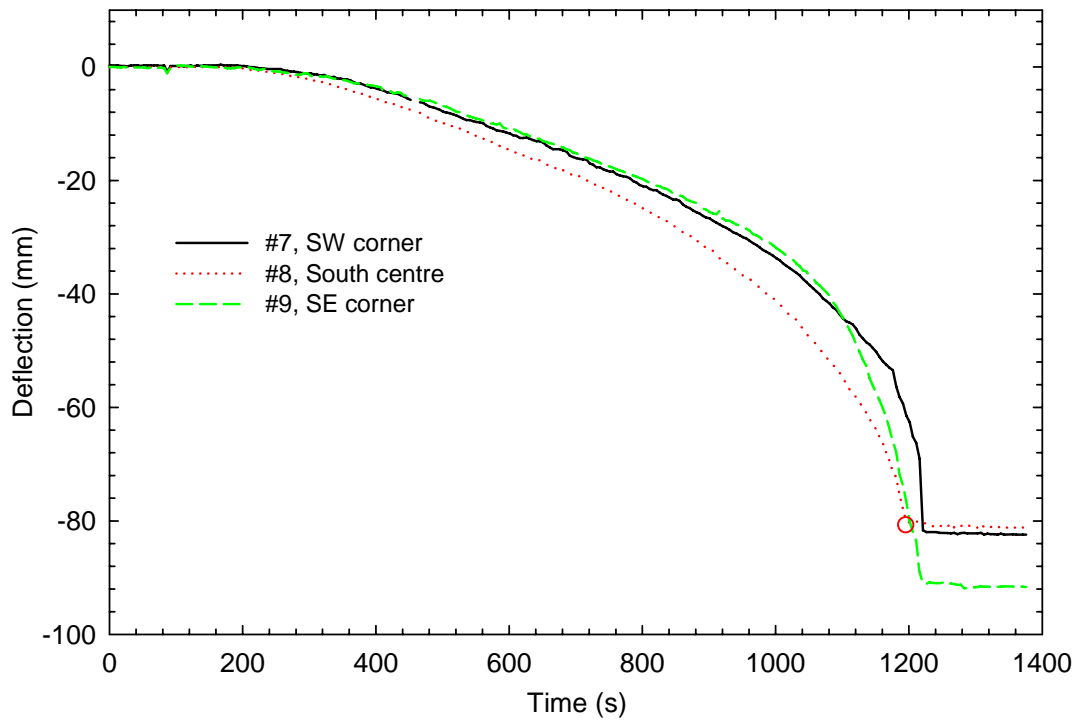


a) Floor Deflection, for Row 1, Joist E-1

**Figure 43 (a). Deflection measurements for rows 1, 2 and 3 for UF-02**



b) Floor Deflection, for Row 2, Joist H-1



c) Floor Deflection, for Row 3, Joist K-1

**Figure 43 (b and c). Deflection measurements for rows 1, 2 and 3 for UF-02**



**Figure 44. Picture showing the north side holding the concrete blocks for UF-02**

### **3.5 Flame Penetration Results**

Flame penetration through the floor assembly is one of the important aspects of fire performance that is of interest in this project since this is also a failure criterion in standard fire resistance testing. Flames and combustion products penetrating through the subfloor can impact on the time available for evacuation. Any opening(s) created by the flames penetrating the subfloor or excessive deflection would provide a means for hot fire gases to migrate from the basement fire room to the upper storey(s). As well, the holes would add to the overall weakening of the subfloor. To determine whether there was flame penetration through the floors, both a flame-sensing device and the time-temperature curves on the unexposed side of the floors were used. As mentioned before, the flame-sensing device was only employed in Test UF-02 after it was found that cameras were unable to monitor flame penetration in Test UF-01.

### 3.5.1 For Test UF-01

Since the flame-sensing device was not used in Test UF-01, Figure 37 (a) and Figure 24 were used in helping to determine time to flame penetration. As shown in Figure 37 (a) (Thermocouples 1 to 9 on the unexposed side), locations 1, 3, 6, 7 and 9 all show a sharp increase in temperatures at about 720 s, 780 s, 780 s, 760 s and 760 s, respectively. This may be an indication that flames started penetrating at these times. In addition, Figure 24 (a) shows the time-temperature curves at different heights at the middle of the South-East quadrant of the first storey. As illustrated in the figure, there was an increase in temperatures at about 760 s indicating the possibility of flames penetrating to the unexposed side of the floor and hot smoke migrating to the upper storeys. Figure 24 (b, c and d) (SW, NE and NW on the 1<sup>st</sup> storey) shows similar trends to Figure 24 (a) (SE) probably due to the additional heat and smoke spreading from the basement to the first storey through the floor. The temperature levels were however lower in these quadrants.

### 3.5.2 For Test UF-02

Figure 45 shows the results from the three flame-sensing devices, which were installed on the top of three joints (East, Centre and West) on the unexposed side of the floor as shown in Figure 19 (instrumentation figure). There was an increase in the voltage output of the device when flames penetrating through the floor struck the device. As indicated by Figure 45, the flame penetrated first through the East joint at 615 s, then the Centre joint at 1115 s, and finally the West joint at 1260 s.

Figure 38 (Thermocouples 1 to 9 and 92 to 97 on the unexposed side) shows an increase in temperatures at locations 1, 3, 4, 7, 8 and 9 at about 640 s, 1180 s, 1220 s, 1160 s, 1100 s and 1040 s, respectively. This may be an indication of flame penetration through the floor at these times. These times are also close to the times recorded by the flame-sensing device. In addition, Figure 25 (a) shows time-temperature curves at different heights at the middle of the South-East quadrant of the first storey. As illustrated in the figure, there was an increase in temperatures at about 1180 s indicating the possibility of flames penetrating to the unexposed side of the floor and hot smoke migrating to the upper storeys. Figure 25 (b, c and d) (SW, NE and NW on the first storey) shows similar trends to Figure 25 (a) (SE) probably due to the additional heat from the flames and smoke spreading from the basement to the first storey through the floor. The temperature levels were however lower in these quadrants.

For Test UF-02, the flame penetration started first in the east side of the floor assembly. This can be attributed to the fact that the opening of the basement window and the door to the outside (1<sup>st</sup> door storey) may have created path for air to travel between the two openings (window and door) with the east side of the fire compartment as the easier path for this air movement. This also resulted in earlier flame penetration through at least one joint on the east side of the assembly. The times for flame penetration through the other joints were much later (almost double). This was not the case for UF-01, because having the basement doorway open, at the start of the test, facilitated the movement of air without the need to find any other paths through the floor assembly.

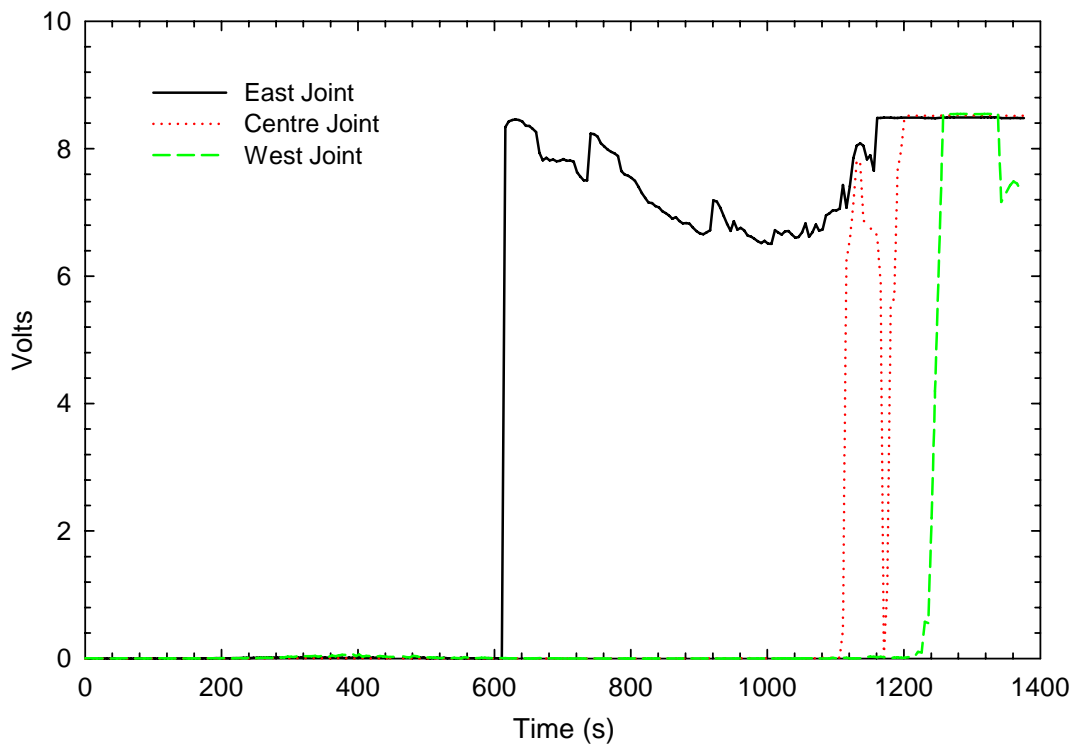


**Figure 45. Results of flame sensors at different joints**

### 3.6 Detection Times

Residential photoelectric and ionization smoke alarms were installed on the ceiling in each bedroom, second storey corridor, first storey and the basement fire compartment. These smoke alarms were powered by batteries and were not interconnected. The ionization smoke alarm was not installed in the basement fire room in order to avoid dealing with radioactive materials in the cleanup of debris after the fire tests. Since photoelectric smoke alarms are generally slower in detecting flaming fires than ionization smoke alarms, using the photoelectric smoke alarms in the basement resulted in more conservative estimates for activation times for the fire scenarios used in the experiments. New smoke alarms were used in each experiment.

Table 2 shows the activation times of the smoke alarms installed in the test facility. The photoelectric smoke alarms in the basement fire compartment took 40-42 s to activate. With the open basement doorway, it took up to 95 s longer for the smoke alarms in the second storey corridor to activate and up to 165 s longer for the smoke alarms in the closed bedroom to activate. With the closed basement doorway, the smoke alarms installed on the upper storeys took even longer to activate – up to 140 s longer for the smoke alarms in the second storey corridor and up to 500 s longer for the smoke alarms in the closed bedroom. This highlights the importance of having the smoke alarms interconnected to activate simultaneously when one of them detects a fire.

Note that in Test UF-02 the ionization smoke alarm on the first storey activated as quickly as the one in Test UF-01. This may be attributed to the fact that although the door to the basement was closed in Test UF-02, smoke was migrating through perimeter/edges of the floor assembly and the basement door in the first few minutes of the test. In Test UF-02, the photoelectric smoke alarm in the SW bedroom on the second storey did not activate and it is believed that this smoke alarm malfunctioned.

**Table 2. Smoke Alarm Activation Times after Ignition (in seconds)**

Location	Basement fire room	First storey		Second storey corridor		SE bedroom (door closed)		SW bedroom (door open)	
Type of Smoke Alarm	P	I	P	I	P	I	P	I	P
UF-01	40	75	85	125	135	200	205	140	150
UF-02	42	72	97	172	182	427	541	212	N/A

Notes:

1. See section on instrumentation in compartment (Figure 8 to Figure 10)
2. I: ionization, P: photoelectric, SE: South East, SW: South West, N/A: no activation

### 3.7 Results of Smoke and Gas Measurements and Tenability Analysis

Fires produce heat, narcotic and irritant gases, and smoke that obscures vision. The temperature and the production of combustion products depend upon the fire characteristics, enclosure geometry and ventilation. The increased temperature and combustion products can, either individually or collectively, create conditions that are potentially untenable for occupants.

Tenability analysis involves examination of the production of heat and toxic products of combustion during the fire tests. It also involves estimation of the potential exposure of occupants, who would have been in the test house, to heat and toxic smoke and of the potential effects as a result of the exposure. The purpose of tenability analysis is to provide an estimation of the time available for escape — the calculated time interval between the time of ignition and the time after which conditions become untenable for an individual occupant.

There are various endpoints for tenability analysis, such as incapacitation, lethality/fatality, etc. For this project, *incapacitation* – a state when people lose the physical ability to take effective action to escape from a fire – was chosen as the endpoint for the tenability analysis related to heat and toxic products of combustion. The time available for escape thus calculated is the interval between the time of ignition and the time after which conditions become incapacitating for an individual occupant.

ISO 13571 and the SFPE Handbook of Fire Protection Engineering provide guidance and methodologies for evaluating the time available for occupants to escape from a fire [15, 16]. These methodologies are used in this report to calculate the time available for escape as an input to the hazard analysis for each fire scenario used in the project. The methodologies include a fractional effective dose (FED) approach to quantify the time at which the accumulated exposure to each fire effluent exceeds a specified threshold

criterion for incapacitation. This time then is taken to represent the time available for escape relative to the specified threshold.

The calculated time available for escape depends not only on the time-dependent temperatures, concentrations of combustion gas products and density of smoke in the test house, but also on the characteristics of occupants. The age and health of the occupants (such as body weight and height, lung and respiratory system function, blood volume and hemoglobin concentration, skin, vision, etc.) as well as the degree of activity at the time of exposure have an effect on the consequences of exposure to fire effluents and heat. Since the general population has a wide range of susceptibility to fire effluents and heat, the exposure thresholds for incapacitation can change from subpopulation to subpopulation. Thus, each occupant is likely to have a different time available for escape.

This section of the report does not try to debate what FED criterion should be used as the incapacitation threshold but rather to present the results of the analysis for 2 typical FED values (e.g.  $FED = 1$  and  $FED = 0.3$ ). The methodology can be used to estimate the time available for escape associated with other FED values, if required.

The time available for escape calculated based on  $FED = 1$  represents the time available for a healthy adult of average susceptibility. The distribution of human responses to the fire effluents is unknown but is assumed to be a logarithmic normal distribution [15]. Under this distribution, the time available for escape calculated at  $FED = 1$  also represents statistically the time by which 50% of the general population would have been incapacitated but the conditions would still be tenable for the other 50% of the population.

For a more susceptible person, the threshold can be lower and the time available for escape would be shorter than for an average healthy adult. If  $FED = 0.3$  is used as a criterion to determine the time available for escape, it would statistically represent the time by which 11% of the population would have been incapacitated but the conditions would still be tenable for the other 89% of the population [15].

The location of the occupant who would have been in the test house has an effect on the time available for escape. The analysis focused on the fire conditions affecting tenability, as measured on the first and second storeys of the test facility, and the impact on any occupant assumed to be present on the upper storeys of the test house at the time of ignition. In real fire situations, the occupant would move through different locations during egress. Therefore, the time to incapacitation would be in-between the times calculated for different locations. The conditions in the basement fire room would not be survivable once flashover occurred.

The methodology used does not address quantitatively any interaction (combined effects) between heat, combustion gas products and smoke obscuration. Each component is treated as acting independently on the occupants to create incapacitating conditions and the time available for escape is the shortest of the times estimated from consideration of exposure to combustion gas products, heat and visual obscuration.

It is necessary to recognize that 2 types of uncertainty exist in the tenability analysis: the uncertainties associated with the experimental data and the uncertainties associated with the equations used for FED calculations. Fortunately, with the fast-growing fire

used in the project, the resulting uncertainty in the estimated time available for escape is much smaller than the uncertainty in the calculated FED due to their non-linear relationship. More details are provided in the following sections.

### 3.7.1 Exposure to Toxic Gases

Exposure to toxic products of combustion from fires has been a major cause of death and injury in many fire incidents. Understanding the toxic effect of the smoke products and predicting the exposure time necessary to cause incapacitation are complex problems.

In regards to the fuel package used in this study, with the combined flaming combustion of polyurethane foam and wood cribs, the primary gas products were toxic carbon monoxide (CO) and asphyxiant carbon dioxide (CO<sub>2</sub>) in a vitiated oxygen (O<sub>2</sub>) environment. Given the amount of polyurethane foam in the fuel package and the volume of the test house, hydrogen cyanide (HCN) produced from the combustion of polyurethane foam would not reach a concentration of concern for occupant life safety. A literature review by Beyler concluded that exposure to products of flaming combustion of flexible polyurethane foam would result in CO levels in the blood of test animals generally consistent with simple CO exposure, despite the toxicological role of HCN [17]. The fuel package contained no chemical components that would produce acid halides in the combustion gases. In this report, the analysis involved CO and CO<sub>2</sub> and oxygen vitiation only.

Table 3 shows the maximum CO and CO<sub>2</sub> concentrations and the minimum O<sub>2</sub> concentrations for Tests UF-01 and UF-02. Data from the fire scenario Tests FS-1 and FS-4 are also included in Table 3 for comparison; more information on Tests FS-1 and FS-4 can be found in a data compilation report [6]. The O<sub>2</sub> vitiation, CO and CO<sub>2</sub> production were much larger in Tests UF-01 and UF-02 than in Tests FS-1 and FS-4, respectively. All gas analyzers used had an upper limit of 10% for CO<sub>2</sub> measurements. The gas analyzer used for the first storey at the 1.5 m height had an upper measurement limit of 5% CO. All other gas analyzers had a measurement limit of 1% CO.

Figure 46 to Figure 48 and Figure 50 to Figure 52 (figures commence on page 89) show the CO, CO<sub>2</sub> and O<sub>2</sub> concentration-time profiles measured during Tests UF-01 and UF-02. Note that in Test UF-01 (see Figure 48) the CO<sub>2</sub> concentration profile above the 10% measurement range for the analyzer was calculated for the first storey at the 1.5 m height using the measured O<sub>2</sub> and CO concentrations ( $\text{CO}_2\% = 20.9\% - \text{O}_2\% - \frac{1}{2} \text{CO}\%$ ).

In Test UF-01, the fire quickly changed from a well-ventilated flaming to an under-ventilated post-flashover fire, as indicated by a decrease in the CO<sub>2</sub>/CO ratio from 50 to 4 in 180 s. The gases were well mixed in the house in Test UF-01.

The SFPE Handbook of Fire Protection Engineering contains information on the tenability limits for incapacitation or death after a 5-min exposure [16], shown in Table 4, which indicate the test results that need to be analyzed. In the following sections, tenability due to each gas is first analyzed independently; the interaction between gases is then considered.

**Table 3. Maximum CO and CO<sub>2</sub> Concentrations and Minimum O<sub>2</sub> Concentration (%)**

		Test FS-1	Test FS-4	Test UF-01	Test UF-02
2 <sup>nd</sup> storey 1.5 m high	CO	0.62 @ 300 s	0.08 @ 760 s	>1 @ 215 s	>1 @ 730 s
	CO <sub>2</sub>	9.4 @ 450 s	1.0 @ 1200 s	>10 @ 335 s	7.0 @ 1180 s
	O <sub>2</sub>	10.8 @ 430 s	19.5 @ 1200 s	3.0 @ 740 s	13.4 @ 1180 s
2 <sup>nd</sup> storey 0.9 m high	CO	0.61 @ 305 s	0.08 @ 760 s	>1 @ 225 s	>1 @ 756 s
	CO <sub>2</sub>	9.5 @ 460 s	1.2 @ 1200 s	>10 @ 350 s	7.1 @ 1180 s
	O <sub>2</sub>	10.9 @ 430 s	19.6 @ 1200 s	3.6 @ 740 s	13.5 @ 1180 s
1 <sup>st</sup> storey 1.5 m high	CO	0.57 @ 285 s	0.06 @ 760 s	3.5 @ 450 s	2.5 @ 1060 s
	CO <sub>2</sub>	9.1 @ 420 s	0.95 @ 1200 s	>10 @ 320 s 16* @ 740 s	6.2 @ 1180 s
	O <sub>2</sub>	11.0 @ 420 s	19.8 @ 1200 s	2.9 @ 740 s	14.1 @ 1180 s
1 <sup>st</sup> storey 0.9 m high	CO	0.58 @ 285 s	0.06 @ 840 s	>1 @ 215 s	>1 @ 806 s
	CO <sub>2</sub>	9.3 @ 435 s	0.95 @ 1200 s	>10 @ 335 s	7.0 @ 1180 s
	O <sub>2</sub>	10.9 @ 430 s	19.9 @ 1200 s	3.0 @ 740 s	13.9 @ 1180 s

Notes:

1. ">" indicating the concentration beyond the measurement range of the gas analyzer;
2. For UF-01 and UF-02, all concentrations before the structural failure;
3. \*calculated: CO<sub>2</sub>% = 20.9% - O<sub>2</sub>% - ½ CO%
4. For FS -1 and FS-4, all concentrations before fire suppression.

**Table 4. Tenability Limits for Incapacitation or Death after 5-min Exposure [16]**

Gas	Incapacitation	Death
CO	6000 – 8000 ppm (0.6 – 0.8%)	12,000 – 16,000 ppm (1.2 – 1.6%)
Low O <sub>2</sub>	10 – 13%	< 5%
CO <sub>2</sub>	7 – 8%	> 10%

### 3.7.1.1 Exposure to O<sub>2</sub> vitiation

Fires consume oxygen and create a low oxygen atmosphere. Past human experiments in an oxygen-depleted atmosphere indicated that most people could tolerate a 15% O<sub>2</sub> atmosphere [16]. Healthy individuals could also tolerate a 12% O<sub>2</sub> level for a short period (<5 min) [18]. When oxygen diminished to below 10%, unconsciousness could occur rapidly. For healthy adults, the following equation was derived from the experiments with human subjects [16] and can be used to predict the time,  $t_{in,O_2}$  (minute), to loss of consciousness due to lack of oxygen alone.

$$t_{in,O_2} = \exp[8.13 - 0.54(20.9 - \%O_2)]$$

With the changing O<sub>2</sub> concentration, the fractional effective dose approach has to be used in the analysis. The incapacitation dose for oxygen vitiation can be expressed by  $(20.9 - \%O_2) \times t_{in,O_2}$ . The fractional effective dose is the accumulation of the ratio of the actual exposure dose  $(20.9 - \%O_2) \times \Delta t$  and the incapacitation dose at each discrete increment of time:

$$F_{in,O_2} = \sum_{t1}^{t2} \frac{(20.9 - \%O_2) \cdot \Delta t}{(20.9 - \%O_2) \cdot t_{in,CO_2}} = \sum_{t1}^{t2} \frac{\Delta t}{\exp[8.13 - 0.54(20.9 - \%O_2)]}$$

where  $\Delta t$  (*minute*) is the discrete increment of time, i.e. the time interval for data sampling. Table 5 shows the calculated times for the fractional effective dose reaching 0.3 and 1.0 for exposure to  $O_2$  vitiation alone.

In Test UF-01 (see Figure 47), the  $O_2$  concentration on both the first and second storeys dropped to below 10% in 300 s and to 3% at the end of the test. The  $O_2$  vitiation alone would cause incapacitation after 440-450 s (1<sup>st</sup> storey-2<sup>nd</sup> storey) using  $F_{in,O_2} = 1$  as a criterion, or after 370-380 s (1<sup>st</sup> storey-2<sup>nd</sup> storey) using  $F_{in,O_2} = 0.3$ .

In Test UF-02 (see Figure 51), the  $O_2$  concentrations in both storeys were above 15% for the first 18 min (1080 s). The  $O_2$  concentrations fell from 14 to 2-3% at 20 min (1200 s). The fractional effective dose increased from  $F_{in,O_2} = 0.07$  at 1200 s to  $F_{in,O_2} > 1$  in less than 30 s. The  $O_2$  vitiation alone would not result in incapacitation until 20 min after ignition.

### 3.7.1.2 Exposure to $CO_2$

$CO_2$  is not toxic at concentrations of up to 5%. Above 7%,  $CO_2$  becomes an asphyxiant gas; the danger of loss of consciousness of an exposed person increases. Loss of consciousness could occur in approximately 2 minutes at 10%  $CO_2$ , for example. The following equation can be used to predict the time,  $t_{in,CO_2}$  (*minute*), to loss of consciousness due to the  $CO_2$  asphyxiant effect [16]:

$$t_{in,CO_2} = \exp(6.1623 - 0.5189 \cdot \%CO_2)$$

With the changing  $CO_2$  concentration, the fractional effective dose approach has to be used. The incapacitation dose for  $CO_2$  exposure can be expressed by  $\%CO_2 \times t_{in,CO_2}$  above which loss of consciousness would occur for people of average susceptibility. At each discrete increment of time, the increment of the fractional effective dose was calculated as the actual exposure dose ( $CO_2$  concentration  $\times$  time increment) divided by the incapacitation dose. The fractional effective dose values expressed in Table 5 are the accumulation of this ratio of each time increment:

$$F_{in,CO_2} = \sum_{t1}^{t2} \frac{\%CO_2 \cdot \Delta t}{\%CO_2 \cdot t_{in,CO_2}} = \sum_{t1}^{t2} \frac{\Delta t}{\exp(6.1623 - 0.5189 \cdot \%CO_2)}$$

In Test UF-01 (see Figure 48), the  $CO_2$  concentration exceeded 10% (measurement range limit of the gas analyzers) in 360 s. Note that the  $CO_2$  concentration profile above the 10% measurement range was calculated for the first storey at the 1.5 m height using the measured  $O_2$  and CO concentrations ( $CO_2\% = 20.9\% - O_2\% - \frac{1}{2} CO\%$ ). The increased concentration of  $CO_2$  alone would cause incapacitation after 390-420 s (1<sup>st</sup>

storey-2<sup>nd</sup> storey) using  $F_{in,CO_2} = 1$  as a criterion, and after 320-335 s (1<sup>st</sup> storey-2<sup>nd</sup> storey) using  $F_{in,CO_2} = 0.3$ . These times (320-335) are slightly shorter than that in Test FS-1 (i.e., 380 s for  $F_{in,CO_2} = 0.3$  on both storeys) without the presence of any combustible floor assembly.

In Test UF-02 (see Figure 52), the CO<sub>2</sub> concentrations in both storeys were below 5% for the first 15 min. Even if using  $F_{in,CO_2} = 0.3$  as a criterion, CO<sub>2</sub> alone would not cause incapacitation until 20 min after the ignition.

### 3.7.1.3 Exposure to CO

CO is known to be the most important toxicant of the fire gases. The lowest CO concentration in air that has been reported to cause human death is 5,000 ppm for a 5 min exposure [19]. The toxic effect of CO is due to its affinity with the hemoglobin in human blood to form carboxyhemoglobin (COHb), which reduces the transport of oxygen in the blood to various parts of the body. When COHb in the blood increases to a threshold concentration, loss of consciousness or death may occur. The time for the toxic effect to occur depends on the uptake rate of CO into the blood of a victim and the threshold COHb concentration for that victim.

The CO uptake rate is determined by the difference between the CO concentration inhaled and that already in the body, and varies with the breathing rate, the degree of activity, the lung function, the body size, the blood volume and hemoglobin concentration of the victim and the exposure duration. The complexity of the CO uptake is described by the theoretical Coburn-Forster-Kane (CFK) equation, which takes account of a wide range of variables to predict the COHb concentration [20]. For high-concentration and short-duration exposures such as the fire scenarios used in the FPH tests, one can use a simpler equation that was derived from human exposure experiments with healthy adults [16, 21]:

$$\%COHb = 3.317 \times 10^{-5} [CO]^{1.036} RMV \cdot t$$

where  $[CO]$  is the inhaled carbon monoxide concentration in *parts per million*,  $RMV$  (respiratory minute volume) is the volume of air breathed in *litres per minute*, and  $t$  is the exposure duration in *minutes*. This equation gives equally good predictions as the CFK equation for average healthy adults. Since the CO concentration in the experiments varied with time, %COHb was calculated as a summation of the CO uptake at each discrete time step:

$$\%COHb = \sum_{t_0}^t 3.317 \times 10^{-5} [CO]^{1.036} RMV \cdot \Delta t$$

For an average adult, the normal breathing rate is 20 L/min with light activity. The breathing rate is affected by the presence of CO<sub>2</sub> in a fire situation. In the concentration range of 2 to 6%, CO<sub>2</sub> can stimulate breathing. A CO<sub>2</sub>-induced hyperventilation factor,  $VCO_2$ , for breathing can be estimated using [16]:

$$VCO_2 = \exp\left(\frac{\%CO_2}{5}\right)$$

The hyperventilation increases the uptake rate of other toxic gases, such as CO, from the fire. This effect should be considered when CO<sub>2</sub> concentration is above 2%. The presence of 5% CO<sub>2</sub> could triple the normal breathing rate, for example. Considering the CO<sub>2</sub>-induced hyperventilation in a fire situation, the breathing rate would be

$$RMV = 20 \cdot \exp\left(\frac{\%CO_2}{5}\right)$$

For the same individual, the CO uptake rate changes if the breathing rate changes, which also depends on the degree of activity of that individual. The CO uptake rate varies from person to person for a given smoke atmosphere.

The COHb incapacitating concentration at which loss of consciousness may occur is in the range of 25-40% depending on the degree of activity of the occupant among other variables [16, 22]. The threshold of 40% is more appropriate for those at rest and 30% for those engaged in light activity [16]. Certain susceptible populations may be incapacitated at lower COHb concentrations.

With the rate of CO uptake and the likely incapacitating concentration of COHb, time to incapacitation due to CO exposure can be predicted. For those engaged in light activity, the fractional effective dose for incapacitation due to the CO uptake can be expressed as the COHb concentration in the blood divided by the incapacitating COHb concentration

$$F_{in,CO} = \frac{\%COHb}{30} = 2.2113 \times 10^{-5} \sum_{t_0}^t [CO]^{1.036} \Delta t \cdot \exp\left(\frac{\%CO_2}{5}\right)$$

Alternatively, the fractional effective dose for incapacitation due to CO can also be calculated using the approach given in ISO TS 13571 for short exposure to CO at high concentrations [15]:

$$F_{in,CO} = \sum_{t_1}^{t_2} \frac{[CO] \cdot \Delta t}{35000} \exp\left(\frac{\%CO_2}{5}\right)$$

where the incapacitation dose is 35000 ppm-min, which is consistent with the tenability limits of 6000 to 8000 ppm for incapacitation for 5-min exposure given in the SFPE Handbook of Fire Protection Engineering [16]. For the FPH tests, the difference between the incapacitation times predicted using these two equations is relatively small.

The time to incapacitation determined using  $F_{in,CO} = 1$  as a criterion represents the time available for escape for healthy adults of average susceptibility. For more susceptible people, the exposure thresholds could be lower. The CO uptake and the COHb increase are known to be faster in small children than in adults [23]. Therefore, the incapacitation time for small children or a more susceptible subpopulation would be shorter than for average healthy adults. These can be addressed, to a certain degree,

by using  $F_{in,CO}=0.3$  as a criterion to determine the incapacitation time. Table 5 shows the calculated times for the fractional effective dose reaching 0.3 and 1.0. Calculation for the CO fractional effective dose was done with and without the CO<sub>2</sub> hyperventilation factor  $\exp(\%CO_2/5)$ .

In Test UF-01 (see Figure 46), the maximum CO concentration prior to failure of the floor assembly was 35000 ppm, which occurred at 450 s. The increased concentration of CO alone would cause incapacitation after 225-245 s (1<sup>st</sup> storey-2<sup>nd</sup> storey) using  $F_{in,CO} = 0.3$  as a criterion, and after 290-310 s (1<sup>st</sup> storey-2<sup>nd</sup> storey) using  $F_{in,CO} = 1.0$ . With CO<sub>2</sub>-induced hyperventilation, these times were reduced to 205-225 s (1<sup>st</sup> storey-2<sup>nd</sup> storey) for  $F_{in,CO} = 0.3$  and 235-255 s (1<sup>st</sup> storey-2<sup>nd</sup> storey) for  $F_{in,CO} = 1.0$ .

In Test UF-02 (see Figure 50), closing the door to the basement prolonged the time available for escape, compared to Test UF-01. In Test UF-02, the second storey became untenable earlier than did the first storey. Using  $F_{in,CO} = 0.3$  as a criterion, the increased concentration of CO alone would cause incapacitation after 382 s on the second storey and 491 s on the first storey; with CO<sub>2</sub>-induced hyperventilation, these times were reduced to 362 s on the second storey and 466 s on the first storey. Using  $F_{in,CO} = 1.0$  as a criterion, the increased concentration of CO alone would cause incapacitation after 571 s on the second storey and 741 s on the first storey; with CO<sub>2</sub>-induced hyperventilation, these times were reduced to 501 s on the second storey and 676 s on the first storey.

**Table 5. Time (in seconds) to the Specified Fractional Effective Dose for Exposure to O<sub>2</sub> Vitiation, CO<sub>2</sub> and CO**

	Test UF-01		Test UF-02	
Fractional Effective Dose	FED = 0.3	FED = 1.0	FED = 0.3	FED = 1.0
CO alone – 1 <sup>st</sup> storey	225	290	491	741
CO with CO <sub>2</sub> hyperventilation – 1 <sup>st</sup> storey	205	235	466	676
Low O <sub>2</sub> hypoxia – 1 <sup>st</sup> storey	370	440	1211	1216
CO alone – 2 <sup>nd</sup> storey corridor	245*	310*	382	571
CO with CO <sub>2</sub> hyperventilation – 2 <sup>nd</sup> storey corridor	225	255*	362	501
Low O <sub>2</sub> hypoxia – 2 <sup>nd</sup> storey corridor	380	450	1231	1253
High CO <sub>2</sub> hypercapnia – 1 <sup>st</sup> storey	320	390	1200	1270
High CO <sub>2</sub> hypercapnia – 2 <sup>nd</sup> storey corridor	335	420	1200	1290

Notes:

1. \* estimated using the CO profile on the first storey with a time shift (since the CO concentration on the second storey exceeded the measurement range of the gas analyzer, it was assumed that the CO profile on the second storey was the same as that on the first storey with a 20-s time shift);
2. Based on concentrations at 1.5 m height

### 3.7.1.4 Interaction of CO, CO<sub>2</sub> and O<sub>2</sub> vitiation

Interactions between these gases and their combined effect are not well understood. The asphyxiant effect of CO<sub>2</sub> is generally treated as being independent of other gases; the effect of O<sub>2</sub> vitiation (low oxygen hypoxia) is generally treated as being additive with the toxic effect of CO [16]. The effect of the smoke gases is determined by  $F_{in,CO_2}$  or  $(F_{in,CO} + F_{in,O_2})$ , whichever is larger (with  $F_{in,CO}$  including the effect of CO<sub>2</sub>-induced hyperventilation).

Table 6 shows examples of this treatment. The calculation shows that the O<sub>2</sub> vitiation did not add much to the effect at the time when CO was capable of producing incapacitation. CO was the most important toxicant of the smoke gases; increased CO uptake by CO<sub>2</sub>-induced hyperventilation was the most important interaction. Therefore, the exposure to CO with CO<sub>2</sub>-induced hyperventilation determined the incapacitation time for the gases analyzed. Assuming the rate of CO uptake remains unchanged, the time required from the incapacitation dose to the lethal dose for an average adult is estimated to be within 1 minute under the conditions of Test UF-01 and 2 minutes under the conditions of Test UF-02.

A recent paper by Gann includes an analysis of incapacitation by exposure to CO alone for a susceptible subpopulation such as people with coronary artery disease or small children; incapacitation could occur at an FED range of 0.14-0.21 (CO alone) [24]. As shown in Table 6, when the FED due to CO exposure with CO<sub>2</sub> hyperventilation reached 0.3, the FED due to CO exposure alone already reached this range. This shows consistency in the estimation of time to incapacitation.

For exposure to the gases, each calculation for estimating incapacitation in this section was associated with a particular position where the concentrations were measured – each calculated time applies to an occupant who would stay at that particular location. In real fire situations, the occupant would move through different locations during egress. Therefore, the time to incapacitation would be in-between the times calculated for different locations.

**Table 6. FED due to CO, CO<sub>2</sub>, O<sub>2</sub> Vitiation at Specified Time**

	<b>Test UF-01</b> 1 <sup>st</sup> storey SW quadrant 1.5 m height		<b>Test UF-02</b> 2 <sup>nd</sup> storey corridor 1.5 m height	
	<b>205 s</b>	<b>235 s</b>	<b>360 s</b>	<b>500 s</b>
Time				
CO alone	0.17	0.42	0.23	0.69
CO × CO <sub>2</sub> hyperventilation	0.34	1.09	0.30	1.0
Low O <sub>2</sub> hypoxia	0.003	0.009	0.003	0.005
CO × CO <sub>2</sub> hyperventilation + low O <sub>2</sub> hypoxia	0.34	1.10	0.30	1.0
High CO <sub>2</sub> hypercapnia	0.02	0.04	0.02	0.03

### 3.7.2 Exposure to Heat

Convected heat is the most important source of heat exposure for occupants in the first and second storeys. Figure 24 to Figure 27 and Figure 31 to Figure 34 show the temperature-time profiles measured on the two upper storeys during the tests. The temperatures at the 1.4 m height above the floor were used for the analysis of convected heat exposure.

The rate of convective heat transfer from hot gases to the skin depends on temperature, ventilation, humidity of the enclosure and clothing over the skin [16]. The tolerable time of exposure to convected heat is 15 min for dry air of 100°C or saturated air of 80°C. For hot air at temperatures above 120°C and with water vapour of less than 10%, pain and skin burns would be likely to occur in minutes; assuming unclothed or lightly clothed subjects, the time to incapacitation due to exposure to convected heat,  $t_{in,conv}$  (minutes), can be estimated for a constant temperature  $T$  (°C) using [15, 16]:

$$t_{in,conv} = 5 \times 10^7 T^{-3.4}$$

Since the temperatures in the FPH experiments were changing, the exposure was estimated using the fractional effective dose analogy at each discrete increment of time,  $\Delta t$  (minutes):

$$\frac{\Delta t}{t_{in,conv}} = \frac{T^{3.4}}{5 \times 10^7} \Delta t$$

When the temperature is increasing or stable, the fractional effective dose for incapacitation due to the convected heat exposure can be calculated using the following equation:

$$F_{in, heat} = \sum_{t_1}^{t_2} \frac{\Delta t}{t_{in, conv}} = \sum_{t_1}^{t_2} \frac{T^{3.4}}{5 \times 10^7} \Delta t$$

The calculated time to incapacitation due to the convected heat exposure is given in Table 7. Radiant heat is important when the hot smoke layer is over 200°C, which corresponds to the threshold radiant heat flux of 2.5 kW·m<sup>-2</sup> required to produce second degree burning of skin [25]. The calculation indicated that the convected heat exposure would result in incapacitation before the radiant heat began to play a major role on the first and second storeys.

Each calculation was associated with a particular position where the temperature was measured; in other words, each calculated time applies to an occupant who would stay at the location of a particular thermocouple tree. In real fire situations, the occupant would move through different locations during egress. Therefore, the time to incapacitation would be in-between the times calculated for different locations.

For Test UF-01, the convective heat exposure alone would produce incapacitation, but the time depended on the location in the test house. In the corridor on the second storey, the incapacitation time would be after 320 s and 435 s for  $F_{in,heat}=0.3$  and  $F_{in, heat}= 1$ ,

respectively. In the open bedroom, the incapacitation time would be after 455 s and 690 s for  $F_{in,heat} = 0.3$  and  $F_{in,heat} = 1$ , respectively. Heat exposure would not contribute to incapacitation in the closed bedroom ( $F_{in,heat} < 0.07$ ). On the first storey, the incapacitation time would be after 230-245 s using  $F_{in,heat} = 0.3$  as a criterion, and 280-300 s using  $F_{in,heat} = 1$ . The heat incapacitation times for Test UF-01 were similar to Test FS-1 (approximately 13 s shorter in average), the latter test being the one where the floor assembly over the basement level was noncombustible.

In Test UF-02, the closed door in the doorway to the basement fire room impeded the transport of hot gases to the upper storeys, as indicated by the temperature profiles (Figure 24 to Figure 34). Incapacitation due to heat exposure would not occur until 1100-1200 s after the ignition, which was near the end of the experiment. Heat exposure would not contribute to incapacitation in the closed bedroom.

**Table 7. Time (in seconds) to the Specified FED for Exposure to Convected Heat**

Fractional Effective Dose	Test UF-01		Test UF-02	
	FED = 0.3	FED = 1.0	FED = 0.3	FED = 1.0
1 <sup>st</sup> storey SE quadrant	235	290	1086	1196
1 <sup>st</sup> storey SW quadrant	230	280	1086	1196
1 <sup>st</sup> storey NE quadrant	245	300	1106	1201
1 <sup>st</sup> storey NW quadrant	245	300	1101	1201
2 <sup>nd</sup> storey corridor	320	435	1171	1241
2 <sup>nd</sup> storey open bedroom	455	690	1263	n.r. (FED<0.5)
2 <sup>nd</sup> storey closed bedroom	n.r. (FED<0.07)	n.r. (FED<0.07)	n.r. (FED<0.02)	n.r. (FED<0.02)

Notes:

1. Based on temperatures at 1.4 m height;
2. n.r. – not reached.

### 3.7.3 Visual Obscuration by Smoke

Visual obscuration by the optically dense smoke tended to be the first hazard to arise that could impede evacuation by the occupants. Although visual obscuration would not directly cause incapacitation, it would cause delays in movement by the occupants and thus prolong exposure of occupants to other hazards. In this report, the smoke obscuration is expressed as the optical density per meter ( $OD$  in  $m^{-1}$ ):

$$OD = \frac{1}{L} \log_{10} \left( \frac{I_0}{I} \right)$$

where  $I_0$  is the intensity of the incident light,  $I$  is the intensity of the light transmitted through the path length,  $L$  (m), of the smoke. The optical density is related to the extinction coefficient ( $k$  in  $m^{-1}$ ) by  $OD = k/2.303$ .

Studies by Jin indicated that the optical density of smoke and visibility through smoke are related (the visibility is proportional to the reciprocal of the  $OD$  for non-irritating smoke, for example) [26]. Various threshold  $OD$  values related to the loss of visibility have been suggested for small buildings with occupants familiar with the egress route.

The limiting  $OD$  value was suggested to be  $0.5 \text{ m}^{-1}$  for non-irritating smoke and  $0.2 \text{ m}^{-1}$  for irritating smoke [16,26]. A limiting  $OD$  value of  $0.5 \text{ m}^{-1}$  was also set by Babrauskas using the results of full-scale burns of upholstered chairs and mattresses [22,27]. A recent home smoke alarm study used an  $OD$  of  $0.25 \text{ m}^{-1}$  as the tenability limit for smoke obscuration [28]. In ISO 13571[15], the minimum visible brightness difference between an object and a background is used to estimate the smoke obscuration limit at which occupants cannot see their hands in front of their faces (a distance of 0.5 m or less). These calculations indicate that occupants cannot see their hands in front of their faces and become disoriented at an optical density of  $3.4 \text{ m}^{-1}$ . For an occupant whose vision is impaired, this can happen at an optical density of  $2 \text{ m}^{-1}$  or less.

Video records were also analyzed for visual obscuration. The video images became completely obscure when the optical density was approaching  $2 \text{ m}^{-1}$ . Note that there were at least 2 halogen lamps (2 x 500 Watts) providing lighting in the view direction of each video camera on the first and second storey. This lighting condition was much better than that in a real house.

In this report, a tenability limit for optical density is set at  $OD_{Limit} = 2 \text{ m}^{-1}$ , recognizing that this limit could be lower for people with impaired vision. The time to untenable smoke obscuration is the moment when the optical density reaches this limit. Times to reach other smoke levels are also provided for discussion.

Figure 49 and Figure 53 show the optical density-time profiles measured on the first and second storeys. The times to reach various optical density levels at different locations for this series of the tests are listed in Table 8. It must be pointed out that the smoke density meters used for the first storey had a narrower range of signal output (0.15 to 0 V) while the smoke density meters used for the second storey had a wider working range (1 to 0 V). The starting voltage (0.15 or 1 V when there was no smoke) decreased due to smoke residue left over from the preceding tests on the light source and the detector inside the meters. This reduced the working range particularly for the smoke density meters used for the first storey, which became saturated at a lower  $OD$  level than the meters used for the second storey. The smoke density meters used for the first storey were not able to measure the smoke obscuration of  $OD = 2 \text{ m}^{-1}$  and beyond. The analysis of video records indicated that by the time when  $OD = 2 \text{ m}^{-1}$  was reached in the corridor on the second storey, there was complete smoke obscuration in the test house.

In Test UF-01, the increase in the optical density at each measurement location was quite fast. The times to reach various optical density levels of interest were very similar to the fire scenario Test FS-1. The combustion of the polyurethane foam produced sufficient smoke for conditions to reach the smoke obscuration limit. Both the optical density measurements and video records indicate that complete visual obscuration occurred around 180 s in the test house.

With the basement door closed in Test UF-02, the increase in  $OD$  was slower at various measurement points than in Test UF-01 (compare Figure 49 and Figure 53). Due to the exterior door was opened at 180 s, the optical density on the first storey temporarily decreased after opening the exterior door then increased again (see Figure 53a). The  $OD_{Limit} = 2 \text{ m}^{-1}$  was reached at 297-347 s in the corridor on the second storey. Both the optical density measurements and video records indicate that complete visual obscuration occurred in this timeframe in the test house.

Psychological effects of smoke on occupants may accelerate the loss of visibility [26]. Possible reduction of time to untenable smoke level due to psychological effect is not addressed in this report.

**Table 8. Time (in seconds) to the Specified Smoke Optical Density**

OD (m <sup>-1</sup> ) =	Test UF-01				Test UF-02			
	0.25	0.50	1.0	2.0	0.25	0.50	1.0	2.0
1 <sup>st</sup> storey SW quadrant 1.5 m height	125	140	155	n.a.	137	147	187/ 342*	n.a.
1 <sup>st</sup> storey SW quadrant 0.9 m height	155	170	195	n.a.	252	292	357	n.a.
2 <sup>nd</sup> storey corridor 1.5 m height	150	160	170	185	202	232	247	297
2 <sup>nd</sup> storey corridor 0.9 m height	160	170	180	195	237	252	277	347

Notes:

1. \*OD = 1.0 m<sup>-1</sup> first reached at 187 s on the first storey but OD then decreased due to the exterior door was opened at 180 s; OD = 1.0 m<sup>-1</sup> reached again at 342 s.
2. n.a. – not available due to limited measurement range of the smoke meters used for the first storey.

### 3.7.4 Summary of Estimation of Time to Incapacitation

Tenability was analyzed independently for gas exposure, heat exposure and smoke obscuration to estimate the time available for escape, using incapacitation as the endpoint. The combined incapacitating effect as a result of simultaneous exposure to the combustion gases, heat and smoke obscuration is not well understood. Table 9 summarizes the estimated times to the onset of untenable conditions, where each value is the shortest time among each set of values from Table 5, Table 7 and Table 8.

The uncertainty in the calculation of the FED is estimated to be  $\pm 25\%$  for the heat exposure and  $\pm 40\%$  for the CO exposure (with CO<sub>2</sub> induced hyperventilation) [15]. With the fast-growing fire used in the FPH project, the resulting uncertainty in the estimated time is much smaller than the uncertainty in the calculated FED due to the non-linear relationship. The uncertainty in the timing of the optical density measurement is  $\pm 5$  s. Table 9 lists the uncertainty in the estimated time.

**Table 9. Summary of Estimation of Time to Specified FED and OD (in seconds)**

Test	OD = 2 m <sup>-1</sup>	FED = 0.3		FED = 1	
	2 <sup>nd</sup> storey	1 <sup>st</sup> storey	2 <sup>nd</sup> storey	1 <sup>st</sup> storey	2 <sup>nd</sup> storey
Tests with open basement doorway					
FS-1	190 $\pm$ 5	245 $\pm$ 15	260 $\pm$ 15	290 $\pm$ 20	325 $\pm$ 30
UF-01	185 $\pm$ 5	205 $\pm$ 10	225 $\pm$ 10	235 $\pm$ 15	255 $\pm$ 15
Tests with closed basement doorway					
FS-4	not reached	1550 $\pm$ 410	1100 $\pm$ 300	not reached	not reached
UF-02	297 $\pm$ 5	466 $\pm$ 60	362 $\pm$ 30	676 $\pm$ 90	501 $\pm$ 70

Notes:

1. Values determined using the measurements at 1.5 m height (for gas concentrations and OD) or 1.4 m height (for temperatures);
2. Data for the fire scenario Tests FS-1 and FS-4 included for reference.

Smoke obscuration was the first hazard to arise. Although smoke obscuration would not directly cause incapacitation, it could impede evacuation and prolong exposure of occupants to other hazards. In Test UF-01, the time to reach various optical density levels of interest was very similar to that of Test FS-1 and the combustion of polyurethane foam was mainly responsible for reaching the smoke obscuration limit. With the basement door closed in Test UF-02, the increase in *OD* was slower than in Test UF-01. It must be pointed out that people with impaired vision could become disoriented at a lower optical density.

Because of the variation in susceptibility to heat and/or gas exposure, the time to untenable conditions was not a single value. The times corresponding to  $FED = 0.3$  and  $FED = 1$  in Table 9 represent this variation to a certain extent. There was also a slight variation of the corresponding time on the 2 different storeys, which is reflected by the time range for each  $FED$  in Table 9. It should be pointed out that in Test UF-01, the heat exposure and the CO exposure (with hyperventilation) would cause incapacitation at a similar time on the first storey, independently. Closing the door to the basement fire room prolonged the time available for escape.

Closing the door to the basement fire room prolonged the time available for escape for occupants on the upper storeys. For Test UF-02 with the door to the basement closed, the products of combustion were initially transported into the first storey through the undercut of the basement door. It was recognized that the air-tightness around the perimeter of the floor-ceiling test assembly could have an impact on the time to untenable conditions on the upper storeys. Efforts were made during the construction of the test assembly to minimize potential leakage by putting ceramic fibre blankets in the small gaps around the perimeter but actual leakage was not measured.

For the closed bedroom, only heat exposure could be estimated. Based on the temperature measurements and the heat exposure calculation, during both tests, the conditions in the closed bedroom on the second storey would not reach untenable conditions associated with  $FED = 0.3$  or 1.

The analysis so far addressed a potential exposure that started at the time of ignition, which applies to occupants who would have been in the open spaces of the house.

Further analysis was also conducted for exposure starting at times later than ignition. This further analysis is important for occupants who would have been in the closed bedroom but tried to open the bedroom door to escape through the normal routes. Figure 54 and Figure 55 show the time remaining to incapacitation calculated from the convected heat and hyperventilated CO exposure for people of average susceptibility ( $FED=1$ ) and for more susceptible occupants ( $FED=0.3$ ) as a function of onset of exposure. Again, this calculation was associated with particular positions where the concentrations or temperatures were measured (each calculated time applies to an occupant who would have stayed at that particular location). The actual time to incapacitation would be in between the times calculated for different locations since an occupant would have moved through different locations during egress. The time remaining to incapacitation tended to be dictated by the gas exposure in both tests. The convected heat became more severe as time advanced and also became the determining factor on the first storey in Test UF-01.

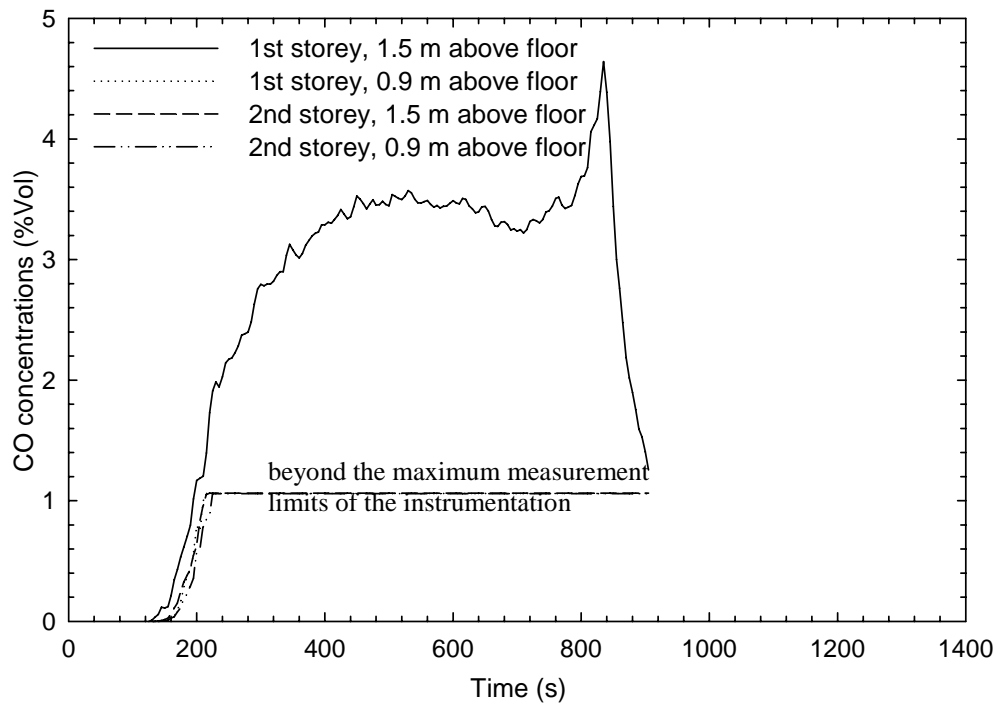


**Figure 46. CO measurements for Test UF-01**

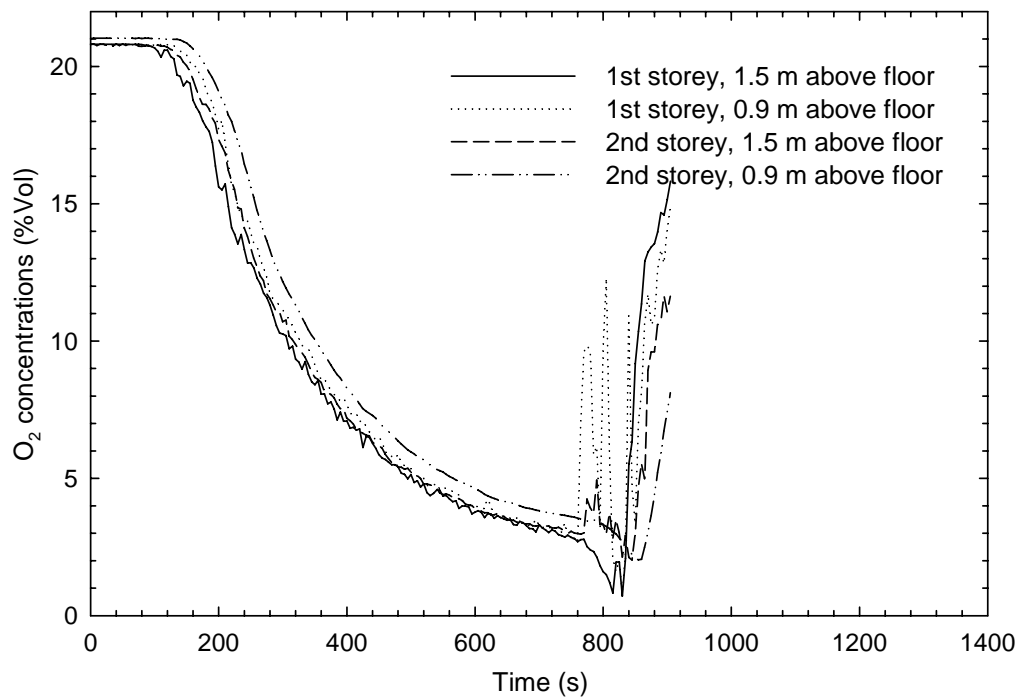


**Figure 47. O<sub>2</sub> measurements for Test UF-01**

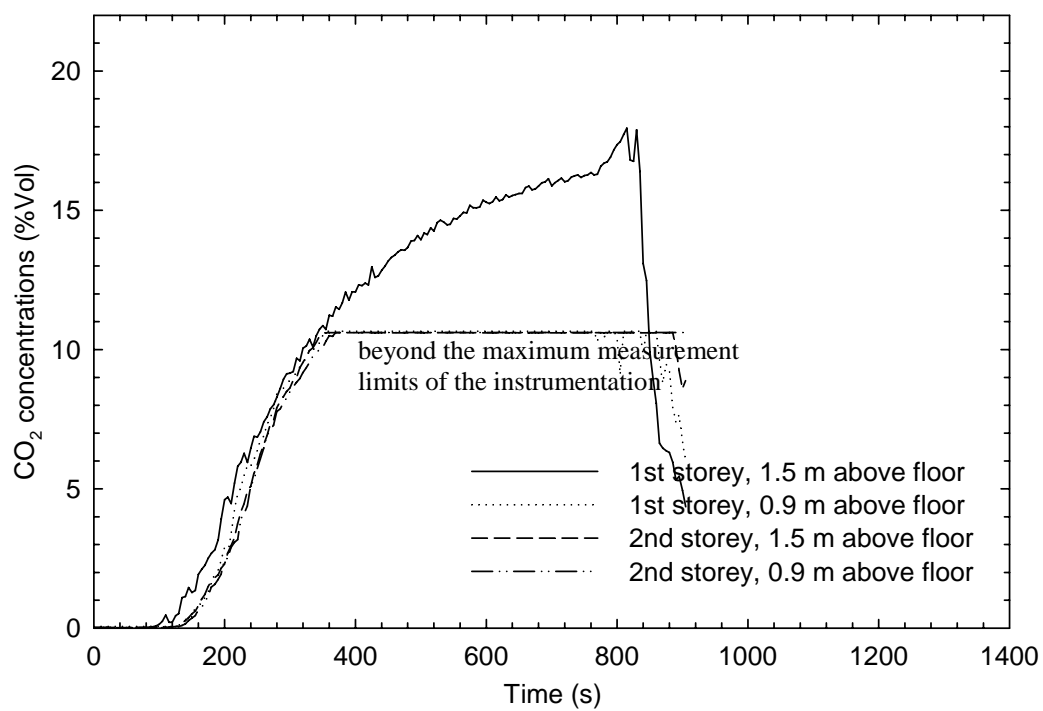
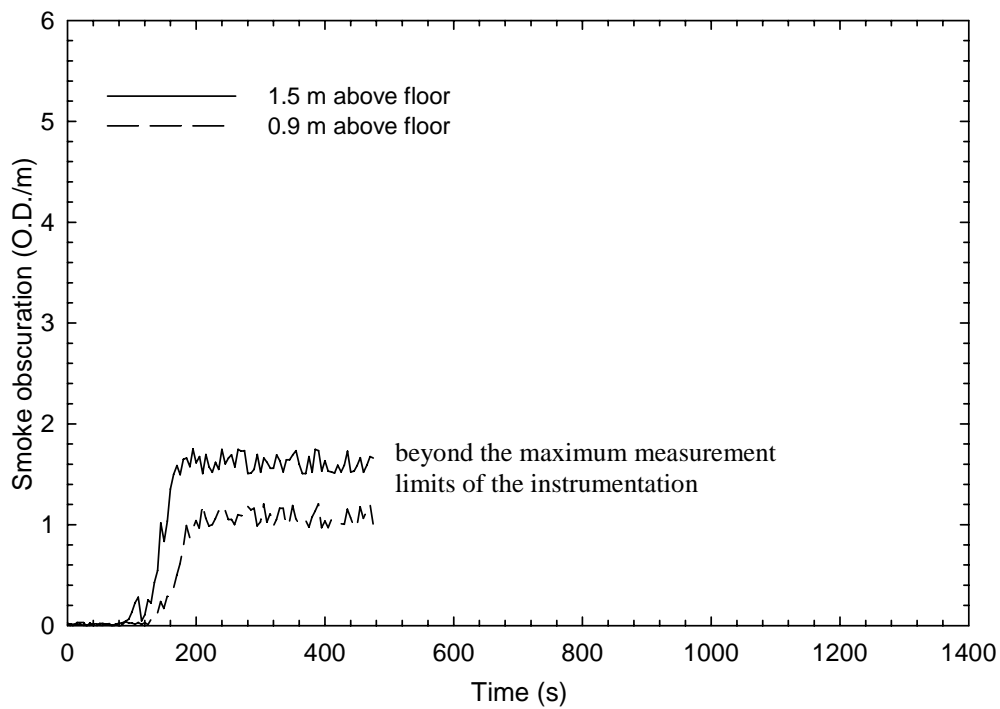
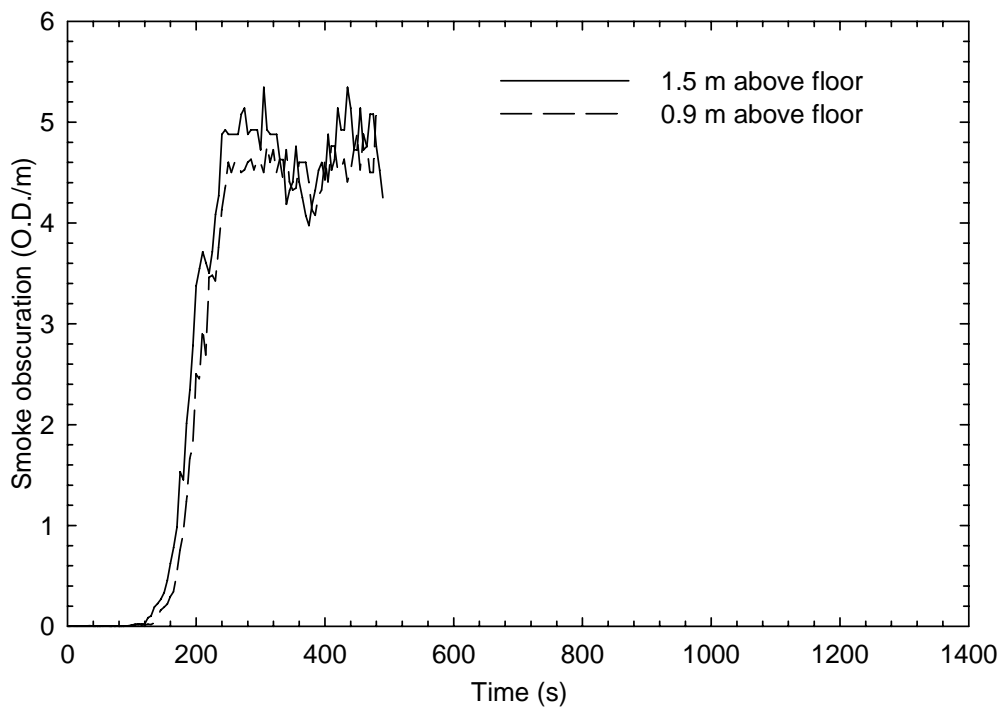


Figure 48. CO<sub>2</sub> measurements for Test UF-01



a) Smokemeters - 1st storey SW quadrant.



b) Smokemeters - 2nd storey corridor.

**Figure 49. Optical density measurements for Test UF-01**

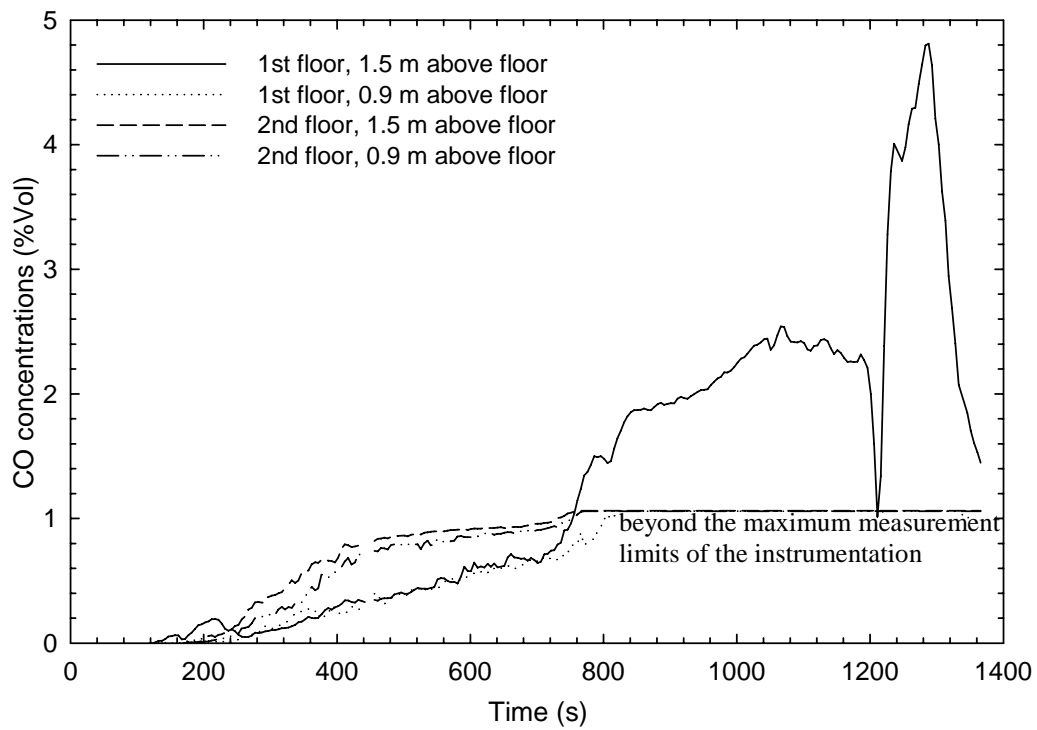


**Figure 50. CO measurements for Test UF-02**

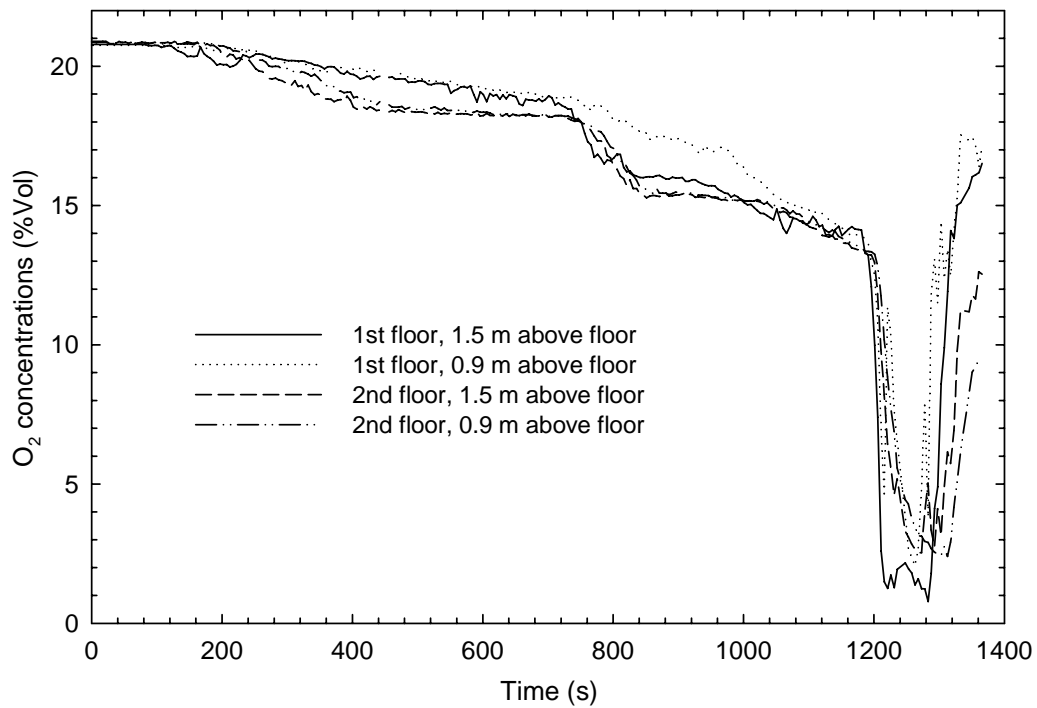


**Figure 51. O<sub>2</sub> measurements for Test UF-02**

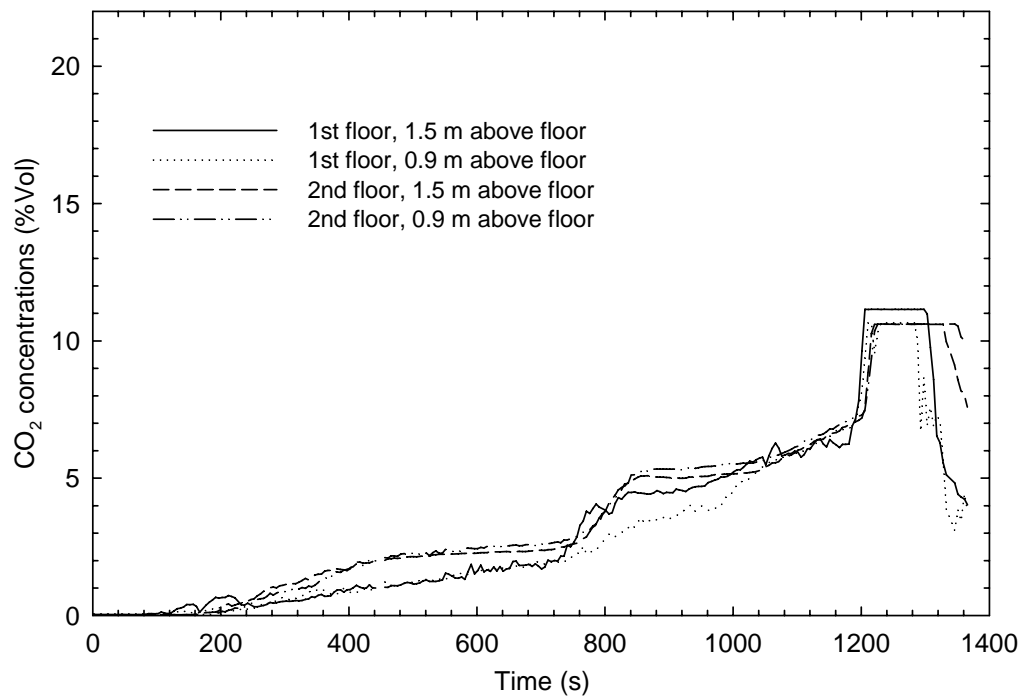
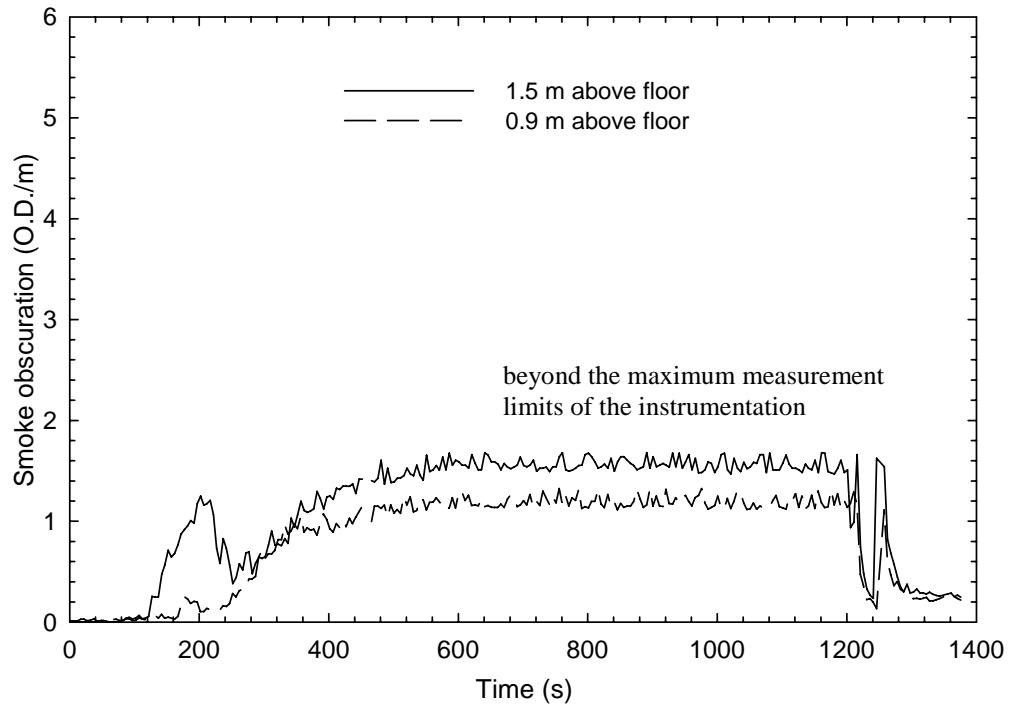
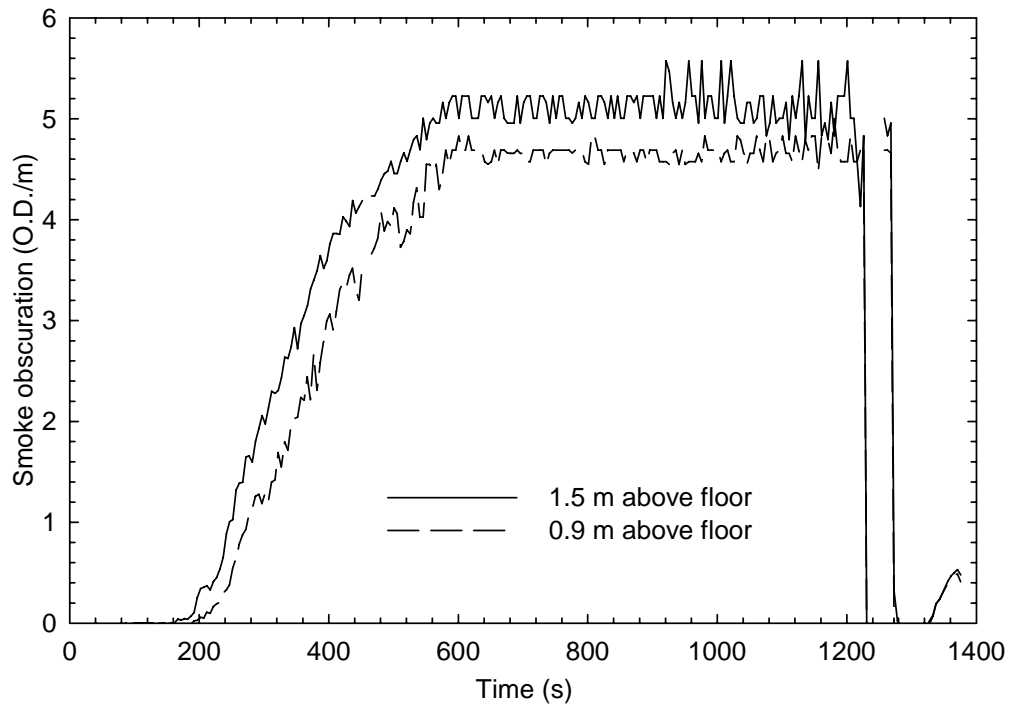


**Figure 52. CO<sub>2</sub> measurements for Test UF-02**



a) Smokemeters - 1st storey SW quadrant.



b) Smokemeters - 2nd storey corridor.

**Figure 53. Optical density measurements for Test UF-02**

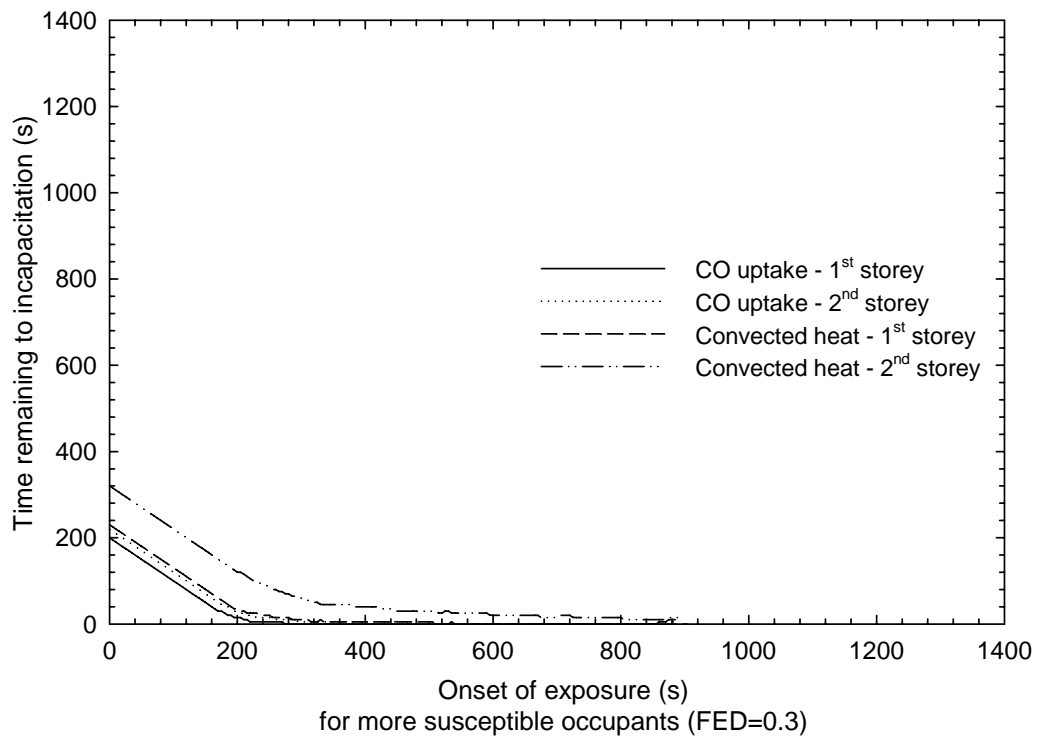
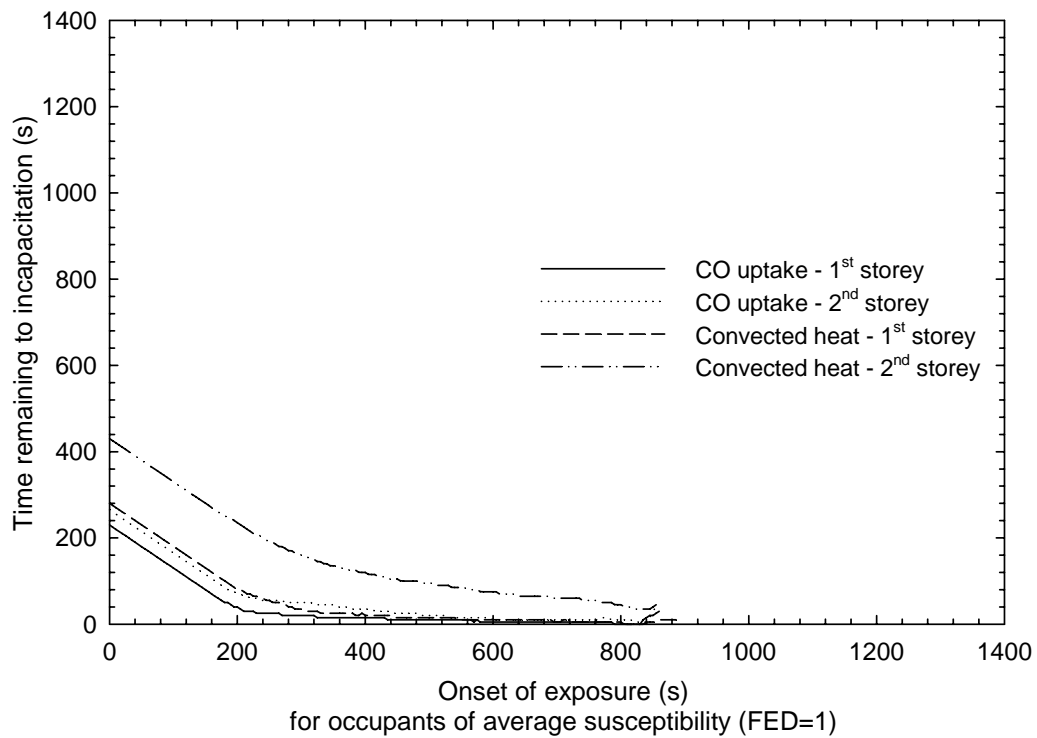


**Figure 54. Time remaining to incapacitation versus onset of exposure for Test UF-01 (ignition at time zero)**

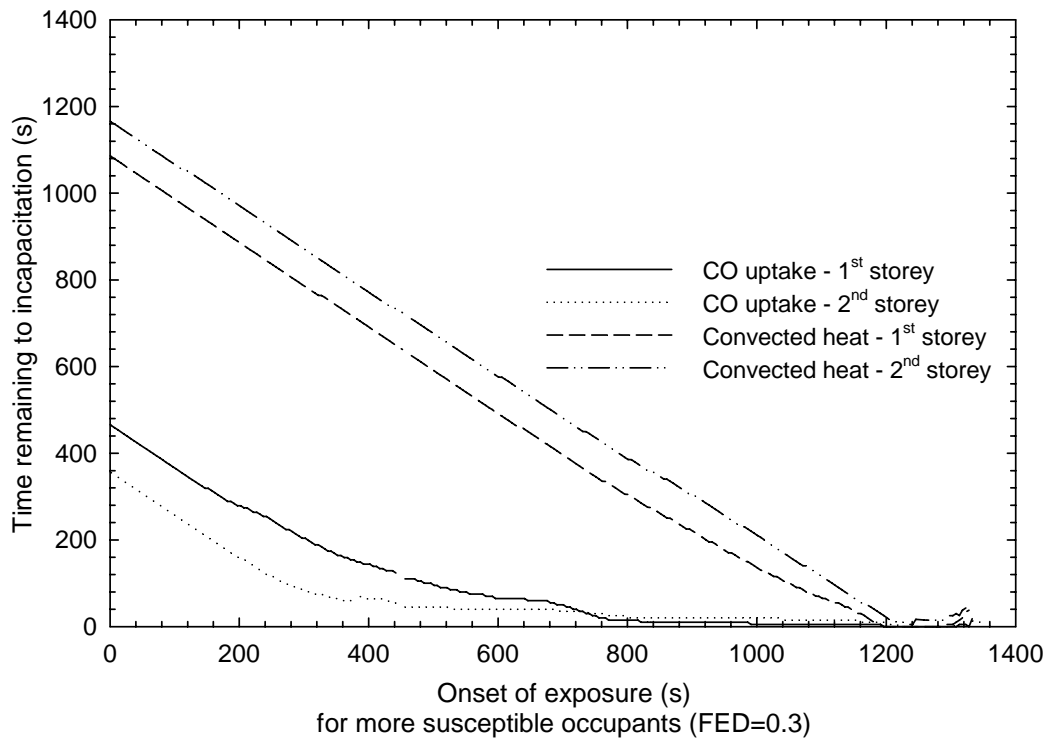
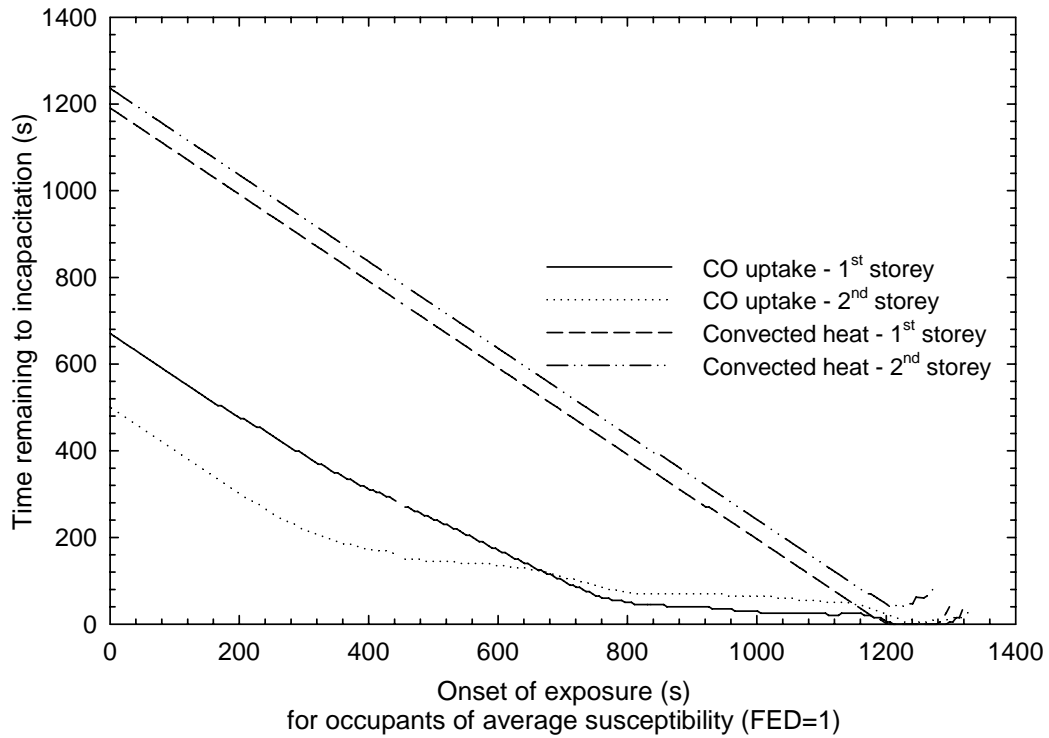


**Figure 55. Time remaining to incapacitation versus onset of exposure for Test UF-02 (ignition at time zero)**

### 3.8 The Sequence of Events

Figure 56 and Figure 57 show the chronological sequence of the fire events in Tests UF-01 and UF-02, respectively.

The smoke alarms in the basement detected the fire quickly. The smoke alarm (photoelectric) located in the basement activated at 40 s in Test UF-01 and at 42 s in Test UF-02. Interconnecting all of the smoke alarms in the house would help ensure an early fire alert.

The basement window was opened after it reached 300°C at 105 s in Test UF-01 and at 97 s in Test UF-02. The exterior door on the first storey was opened at 180 s in both tests.

The timing for onset of potentially untenable conditions includes those for the complete smoke obscuration ( $OD \geq 2 \text{ m}^{-1}$ ) and for exposure to heat and narcotic gases for susceptible ( $FED = 0.3$ ) and average ( $FED = 1.0$ ) occupants (see Section 3.7 for detailed discussions). The time after which the floor structure would be no longer usable for egress (740 s for UF-01 and 1200 s for UF-02) was based on the shortest time to reach the maximum deflection.

In both tests the untenable conditions were reached before the failure of the floor assembly based on falling of the concrete blocks. In the case of UF-01 scenario (door to the basement was open), every event happened earlier than in the case of the UF-02 scenario (door to the basement was closed). This is due to the fact that having the door closed slowed down the fire development and limited the migration of hot gases to the upper storeys until gaps in the floors and/or the door were formed to allow for this migration.

It should be mentioned that there appears to be a slightly earlier flame penetration in UF-02 compared to UF-01. This may be attributed to the lack of air in UF-02 and the fire creating a path for air and smoke to move between the basement and the first storey. The tests were terminated after some concrete blocks had started falling through the subfloor.

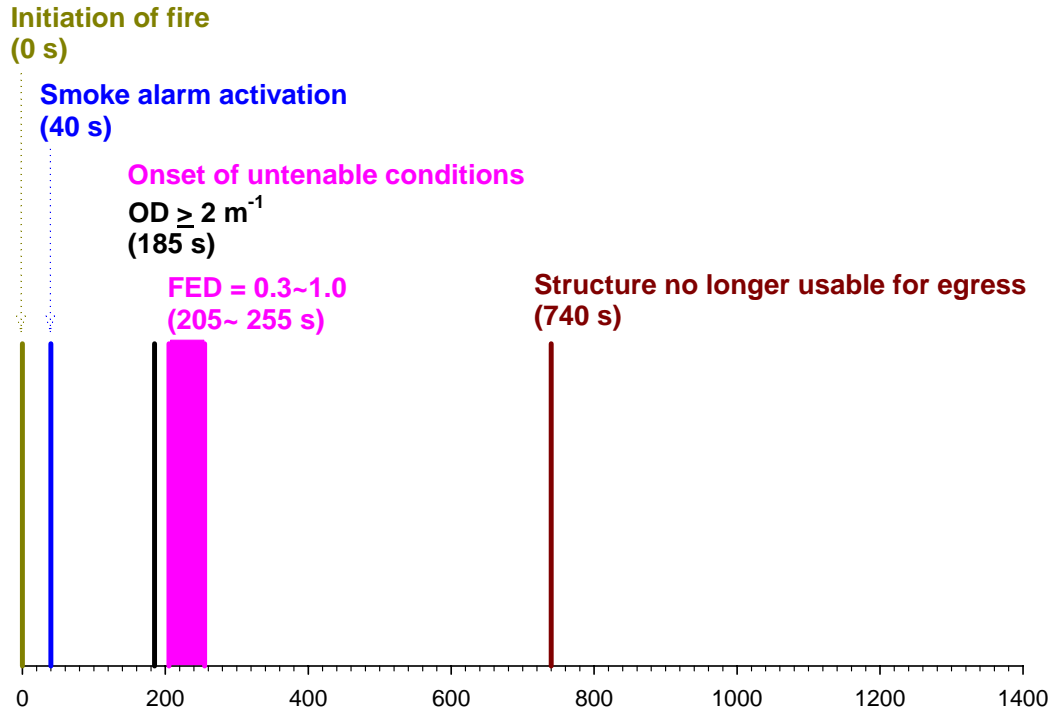


**Figure 56. Sequence of fire events in Test UF-01 (s)**

(Flame penetration at 12 min or 720 s)

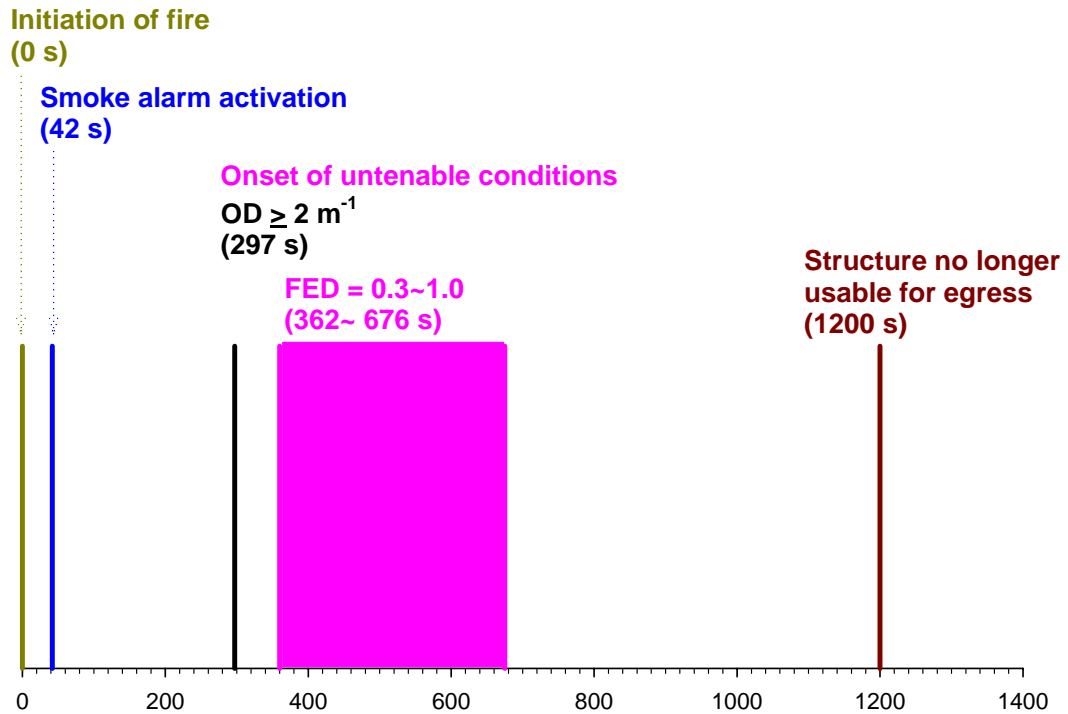


**Figure 57. Sequence of fire events in Test UF-02 (s)**

(Flame penetration at 10 min 15 s or 615 s)

## 4 SUMMARY

This report presents the results and analysis of Tests UF-01 and UF-02 as part of the research project on fire performance of houses. The tests were conducted in the test facility that simulated a typical two-storey single-family house complying with the minimum code requirements in the NBCC. The two tests were identical except for the state of the door in the basement doorway. In Test UF-01, there was no door in this doorway (open basement doorway) while in Test UF-02 there was a door in this doorway in the closed position (closed basement doorway).

The tests were conducted on loaded unprotected solid wood joist floors (also basement ceilings) using fire scenarios that were characterized in a study documented in references [6,29]. A number of measurements were conducted during the tests including temperatures at various locations (in the compartments and on the floor assemblies), fire detection times at various locations, gas measurements, smoke density measurements, flame penetration and deflection measurements for the floor assemblies.

The results showed that, in a basement fire test scenario, closing the door to the basement delayed the onset of untenable conditions on the first and second storeys as well as delayed the failure of the unprotected floor assemblies constructed over the basement.

For both scenarios, floor failure occurred after the onset of untenable conditions (using incapacitation as an end point). On the other hand, the activation times of smoke alarms in the basement and times for flame penetration through the floor assemblies were very close for the two tests. But the time for flame penetration was much closer to floor failure in Test UF-01 (difference of 20 s) than in Test UF-02 (difference of almost 600 s).

The test results must be interpreted within the context of the fire scenarios used in the experiments. Two relatively severe basement fire scenarios were used in the full-scale fire experiments to establish the sequence of the events that would affect the ability of occupants to escape the house in the event of a basement fire.

## 5 ACKNOWLEDGMENTS

The National Research Council Canada gratefully acknowledges the financial and technical support of the following organizations that provided valuable input to the research as the project partners:

- Canada Mortgage and Housing Corporation
- Canadian Automatic Sprinkler Association
- Canadian Wood Council
- Cement Association of Canada
- City of Calgary
- FPInnovations - Forintek Division
- North American Insulation Manufacturers Association
- Ontario Ministry of Community Safety and Correctional Services/Office of the Fire Marshal
- Ontario Ministry of Municipal Affairs and Housing
- Wood I-Joist Manufacturers Association

The authors would like to acknowledge H. Cunningham (deceased), B. Di Lenardo, E. Gardin, J. Haysom (retired), I. Oleszkiewicz (retired), G. Proulx and M. Sultan who served on the IRC steering committee for the project. The authors also wish to acknowledge Don Carpenter, George Crampton, Eric Gibbs, Jocelyn Henrie, Malgosia Kanabus-Kaminska, Roch Monette, Richard Rombough, Michael Ryan and Michael Wright who contributed to the construction of the test facility, the setup of and conducting the fire tests.

## 6 REFERENCES

1. Canadian Commission on Building and Fire Codes; National Building Code of Canada; National Research Council of Canada, Ottawa, Canada, 2005.
2. Canadian Commission on Building and Fire Codes, User's Guide – NBC 2005, Application and Intent Statements, National Research Council of Canada, Ottawa, Canada, 2006.
3. Proulx, G., Cavan, N.R., Tonikian, R., Egress Times From Single Family Houses, Research Report 209, Institute for Research in Construction, National Research Council Canada, 2006.
4. Bwalya, A.C., An Extended Survey of Combustible Contents in Canadian Residential Living Rooms, Research Report 176, Institute for Research in Construction, National Research Council Canada, 2004
5. Leroux, P., Kanabus-Kaminska, J.M., Séguin, Y.P., Henrie, J.P., Loughheed, G.D., Bwalya, A.C., Su, J.Z., Bénichou, N., Thomas, J.R. Small-Scale and Intermediate-Scale Fire Tests of Flooring Materials and Floor Assemblies for the Fire Performance of Houses Project, Research Report 211, Institute for Research in Construction, National Research Council Canada, 2007.
6. Taber, B.C., Bwalya, A.C., McCartney, C., Bénichou, N., Bounagui, A., Carpenter, D.W., Crampton, G.P., Kanabus-Kaminska, J.M., Kashef, A., Leroux, P., Loughheed, G.D., Su, J.Z., Thomas, J.R., Fire Scenario Tests in Fire Performance of Houses Test Facility - Data Compilation, Research Report 208, Institute for Research in Construction, National Research Council Canada, 2006.
7. "ASTM E1537-02a: Standard Test Method for Fire Testing of Upholstered Furniture", American Society for Testing and Materials, PA, USA, 2002.
8. Crampton, G.P. The Design and Construction of a Flame Conductivity Device to Measure Flame Penetration through Floor Systems, Research Report 223, Institute for Research in Construction, National Research Council Canada, 2006.
9. Forte, N. and Crampton, P., The Design and Construction of Electronic Deflection Gauges to Measure the Movement of Floor Assemblies in a Fire, Research Report 202, Institute for Research in Construction, National Research Council Canada, 2005.
10. EC1, Eurocode 1, "Basis of design and design actions on structures", Part 2-2: Actions on Structures Exposed to Fire, ENV 1991-2-2, European Committee for Standardization, Brussels, Belgium, 1994.
11. SNZ, "Code of practice for the general structural design and design loadings for buildings", SNZ 4203, Standards New Zealand, Wellington, New Zealand. 1992.
12. AS/NZS, "Structural design actions, Part 0: General principles", AS/NZS 1170.0, Australia/New Zealand Standard, 2002.

13. ASCE 7-98, ASCE Standard, "Minimum design loads for buildings and other structures", American Society of Civil Engineering, Reston, Virginia, 2000.
14. CAN/ULC-S101-04; Standard Methods of Fire Endurance Tests of Building Construction and Materials; Underwriters' Laboratories of Canada, Scarborough, Canada, 2004.
15. ISO Technical Specification 13571, "Life-threatening Components of Fire—Guidelines for the Estimation of Time Available for Escape Using Fire Data," International Organization for Standardization, Geneva, 2002.
16. Purser, D.A., "Toxicity Assessment of Combustion Products," in The SFPE Handbook of Fire Protection Engineering, ed. P.J. DiNenno, D. Drysdale, C.L. Beyler, W.D. Walton, R.L.P. Custer, J.R. Hall, Jr. and J.M. Watts, Jr., 3rd edition, Society of Fire Protection Engineers /National Fire Protection Association, Quincy, Massachusetts, 2002, Section 2, Chapter 6.
17. Beyler, C., "Toxicity Assessment of Products of Combustion of Flexible Polyurethane Foam," Fire Safety Science -- Proceedings of the Eighth International Symposium, International Association for Fire Safety Science, 2005, pp.1047-1058
18. Laursen, T., "Overview of Toxicity/Effectiveness Issues", Proceedings of Halon Alternatives Technical Working Conference, Albuquerque, NM, 1993, pp. 357-367.
19. Sax, N.I. and Lewis, R.J., "Dangerous Properties of Industrial Materials" (7th ed.), Van Nostrand Reinhold, New York, 1989.
20. Peterson, J.E. and Stewart, R.D., "Predicting the carboxyhemoglobin levels resulting from carbon monoxide exposures," Journal of Applied Physiology, Vol. 39, No. 4, pp. 633-638, 1975
21. Stewart, R.D., Peterson, J.E., Fisher, T.N., Hosko, M.J., Baretta, E.D., Dodd, H.C. and Herrmann, A.A., "Experimental Human Exposure to High Concentrations of Carbon Monoxide," Archives of Environmental Health, Vol. 26, pp. 1-7, 1973
22. Babrauskas, V., "Combustion of Mattresses Exposed to Flaming Ignition Sources, Part I. Full-Scale Tests and Hazard Analysis," NBSIR 77-1290, National Bureau of Standards, Washington, DC, September 1977.
23. Hauck, H. and Neuberger, M., "Carbon monoxide uptake and the resulting carboxyhemoglobin in man," European Journal of Applied Physiology, Vol. 53, pp.186-190, 1984.
24. Gann, R.G., "Estimating Data for Incapacitation of People by Fire Smoke," Fire Technology, Vol. 40, pp.201-207, 2004.
25. Christopher J. Wiecek and Nicholas A. Dembsey, "Human Variability Correction Factors for Use with Simplified Engineering Tools for Predicting Pain and Second Degree Skin Burns", Journal of Fire Protection Engineering, Vol. 11, No. 2, 88-111, 2001
26. Jin, T., "Visibility and Human Behavior in Fire Smoke," in The SFPE Handbook of Fire Protection Engineering, ed. P.J. DiNenno, D. Drysdale, C.L. Beyler, W.D. Walton, R.L.P. Custer, J.R. Hall, Jr. and J.M. Watts, Jr., 3rd edition, Society of Fire Protection Engineers /National Fire Protection Association, Quincy, Massachusetts, 2002, Section 2, Chapter 4.
27. Babrauskas, V., "Full-Scale Burning Behavior of Upholstered Chairs," NBS Technical Note 1103, National Bureau of Standards, Washington, DC, August 1979.
28. Bukowski, R.W., Peacock, R.D., Averill, J.D., Cleary, T.G., Bryner, N.P., Walton, W.D., Reneke, P.A., Kuligowski, E.D., "Performance of Home Smoke Alarms - Analysis of the Response of Several Available Technologies in Residential Fire Settings," NIST Technical Note 1455, National Institute of Standards and Technology, December 2003.

29. Su, J., Bwalya, A., Lougheed, G., Bénichou, N., Taber, B., Kashef, A., Leroux, P. and Thomas, R., Fire Scenario Tests In Fire Performance Of Houses Test Facility – Data Analysis, Research Report 210, Institute for Research in Construction, National Research Council Canada, 2007.

**Table A 1. Test Summary for Test UF-01**

- Test ID: UF-01
- Test Date: June 7, 2005
- Atmospheric Conditions: Temp: 25°C      RH: 68%      Pres: 100.5 kPa↓
- Structure Tested:
  - 38x235 mm (2x10) solid lumber (SPF)
  - 15.1 mm (5/8") OSB floor
  - 0.95 kPa load (144 concrete blocks, 2490 kg, 61 m pipe, 143 kg)
  - MC 9%
- Fire Load:
  - Mock-up sofa at centre of basement (9.32 kg foam)
  - Wood crib located 200 mm behind mock-up sofa (64.7 kg, 10% MC)
  - Wood crib located 200 mm from west side of mock-up sofa (65.9 kg, 10% MC)
  - Two wood cribs located under the mock-up sofa (32.6 kg, 30.3 kg, 10% MC)
  - 80 s ignition with 19 kW burner (13 l/min)
- Ignition time after start of data: 1:00
- Doors:      SE bedroom door closed / SW bedroom door open  
                  Door at top of basement stairs open  
                  First floor exterior door opened at 3:00 after ignition
- Window:   Window opened at 1:45 after ignition (300°C)
- Extinguishment: Water applied at 13:40 (820 s) after ignition
- Smoke Alarm Activation Times:
 

	Activation <i>(time from ignition)</i>
Smoke Alarm #2, Photoelectric, Basement, bottom of stairs	0:40
Smoke Alarm #3, Ionization, 1 <sup>st</sup> Floor, top of stairs	1:15
Smoke Alarm #4, Photoelectric, 1 <sup>st</sup> Floor, top of stairs	1:25
Smoke Alarm #5, Ionization, 2 <sup>nd</sup> Floor, top of stairs	2:05
Smoke Alarm #6, Photoelectric, 2 <sup>nd</sup> Floor, top of stairs	2:15
Smoke Alarm #7, Ionization, SE bedroom, closed	3:20
Smoke Alarm #8, Photoelectric SE bedroom, closed	3:25
Smoke Alarm #9, Ionization, SW bedroom, open	2:20
Smoke Alarm #10, Photoelectric, SW bedroom, open	2:30

**Table A 2. Test Summary for Test UF-02**

- Test ID: UF-02
- Test Date: Sept. 21, 2005
- Atmospheric Conditions: Temp: 19°C      RH: 94%      Pres: 101.5 kPa↓
- Structure Tested:
  - 38x235 mm (2x10) solid lumber (SPF)
  - 15.1 mm (5/8") OSB floor
  - 0.95 kPa load (144 concrete blocks, 2490 kg, 61 m pipe, 143 kg)
  - MC 10%
- Fire Load:
  - Mock-up sofa at centre of basement (9.26 kg foam)
  - Wood crib located 200 mm behind mock-up sofa (62.5 kg, 9% MC)
  - Wood crib located 200 mm from west side of mock-up sofa (65.3 kg, 9% MC)
  - Two wood cribs located under the mock-up sofa (32.1 kg, 29.3 kg, 9% MC)
  - 80 s ignition with 19 kW burner (13 l/min)
- Ignition time after start of data: 0:57
- Doors:      SE bedroom door closed / SW bedroom door open  
                  Door at top of basement stairs closed  
                  First floor exterior door opened at 3:00 after ignition
- Window:    Window opened at 1:37 after ignition (300°C)
- Extinguishment: Water applied at 21:20 (1280 s) after ignition
- Smoke Alarm Activation Times:
 

	Activation <i>(time from ignition)</i>
Smoke Alarm #2, Photoelectric, Basement, bottom of stairs	0:42
Smoke Alarm #3, Ionization, 1 <sup>st</sup> Floor, top of stairs	1:12
Smoke Alarm #4, Photoelectric, 1 <sup>st</sup> Floor, top of stairs	1:37
Smoke Alarm #5, Ionization, 2 <sup>nd</sup> Floor, top of stairs	2:52
Smoke Alarm #6, Photoelectric, 2 <sup>nd</sup> Floor, top of stairs	3:02
Smoke Alarm #7, Ionization, SE bedroom, closed	7:07
Smoke Alarm #8, Photoelectric SE bedroom, closed	9:01
Smoke Alarm #9, Ionization, SW bedroom, open	3:32
Smoke Alarm #10, Photoelectric, SW bedroom, open	Failed to operate